FABRICATION AND CHARACTERIZATION OF SURFACE MODIFIED NANOFIBRILLATED CELLULOSE INCORPORATED POLYPROPYLENE COMPOSITES

K. D. H. N. Kahawita

139454T

Degree of Master of Science

Department of Materials Science and Engineering

University of Moratuwa

Sri Lanka

June 2018

FABRICATION AND CHARACTERIZATION OF SURFACE MODIFIED NANOFIBRILLATED CELLULOSE INCORPORATED POLYPROPYLENE COMPOSITES

Kahawitage Dona Himanthi Nimrekha Kahawita

139454T

Thesis submitted in partial fulfillment of the requirements for the degree Master of Science in Materials Science

Department of Materials Science and Engineering

University of Moratuwa

Sri Lanka

June 2018

Declaration

I declare that this is my own work and this thesis/dissertation does not incorporate without acknowledgement any material previously submitted for a Degree or Diploma in any other University or institute of higher learning and to the best of my knowledge and belief it does not contain any material previously published or written by another person except where the acknowledgement is made in the text.

Also, I hereby grant to University of Moratuwa the non-exclusive right to reproduce and distribute my thesis/dissertation, in whole or in part in print, electronic or other medium. I retain the right to use this content in whole or part in future works (such as articles or books).

Signature: Date:

The above candidate has carried out research for the PG Diploma Dissertation under my supervision.

Name of the supervisor: Mr. A. M. P. B. Samarasekara

Signature of the supervisor: Date:

Abstract

Increasing demand for materials with improved properties leads to acquiring advancement of nanomaterial. Therefore, Interest in nanocellulose has been increasing exponentially in recent years. Nanocellulose extracted from plant materials are divided into two main two categories as nanofibrillated cellulose (NFC) and nanocrystalline cellulose (NCC). Compared to NCC, NFC has gained more attention due to attractive properties such as high mechanical properties, reinforcing ability and aspect ratio. Reinforcement of NFC with synthetic polymer materials is an interesting area in the polymer-based researches over the past decades to enhance mechanical and thermal properties as well as to deplete the environmental pollution. Polypropylene is one of the widely used thermoplastic materials as matrix material in engineering composite applications. In nature, NFC is hydrophilic and polypropylene is hydrophobic. Therefore, surface modification of NFC reinforcement is necessary to prepare a nanocomposite with good performance. The prepared nanocomposite material can be used for many engineering applications. In the present research discuss mechanical, thermal and water absorption properties of polypropylene with up to 5 wt. % loading of unmodified and silane surface modified NFC reinforced composites. Scanning electron microscopic images, Fourier-transform infrared spectra, X-ray diffractograms and thermal gravimetric analysis were used to characterize the raw materials and surface modified NFC samples. The best thermal resistance and mechanical properties were given by the 3.5% silane surface modified NFC loaded polypropylene composite such as the hardness, tensile strength, and impact strength values are respectively 7.4%, 12.6%, and 86.1% higher than that of untreated NFC reinforced composite materials and neat polypropylene. In addition, the composite sample has the intermediate level of water absorption (0.1 wt. %) and processability (21.1 g/10 min) with respect to all the other samples including pure polypropylene.

Keywords: nanofibrillated cellulose; polypropylene; surface modification; silylation; nanocomposite

Acknowledgement

Research is a creative work which discovers the world in a new way. Therefore, I want to express my gratitude through simple words to the people who did a great job to their nation.

In the first instance, I wish to acknowledge to Mr. V. S. C. Weragoda, the head of the Department of Materials Science & Engineering, University of Moratuwa to grant me a valuable opportunity to follow a Master of Science at the University of Moratuwa. Then I am grateful to Mr. A. M. P. B. Samarasekara the research supervisor and Dr. D. A. S. Amarasinghe, for the enthusiasm, guidance, assistance, and encouragement in the research studies and in the preparation of the dissertation. I am especially indebted to Mr. V. Sivahar, the coordinator of MSc/PGDip in Materials Science and the other academic staff members for monitoring and providing specific advice.

Sincere gratitude is extended to Mr. Pubudu, Mr. Premalal and Mr. Mihiranga in the same department at Moratuwa University, to expertly provide me the knowledge about different kinds of testing methods. In addition, I wish to thank all the other non-academic staff members of the Materials Science and Engineering, Moratuwa University for the assistance. Then I wish to express my special thanks to Dr. Dilhara Edirisinghe, the head of rubber technology and development department of Rubber Research Institute, Ratmalana (RRISL), to grant permission for further studies of the research. The research would not become success unless the support I gain from them.

Penultimately, I want to express profound gratefulness to my family for the love, care, support, and scarifications, to my colleagues and to all the other people who helped me even in a single word. Finally, I would like to thanks all the people who help me however, I fail to mention in this Acknowledgement.

Table of Content

List of Figures

List of Tables

List of Abbreviations

PP	Polypropylene
iPP	isotactic Polypropylene
sPP	syndiotactic Polypropylene
aPP	atactic Polypropylene
NFC	Nanofibrillated Cellulose
NCC	Nanocrystalline Cellulose
PE	Polyethylene
PS	Polystyrene
PVC	Polyvinylchloride
PC	Polycarbonate
PET	Polyethylene Terephthalate
NC	Nanocellulose
ILs	Ionic Liquids
TEMPO	2,2,6,6-tetramethylpiperidinyl-1-oxyl
CDMIPS	chlorodimethyl isopropylsilane
SEM	Scanning electron microscope
TEM	Transmission electron microscope
FTIR	Fourier Transform Infrared Spectroscopy
TGA	Thermal gravimetric analyzer
DSC	Differential scanning calorimetry
DTA	Differential thermal analysis
XRD	X-ray diffraction
PLA	Polylactic acid
PHAs	polyhydroxyalkaonates
PHB	polyhydroxybutyrate
PHBV	poly(3-hydroxybutyrate-co-3-hydroxyvalerate)
MFC	Microfibrillated cellulose

MAPP/ MAHgPP	Maleic anhydride grafted polypropylene
MALDPE	Maleic anhydride low-density polyethylene
MFI	Melt flow index
PVA	Polyvinyl alcohol
Si-69	(Bis [3-(triethoxysilyl)propyl] tetrasulfide)

List of Appendices

1 INTRODUCTION

Present days, synthetic polymers or plastics are very popular among people due to their advantages of low cost, lightweight, and simplicity of production process. However, synthetic plastics have low mechanical, thermal and biodegradable properties. Therefore, the production and development of natural polymer based synthetic polymer composites currently perform a significant role in material researches to improve the functionality of the final product. The properties of polymer blends depend not only on the geometry of matrix and fiber materials but also on coupling agents and other additives which are used frequently for effective modification [1].

Polypropylene (PP) is widely used, a thermoplastic material for different applications. There are major two types of PP; homopolymer (contain a single type of repeating unit) and copolymer (contain two or more types of repeating units). The copolymer again divides into two as random and blocks copolymers and produce by polymerization of PP homopolymer typically with ethylene [2]. In general, PP homopolymer offers high tensile strength, strength to weight ratio and stiffness than PP copolymer due to high crystallinity. Based on the spatial arrangement of atoms or tacticity, polypropylene can be again divided into three types; isotactic PP (iPP) syndiotactic PP (sPP) and atactic PP (aPP). Industrial polypropylene resins are mostly isotactic materials due to high strength [3]. However, the thermal stability and biodegradability of PP are considerably low as same as other thermoplastics. Therefore, various PP researches were done to improve the thermal and environmental properties with better mechanical characteristics by combining with natural fibers.

In nature, cellulose is the most abundant biopolymer present in the earth and has been easily extracted using plant waste materials [4, 5, 6, 7, 8]. Compared to cellulose, nanocellulose has better performances because there is a synergistic effect of nanoscale dimensions comparative to large-scale dimensions and the “nano effect” can optimize the ultimate composite [9]. Nanofibrillated cellulose (NFC) and nanocrystalline cellulose (NCC) are two main subgroups of nanocellulose extracted

from plant materials. In the production process, NCC is produced by the complete decomposition of amorphous regions of cellulose fibers and NFC production is mainly based on the application of high shearing forces to the extracted cellulose. NFC has more advantages in nanocomposite materials than NCC, such as better reinforcement ability with different matrices due to the strong nanoporous structure with three-dimensional network [10].

To enhance properties of nanocomposites, a proper surface modification should be done either to the matrix or to fiber materials. However, the most common and simple method is the modification of reinforcement surface. Therefore, there are different methods can be applied to improve the interaction through the reduction of the hydrophilicity of NFC before mixing with hydrophobic PP matrices [11, 10]. Frequently, hydrophobicity of nanocellulose is improved by the chemical surface modification, especially by coupling agents. Therefore, the research is focused on fabrication and characterization of NFC based PP composite with better performances. The prepared nanocomposite material can be used for different engineering purposes for instance packaging, aerospace, automotive and construction applications.

.

2 LITERATURE REVIEW

2.1 Thermoplastics

A thermoplastic material is denoted as a type of a plastic which can be molded at elevated temperature and solidified upon cooling as well as the process could repeat many times without influencing the mechanical properties [12]. Due to the low cost and reusability with better performances, thermoplastics are rapidly spread over the world. The main source of thermoplastics is crude oil. In addition, some researches have been done on the production of thermoplastics using natural gasses and coal [13]**.** Several types of thermoplastics were produced as results of different polymer researches; however, the majority of thermoplastic types are based only on four types of polymers; Polyethylene (PE), Polypropylene (PP), Polystyrene (PS) and Polyvinylchloride (PVC).

2.1.1 Classification of thermoplastics

Depending on the morphology, thermoplastic materials can be theoretically classified into amorphous, crystalline and semi-crystalline groups. However, there are no 100% crystalline materials and the highest achieved the degree of crystallinity of thermoplastics is approximately 80%. Therefore, thermoplastics are categorized into two groups as amorphous and semi-crystalline [14].

2.1.1.1 Amorphous Thermoplastics

Macromolecules of the thermoplastic materials are packed without a pattern called amorphous thermoplastics. Therefore, the material has low ductility and better optical transparency [2]. Ex: PS, PVC, PC

2.1.1.2 Semi-crystalline Thermoplastics

Macromolecules of semi-crystalline thermoplastics are containing both crystalline and amorphous sections and the crystalline regions are closely stacked in a regular pattern. Generally, amorphous areas provide better elastic properties due to week

bonding [15]. Therefore, semi-crystalline materials have better toughness. Ex: PP, PE, PET

2.2 Polypropylene (PP)

Semi-crystalline thermoplastics of polyolefins fulfill greater than 60 % of the thermoplastic requirement in the world plastic market and out of all polyolefins, polypropylene has become second only to polyethylene. Polypropylene (Figure 2.1) is produced by the polymerization of unsaturated monomer propylene (C_3H_6). Propylene is recovered mainly as a byproduct of steam cracking of liquid fuel (ex: naphtha and liquid petroleum gases) and fluid catalytic cracking units (ex: gasoline and distillates) [16]. Then the extracted propylene be subjected for the conventional polymerization process with Ziegler-Natta catalyst [17] to produce polypropylene. Since the industrial revolution, PP has been used in thousands of applications including packaging, automotive, medical, and textile. The wide range of applications of PP is based on the advanced characteristics such as reusability, low toxicity, inexpensiveness, excellent chemical and water resistance, better processability and high shelf life. However, PP has moderate thermal stability and creep resistance with low biodegradability.

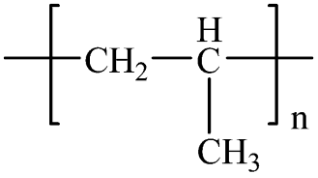

Figure 2.1: Structure of Polypropylene

2.2.1 Classification of Polypropylene

Generally, PP with only single propylene monomer is called the homopolyer. However, in the industry, PP is mixed with another type of simple olefins (especially with PE) with different ratios and produce PP copolymers. Combination of PP with reduced percentages of PE (7% or low) use to produced random copolymers and increased amounts of PE (6-15%) are favorable to fabricate block or impact copolymers. The inclusion of PE can interrupt the uniform stacking of PP and reduce the degree of crystallinity. Therefore, PP copolymers have better stiffness and

processability [18]. However, homopolymer of PP has the unique characteristic properties of thermoplastic PP material. Based on the spatial arrangement of methyl pendent group, polypropylene can be classified into three; atactic, isotactic and syndiotactic polypropylene [19].

2.2.1.1 Atactic polypropylene (aPP)

Methyl groups are in a random orientation to the main carbon chain; therefore, there is no ordered orientation and aPP is considered as amorphous structures. As a result of that aPP has low mechanical and thermal properties [20]; therefore, aPP has the lowest commercial value in respect to other two groups.

2.2.1.2 Syndiotactic Polypropylene (sPP)

Methyl groups are alternatively attached to both sides of the backbone. Therefore, sPP indicates a semi-crystalline structure with better stacking order. However, sPP is not commercially popular because sPP can produce by a specific type of production process (ex: metallocene catalysis) [21].

2.2.1.3 Isotactic Polypropylene (iPP)

The structure consists with one side stacking of $–CH_3$ groups in the main chain. Therefore, iPP considers as high energy, semi-crystalline material with better mechanical properties. iPP can be easily produced by the low cost, a conventional production process of Ziegler–Natta catalysis reaction. Therefore, approximately 95% of commercially available polypropylene is iPP [21, 19].

2.2.2 Properties of Polypropylene

Typical properties of the PP are depending on tacticity, molecular weight, and other structural characteristics. Based on the literature, properties of seven samples which used for researches were summarized in Table 2.1.

Table 2.1: Properties of different types of PP at room temperature [22, 23]

Property	Homopolymer			Copolymer			
				Random		Block	
	1	2	3	1	2	1	2
Melt flow index (g/ 10 min)	3.0	0.7	0.2	9.6		9.7	
Softening point (°C)	148	148	148	103.7	108.4	113	119.6
Tensile strength (MPa)	34	30	29	31.9	29.6	27.2	23.0
Elongation at break (%)	350	115	175	700	610	140	200
Impact strength (J)	34	46	46	14.3	20.0	61.9	106.8

2.3 Natural Fibers

The Natural fibers based on the origin are defined as threads or filaments which are produced naturally by flora (lignocellulose), fauna (proteins) or geographical actions (minerals) [24, 25] as mentioned in Figure 2.2. Plant fibers are the most common fiber type use for composite materials due to the high availability and better mechanical properties compared to animal fibers [26].

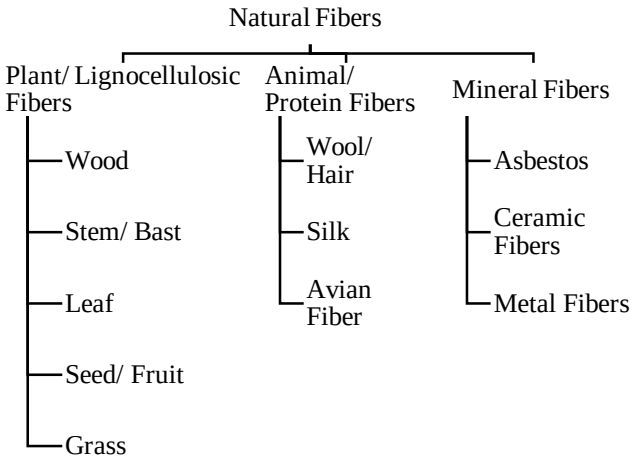

Figure 2.2: Classification of natural fibers according to origin [24, 25]

2.4 Cellulose

Plant lignocellulosic fibers are categorized into three groups; cellulose, hemicellulose and lignin and consist in the plant cell wall [27]. Out of three lignocellulose materials, lignin indicates comparatively low biodegradation, due to the complex three-dimensional polyphenolic structure. The hemicellulose is amorphous, branched, single-chain polysaccharide [28]; however, in respective to cellulose,

hemicellulose has a low degree of polymerization and it leads to obtaining low mechanical properties [29].

In nature, cellulose is a homo-polysaccharide and the most abundant biopolymer present on the earth. Linear, rigid polymer of cellulose consists of glucose subunits which are interconnected by β-1,4-glycosidic bonds and the repeating unit of cellulose is called "cellobiose" (Figure 2.3) [30]. As the result of glycosidic bonds, the axis of cellulose chain is alternately turning by 180 ^{0} [31].

Cellulose is a biodegradable, nontoxic polymer and insoluble in most organic solvents including water. However, cellulose can absorb water less than 14% in presence of 60% of relative humidity at 20 ^{0}C [32].

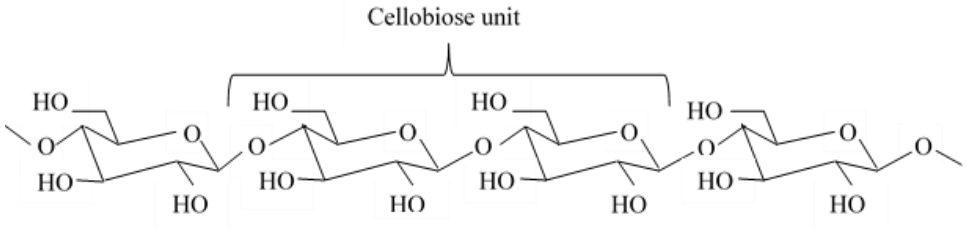

Figure 2.3: Molecular chain structure of cellulose

Source: http://www.namrata.co/category/chemistry-of-carbohydrates/

2.4.1 Sources of Cellulose

Cellulose is mainly extracted from natural plants, other biomass or plant waste materials such as crop and timber residues. In addition, cellulose is present within some bacterial sources (ex: *Acetobacter*, *Achromobacter*, *Pseudomonas* etc.) green algae species (ex: *Valonia*, *Cladophora*) and fungi species (ex: *Dictyostelium discoideum*) [33, 34] Recent researchers have discovered separation of cellulose from tunicates which is the only species that produces cellulose in the animal kingdom [35]. However, the amount of cellulose present in these species is insignificant when compared to plant materials. Except to the natural resources, scientists are focusing on the production of synthetic or man-made cellulose fibers to fill the gap between demand and the supply in the textile industry with the increasing of the world population [36]. Nevertheless, the literature review is focused on the plant waste

materials to reduce the environmental pollution by adding value to a worthless material.

The chemical arrangement of cellulosic fibers in the plant cell wall is quite complicated. Plant cell wall is a naturally occurring composite which has cellulose fibers as reinforcement in lignin-hemicellulose matrix [37]. Out of the total dry weight of hardwood species, cellulose content is approximately 40-50% and hemicellulose and lignin contents are approximately 25-35% and 20-25%, respectively [38]. Table 2.2 illustrates the weight percentages of cellulose with respect to plant sources.

Most of the researches based on cellulose were utilized plant waste to obtain additional value from abundant, priceless materials. Among that, numbers of researches significantly focused on agro waste, for instance, sugarcane bagasse, rice straw, wheat straw, corn stover and denoted lack of attention on forestry wastes.

Table 2.2: Amount of Cellulose present in different plant sources [39, 40]

Plant Source	Amount of Cellulose (wt.%)
Rice straw	28-36
Wheat straw	33-38
Bagasse	35-45
Corn Stover	38-40
Softwood	45-50
Hardwood	40-55
Bamboo	40-55
flax	70-80
Cotton	> 90

2.4.2 Properties of Cellulose

The mechanical properties of cellulose mainly depend on the important parameters of crystallinity, the degree of polymerization and degree of orientation of cellulose fibers to the main axis. These parameters differ from one another on the basis of source of cellulose. Usually, the increase in crystallinity and degree of polymerization lead to obtaining higher tensile strength and modulus. Crystallinity is defined as the portion of a polymer in a regular, ordered state [41]. Therefore, higher crystallinity percentage refers to a great strength or high hardness of a material.

Furthermore, a high degree of polymerization (average number of monomers per molecule) also provides high molecular weight and leads to increase the strength. According to the Table 2.3, algae, bacteria, and animals contain cellulose with good mechanical properties compared to plant cellulose. However, the crystallinity and degree of polymerization are higher; therefore, it increases the melt and glass transition temperatures and indirectly processing and forming become more difficult. Other than that, the separation of cellulose from micro-organisms is not an economical process in relation to yield.

Table 2.3: Degree of polymerization, crystallinity and mechanical properties of cellulose extracted from different sources [42, 43, 44, 45, 46, 47, 48]

Cellulose Source	Crystallinity Range (%)	Degree of Polymerization	Elastic Modulus (GPa)	Tensile Strength (GPa)
Plants	50-80	≈ 925 - 5500	5 - 45	0.2-1
Algae	> 80	26500 - 44 000	130 - 140	-
Bacteria	65-79	2000 - 6000	≈ 114	≈ 2
Animal (Tunicates)	> 85	-	≈ 143	3-6
Man-made Fibers	25-45	300 - 450	1.5 - 2.4	-

Cellulose is non-thermoplastic and non-melting polymer because the decomposition temperature of cellulose exists before the melting point [43]. According to the previous studies cellulose has highly crystalline structure; therefore, softening temperature of cellulose (220-250 ^{0}C) is higher than both hemicellulose and lignin (167-217 ^{0}C and 127-235 ^{0}C, respectively) in the dry state [49]. Additionally, the activation energy for thermal degradation of cellulose is 36-60 kcal/mole while for hemicellulose and lignin calculated as 15–26 kcal/mole and 13–19 kcal/mole respectively [50]. According to the studies, cellulose is the most thermally stable constituent of the lignocellulosic materials. Therefore, cellulose contains many advantages compared to hemicellulose and lignin. Table 2.4 summarized the thermal properties of plant cellulose.

Table 2.4: Thermal properties of plant cellulose [43, 51, 52]

Thermal Property	Value
Decomposition temperature	> 300 °C
Softening point	220 – 250 °C
Ignition point	> 290 °C
Specific heat	1.00 - 1.21 J g^{-1} K^{-1}
Thermal expansion coefficient	1×10^{-7} K^{-1}

When considering the electrical properties, pure dried cellulose is used as an insulating material for many applications. The resistivity of pure dried cellulose at zero relative humidity is measured as 10^{18} Ω cm [43]. However, the electrical conductivity changes with temperature, humidity and ionic impurity content present in the cellulose. At low temperatures presence of moderate humidity, the electrical conductivity of cellulose is nearly 10^{-8} S/cm. When temperature increase above 250 °C, the polarization of cellulose occurs via displacement and rotation of hydroxyl groups present in the cellulose chains. As a result, the conductivity of cellulose rises from 10^{-6} S/cm to 10^{-5} S/cm in temperature between 250 °C to 350 °C. Further application of temperature can reduce the conductivity by splitting the formed polar groups [53]. The characteristics of cellulose polarization process determine the dielectric constant of cellulose and it depends on relative humidity and frequency. At the temperature of 20 °C and frequency 50 Hz, the dielectric constant of oven dried cellulose placed in between 6.0-7.3. At the same temperature and frequency $3x10^{8}$ Hz, the dielectric constant is decreased to 4.9-3.7 [54]. Table 2.5 contains the specific electrical characteristics of plant cellulose.

Table 2.5: Electrical properties of plant cellulose [43, 53, 54, 55]

Electrical Property		Value
Resistivity of pure dry cellulose		10^{18} Ω cm
Insulating value (R-value)		500 kV cm^{-1}
Dielectric constant at	Low frequency	6.0-7.3
	High frequency	4.9-3.7
Dielectric strength		50 V mm^{-1}

2.4.3 Nanocellulose (NC)

Nanocellulose generally defines as a cellulosic material which has one direction as a minimum in nanometer scale [56]. Plant cell wall contains lamella structure of cellulose microfibrils and after separation of the matrix material (mainly hemicellulose and lignin), it is possible to isolate cellulose fibers in the nanometer range. Nanocellulose is popular in food packaging, medical and pharmaceutical, biomedical engineering, paper and paper additives, textiles, cosmetics, paints and coatings due to the natural and nano-dimensional polysaccharide structure. Nanocellulose contains many favorable features than natural cellulose; such as distinctive tensile strength with high stiffness and Young's modulus, high aspect ratio and lightweight [57, 58, 59]. Most of the properties are vary with processing methods, drying methods, surface modification processes of nanocellulose. However, some researchers are attempting to eliminate the disadvantages such as moisture sensitivity, poor compatibility with a hydrophobic polymer matrix and high energy consumption during the production of nanocellulose.

Novel researches of nanocellulose are designed for various applications including sensors [60, 61] and actuators, energy storage devices (ex: solar cells, lithium ion batteries, supercapacitors) [62, 63, 64], electronic devices [65, 66, 67], displays [68] and light-emitting diodes [69]. Naturally, nanocellulose is an electrically resistive material. Electrical, piezoelectrical and magnetostrictive properties can be achieved via modification or improvement of nanocellulose substrate [70]. Therefore, scientists applied different methods, for example, transferring silicon nanomembrane to nanocellulose layer [71], application of polyimide layer to the nanocellulose sheet [72], produce a composite of TEMPO-Oxidized nanocellulose and carbon nanotube [73] to enhance properties of nanocellulose.

Nanocellulose extracted from plant species can be categorized into mainly two types as nanofibrillated cellulose and nanocrystalline cellulose, depending on the preparation method and the structure [74].

2.4.3.1 Nanofibrillated Cellulose (NFC)

NFC consists of a bundle of long chains, flexible cellulose molecules with high aspect ratio [75]. Average diameter is in between 10-100 nm and average length extends 100 nm to several micrometers [76]. NFC is also well known as nanofibrillar cellulose, cellulose nanofibril and cellulose nanofiber [56]. Usually, depending on the quality of raw materials and the homogenous fibrillation process, the difference between the NFC morphology can be changed. Naturally, NFC has three dimensions "Spaghetti" like structure consists of alternating crystalline and amorphous regions [77]. Therefore, NFC can form an entangled network structure and it would lead to increase of the storage modulus.

2.4.3.2 Nanocrystalline Cellulose (NCC)

NCC is a tiny "rod" like shaped cellulose with very narrow flexibility due to the reduced amount of amorphous region [78]. These particles have also been named as cellulose nanocrystals (CNC), rod-like cellulose crystals and nanowhiskers. Compared to NFC, NCC has a very low aspect ratio and flexibility. NCC mainly isolated by strong acid hydrolysis process and the average dimensions of NCC is approximately 5-20 nm in diameter and 100-300 nm in length [79]. Depending on the source of cellulosic material and the hydrolysis conditions, there are considerable differences in the dimensions of the particles and degree of crystallinity. The comparison between general NFC and NCC is given in Table 2.6

Table 2.6: Comparison of properties between NFC and NCC [30, 80, 81, 82]

Property	Nanocellulose	
	NFC	NCC
Length (nm)	≥ 1000	100-500
Aspect ratio	60-100	10-50
Crystallites length (nm)	60-150	70-200
Crystallinity (%)	50-65	72-80
Amorphicity (%)	35-50	20-28
Density (g/cm^3)	1.54-1.56	1.57-1.59
Porosity (cm^3/g)	0.1-0.2	0.01-0.05
Axial modulus (Gpa)	30-40	140-160
Transversal modulus (Gpa)	10-15	15-30
Axial tensile strength (Gpa)	0.8-1	8-10
Transversal tensile strength (Gpa)	≈ 0.1	≈ 1

2.4.4 Isolation of Cellulose from Biomass

The extraction process of nanocellulose includes many pre-treatments and disintegration processes. Plant cell wall consists of the major constituents of cellulose, hemicellulose, and lignin with minor components including resins, proteins, fats, waxes, salts, and other non-volatile hydrocarbons [83]. Therefore, isolation of cellulose explains as separation of cellulose from other extractives together with hemicellulose and lignin. To improve the isolation process, some chemical (ex: steam explosion, liquid hot water treatment, ammonia fiber explosion, CO_2 explosion etc.), physical (ex: chipping, grinding, and milling) and multiple or combine pretreatment methods can be applied to the biomass. The pretreatments can increase the surface area and porosity and help to reduce the energy by 20-30 times as compared with conventional processes [84].

In the steam explosion process, high-pressure steam with temperature 160-260℃ is applied to the biomass. Application of high-pressure steam can modify the plant cell wall and partial hydrolysis of the hemicellulose [85]. Similar as steam explosion process, liquid hot water treatment use water at elevated temperature and pressure [86] and ammonia fiber explosion use liquid anhydrous ammonia under elevated pressure and moderate temperature (60-100℃) [87]. When compared to steam and water explosion methods, ammonia fiber explosion method needs less energy. Therefore, the process is cost-effective. CO_2 explosion is also same as steam explosion and high pressured CO_2 used instead of steam. Then CO_2 react with water and produce diluted H_2CO_3 acid and increase the rate of hydrolysis [88].

The physical pretreatment includes chipping, grinding, and milling. The desired outcome of the process is the reduction of particle size to form a material for comfortable handling and to increase surface/volume ratio. The energy requires to break the biomass is depending on the final particle size. Physical pretreatments assign effective by mixing under shear stresses while applying rapid temperature [89]. The major drawbacks of physical pretreatment methods are high energy consumption and cost (capital and operating cost).

The original or pretreated biomass is then subjected to separation of cellulose. The process can be divided into two as biological and chemical isolations.

2.4.4.1 Biological

Enzymatic treatment is an inexpensive, biological, environmentally friendly process which does not produce harmful waste. When enzymes are used, the main task is the removal of lignin and hemicellulose while surviving the cellulose. As an advantage, enzymes have a selective degradation of specific components. Therefore, other reactions are restricted and provide desired results [90]. However, the time-consuming process of enzymatic treatment needs different types of enzymes to digest different organic compounds. As an example, lignin is mainly degraded by lignin peroxidase (ligninase) and manganese peroxidase (laccase) enzymes produced by white rot basidiomycetes species [91]. Analogous to ligninase, cellulase enzymes have favor reaction on the amorphous region of cellulosic matter. Due to the digestion of cellulose, the method is worthy to separate microfibirllated cellulose [92].

2.4.4.2 Chemical

According to early studies, various chemical methods used to separate cellulose and among them acid-alkaline hydrolysis, ionic liquids, organic solvents and chemical pulping processes are the most common.

a) Acid and alkaline hydrolysis

Concentrated acids (ex: H_2SO_4, HCl) [93], diluted acids (ex: H_2SO_4, H_3PO_4) [94] and bases (ex: NaOH, $Ca(OH)_2$) [95] have been widely used for treat lignocellulosic materials, because they are powerful agents for cellulose hydrolysis. According to the mechanism, H_3O^+ or hydronium ions attack the intermolecular and intramolecular bonds among lignocellulose and as a result, the separation is taken place [77]. Alkali treatment causes degradation of ester and glycosidic side chains resulting in structural alteration of lignin. Acid hydrolysis process has the ability to hydrolyze especially hemicellulose into simple sugar [96]. Therefore, conduct the

acid treatment after the alkaline treatment produces pure cellulose. However, the hydrolysis process is hazardous and toxic. Consequently, careful handling and practice are needed.

b) Ionic liquids

A better solubility of cellulose within ionic liquids (ILs) was found in the early nineties. The development of wood related researches via ILs was improved due to the interesting properties of extracted cellulose; essentially, the chemical and thermal stability. ILs such as 1-butyl-3-methylimidazolium chloride (BMIMCl) and 1-allyl-3-methylimidazolium chloride (AMIMCl) has an ability to dissolve only polysaccharides present in the cellulosic matter by the formation of hydrogen bonds between chloride ions in IL and hydroxyl groups of cellulose [97]. Then the dissolved cellulose separate from the medium and re-precipitated to obtain cellulose. By the addition of ethanol, acetone or water, easily separate cellulose dissolved in the BMIMCl medium [98]. However, reproduced cellulose has a low degree of polymerization such as 50% - 75% and low crystallinity compared to natural cellulose [99]. The main limitations of the process are the high costs of chemicals, time-consumption, and toxicity of some ILs [100].

.

c) Organic solvents

Organic solvents can solubilize lignin and some hemicellulose under tempered conditions by acting as dissolving agents. The reaction is starting by the hydroxyl groups present in the solvents. These OH^- ions break the ether linkage of lignin and minor glycosidic linkage of hemicellulose [101]. Therefore, the method is a selective pretreatment method for lignin extraction and the used organic solvent can be recycled and reused. In practical situations, low boiling point solutions (such as ethanol, methanol, ethyl acetate and acetone) are used as solvents [102]. However, to obtain clean and pure results, washing should be done continuously after the reaction. Additionally, most of the solvents are highly toxic and consume a large amount of energy to recover [100].

d) Chemical pulping

The chemical pulping method converts wood chips or biomass into cellulose fibers by breaking the bonds between lignocellulose. In the process, biomass is reacting with a hot mixture of sodium hydroxide and sodium sulfide under pressure [103]. The term used for the process in the paper industry is "Kraft pulping" and usually used the method of removal of lignin and hemicellulose. Subsequently, the product is bleaching with oxidizing agents such as $NaClO_2$ to solubilize residual lignin. The bleaching process is designated as oxidative delignification and $NaClO_2$, Cl_2, NaOCl, hydrogen peroxide, ozone and peracetic acid used as common bleaching agents [104].

2.4.5 Conversion of Cellulose to Nanofibrillated cellulose

After isolation of cellulose from the biomass, the next step is to convert of cellulose into nanocellulose. The texture of the final result can be either NFC, NCC or mixture depends on the conditions applied during the process (Figure 2.4). In order to obtain uniform size and aspect ratio, a reliable recipe with exact conditions should be used. If not, the final outcome may be the reducing sugar and other unwanted byproducts [105].

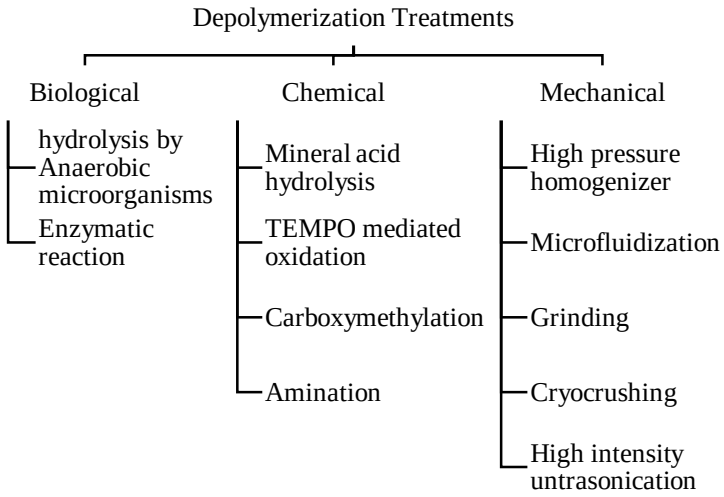

Figure 2.4: Depolymerization methods of cellulose [106, 77]

2.4.5.1 Biological

A biological method of controlled hydrolysis by anaerobic microorganisms is one of the novel methods used to isolate nanocellulose [107]. The process is essential for biomedical applications due to the less use of chemicals and biocompatibility. However, the method is a time consuming and low yielding process. The other method of enzymatic reaction produces nanocellulose with the absence of damages to the cellulose chain [108]. Nevertheless, the method also a prolonged process and better to conduct another mechanical treatment process after enzymatic treatment to improve the yield.

2.4.5.2 Chemical

Chemical methods are well-known nanocellulose isolation techniques due to low energy consumption. The mineral acid process is related to the cleavage of β-1,4-glycosidic bonds in cellulose chains by the action of hydrolysis. The frequently used mineral acids are sulfuric [109, 110] and hydrochloric [111]. The acid easily attacks to loosely packed areas of cellulose chain. Therefore, amorphous regions are more favorable for hydrolysis process and ultimately produce nanocrystalline cellulose. In the TEMPO (2,2,6,6-tetramethylpiperidinyl-1-oxyl) oxidation process, hydroxyl groups in the cellulose converted to carboxylate groups by TEMPO radicals. As a result, surfaces of cellulose fibers lead to improving hydrophilicity. Then the developed surface negative charge can form repulsive forces between cellulose fibers and these forces tend to separate nanofibers [112]. Same as TEMPO oxidation, repulsive forces generate between fibers in carboxymethylation and amination processes due to the replacement of hydroxyl group of cellulose by carboxymethyl [113] and amine [114] groups respectively. However, these processes (except amination) will be produced nanocellulose with negatively modified surfaces. Therefore, the nanocellulose formed by these methods is hydrophilic and unable to mix with hydrophobic thermoplastic polymers.

2.4.5.3 Mechanical

Mechanical treatments are the most commonly used technique for depolymerization of native cellulose into nanofibrillated cellulose. However, the methods consume a high amount of energy; therefore, cellulose separated via chemical methods is preferred for the mechanical depolymerization treatments to reduce the heavy-duty processing [115]. The mechanical isolation of NFC is subcategorized into different methods.

a) High-pressure homogenization

The process consists of transferring cellulose slurry through a tiny nozzle under high pressure. Due to the shear and impact forces applying to the slurry; the defibrillation of cellulose fiber is taken place [116]. Many kinds of research were based on the production of nanocellulose by high-pressure homogenization using deferent raw materials such as sugarcane bagasse [117], sugar beet [118] and skin of prickly pear [119]. The main advantages of the process are efficiency and inessential of organic solvents. However, a blockage may occur because of the very small size of the orifice. Pretreatments are necessary to overcome the problem; especially mechanical methods.

b) Microfluidization

Both homogenization and microfluidization processes are utilized high-pressure energy as the driving force; although, both have distinguishable characteristics. In compared to homogenization, microfluidization required less energy to produce NFC and the pressure applies to cellulose suspensions to passes through a chamber [120]. As a benefit, the process leads to produce NFC with thin and uniform sized nanoparticles and the yield may improve by the combination of one or more pretreatments. In addition, the degree of fibrillation can be increased by repeated application with different sizes of chambers [121].

c) Grinding

The grinding equipment consists of two static and rotating stones. The pulp is passing through the two stone and fibrillation occurs due to the impact and shear

forces [122]. Even though the process is used as a pretreatment of biomass, the conditions applied to NFC preparation are different. Additionally, depending on the applied condition, cellulose can be converted into NFC or NCC. There are two main structures of NFC; twisted and untwisted. The extension of grinding time leads to convert untwisted nanofiber into nanowhiskers with high crystallinity [123].

d) Cryocrushing

In the Cryocrushing process, the cellulose fibers are froze using liquid nitrogen and then shear forces are applied by motor and pestle to break the fibers [106]. The rupturing occurs as a result of the pressure exerted by the ice crystals. The process can also be used as a pretreatment before the homogenization process and apply for a different cellulosic matter such as agricultural crops and by-products. However, cryocrushing method is produced low yield and not economically feasible due to the high energy consumption [82].

e) High-intensity Ultrasonication

The extracted cellulose initially immerses in an aqueous medium and then applies ultrasonic waves. It the beginning, water molecules absorb ultrasonic energy and pass the energy to microscopic gas bubble present inside the cellulose particles. Then the gas bubbles form cavities and they expand to maximum and ultimately explode. The defibrillation occurs as the reaction of hydrodynamic forces generated by ultrasound in the cellulose pulp [82]. In the high-intensity ultrasonication process yields 100% in 25 min and grinding process yields 90% in 40 min. Therefore ultrasonication is more efficient than grinding [124].

2.4.6 Drying of NFC

The drying process is one of the important steps for NFC, to develop natural fiber reinforced thermoplastic composite with better mechanical properties. Furthermore, drying can improve the handling and reduce the transportation cost for aqueous medium. There are two types of material properties; thermal stability and

crystallinity are considered to be critical in the dry process [125]. Cellulose has better thermal stability and crystallinity in respective to hemicellulose and lignin. Therefore, these advanced characteristics should be maintained or improved during the drying. If not, irreversible agglomeration will occur and reduce the properties of NFC due to the affection of nanoparticles dimensions [126].

The agglomeration can be formed within two situations. The agglomeration occurs during compounding can be reduced by surface modification of hydrophilic cellulose in to hydrophobic. In addition, another agglomeration was identified during the drying period and the process is irreversible [127]. During the drying of NFC, water molecules eliminate from the system and as a result of that high-intensity, bonding forces arise between fibers. Therefore, hydrogen bonds formed by water would break and again create strong hydrogen bonds by hydroxyl groups present in the NFC surface [128]. Hence, formed agglomerated cellulose cannot break by adding water because the agglomeration arises during drying called an irreversible process. There are mainly four types of dry methods used for NFC and the features of the methods are discussed in Table 2.7.

Table 2.7: Comparison of Different drying method of NFC [125, 129, 130]

Drying Method	Advantages	Disadvantages
Oven Drying	Simple and low cost	Produce thermally unstable NFC and unable to control nano-scale dimensions due to the formation of bulks
Supercritical drying	Effective for large-scale productions	Complex and expensive method
Freeze Drying	Tend to retain the quality, shape, and size of NFC	Expensive and create agglomeration
Spray Drying	The low labor and maintenance cost	Low rate of efficiency (due to the requirement of low solid content)

Structural properties of the NFC particles changes with the drying method used. Except for the spray drying method, other methods tend to form nano-agglomerates and act as a barrier for uniform distribution of NFC in the fabrication process of nanocomposite materials. Moreover, spray drying method can obstruct the irreversible agglomeration phenomenon [127]. Therefore, out of the four main drying

methods, spray drying method is identified as the best technically suitable process for NFC [129].

2.4.7 Characterization of NFC

Properties of the extracted nanoparticles should be analyzed to examine the quality of the processes used to isolate NFC. Basic properties must be identified before processing and characterization methods of NFC are specified in table 2.8.

Table 2.8: Properties of fibrillated celluloses and characterization methods [131, 132, 133]

Property	Characterization method/ Instrument
Appearance, dimensions and aspect ratio	Scanning electron microscope (SEM), Transmission electron microscope (TEM), atomic force microscopes (AFM)
Chemical properties	Fourier Transform Infrared Spectroscopy (FTIR), Conductometric titration
Thermal	Thermal gravimetric analyzer (TGA), Differential scanning calorimetry (DSC), Differential thermal analysis (DTA)
Crystallinity (%)	X-ray diffraction (XRD)
Purity (%)	High-performance liquid chromatography (HPLC), SEM, TEM, AFM

Microscopic analysis is the most valuable characterization method because the microscopic images can be used to identify the basic information of the samples such as appearance, dimensions, homogeneity, and purity. Generally, NFC forms a porous network with fiber diameter less than 100 nm and length more than 100 nm. Therefore, nanoparticles with high aspect ratio are better for use as reinforcement for polymeric matrices. However, depending on the drying method, morphological properties of NFC change. The average NFC diameters oven dried, supercritical dried and freeze-dried processes are in between 50 - 300 nm [134], about 100 nm [135] and in between 100 - 200 nm respectively [129].

FTIR analysis widely used to identify chemical bonds of materials. Table 2.9 contains the characteristic FTIR absorption peaks of cellulose. Theoretically, there is no difference between chemical bonds present in cellulose and nanocellulose. Therefore, FTIR spectroscopy peaks of both neat materials should be same. However, due to the difference between crystallinity of cellulose and nanocellulose,

peaks intensities of spectra are different. When compared with FTIR spectra of cellulose and cellulose with a high percentage of amorphous regions such as nanofibrillated cellulose, indicates sharper and less intensity peak with high wave numbers due to the reduction of inter and intramolecular hydrogen bonds [136]. Moreover, the water holding capacity of nanocellulose (12.75 g water/g) is higher than cellulose (8.9 g water/g); due to the high surface area [137]. Therefore, intensity improvement slightly exhibits in cellulose and significantly improves in NCC. The NFC exists in the middle of the two values.

Table 2.9: Characteristic absorption bands of functional groups present in the cellulose [137, 138, 139]

Functional group	Compound		Wave number (cm^{-1})
O-H	Stretching vibrations of methanol		3200-2500
	Stretching vibrations, attached to pyranose ring		3500-3200
C-O	C-OH	$-CH_2OH$ (primary)	1025-1050
		Attached to pyranose ring (secondary)	1040-1060
	C-O-C	Within pyranose ring	1170-1025
		Glycosidic linkage	≈ 900
C-H	Aliphatic stretching		≈ 2900
	Within pyranose ring		≈ 1366

2.4.8 Surface Modification of NFC

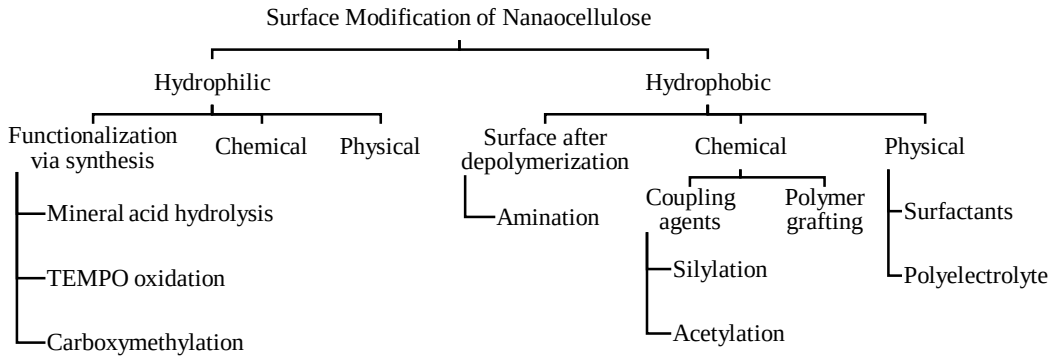

Figure 2.5: Classification of Surface Modification Methods of Nanocellulose

The ultimate goal of the isolated NFC is to produce a nanocomposite material with better mechanical and environmental performances. Therefore, reinforcing NFC should compatible with the matrix material. Cellulose is hydrophilic in nature and most of the thermoplastic matrix materials (ex: polyethylene, polypropylene) are nonpolar [140]. Therefore, the serious issues may form during the production of the nanocomposites such as dispersion difficulties of NFC in the matrix due to incompatible nature [141], poor interfacial adhesion between NFC and matrix materials [58] and low resistance for moisture. Hence, the surface modification of NFC is required to overcome the problems. Furthermore, the modification should not harm the structure of the cellulose and should improve or maintain the qualities of NFC. Therefore, the literature review is only focused on hydrophobic surface modification nanocellulose.

The surface modification processes can be classified as functionalization via synthesis, chemical surface modification (ex: coupling agents and polymer grafting) and physical surface modification (ex: coating of surfactants and polyelectrolytes) [142, 143] as mentioned in Figure 2.5. The functionalization via synthesis explains the indirect surface modification during the defibrillation or nanocellulose extraction process. However, most of the time hydrophilicity of nanocellulose surfaces is improved by the chemical depolymerization treatments. To improve the surface modification, scientists are applied multiple modification methods to nanocellulose. After the surface modification process NFC can be dried using the same drying methods (oven drying, supercritical drying, freeze drying and spray drying) and use for further processing. Additionally, some surface modifications can be carried out during the fabrication of the nanocomposite, such as melt processing.

2.4.8.1 Chemical surface modification

The process used chemical compounds to convert the native hydrophilic surface of cellulose nanofibers to hydrophobic [140]. There are different chemical modification methods; however, the review covers the methods used to produce nonpolar NFC surfaces after the modification because the ultimate target of the surface modification is to produce a nanocomposite with a nonpolar synthetic matrix. The most common

chemical surface modification methods are coupling agents (derivatization) and polymer grafting.

Coupling agents define as the minor quantities of chemical compounds which can attach two different materials together by creates bonds between the two surfaces [144]. Coupling agents are subcategorized as organic, inorganic and organic-inorganic depending on the chemical composition of the compound [145]. There are more than forty coupling agents are used in the industry and among them silylation and acetylation methods are the most common coupling methods used to combine NFC and nonpolar matrixes.

2.4.8.1.1 Silylation

Generally, silylation is the attachment of silyl group (-SiR_3) to host molecular surface by removing hydrogen atoms bonded to hetero atoms such as –OH, =NH, –SH [146]. Therefore, silylation process converts the hydrophilic surface of NFC in to hydrophobic by attaching silyl groups to the –OH groups in the cellulose at elevated temperature with the presence of water [103]. A wide variety of reagents are available with silyl groups; therefore, the reactivity, conditions, and byproducts are depending on the derivative groups attach to the reagent. Significant literature is available to assist the researcher in the selection of preferred reagent for the particular compounds and chlorosilanes and silazanes are the most frequently used silyl reagents for cellulose [147].

In general, silylation process with natural fibers contains four steps. They are hydrolysis, self-condensation, adsorption and chemically grafting (Figure 2.6). Initially, silane monomers are hydrolyzed and form Si-OH oligomer. The self-condensation reaction occurs through the hydroxyl groups present in the oligomers react with another oligomer and form Si-O-Si bonds. If the reaction is not controlled, it can form bulk molecules. Therefore, by adjusting pH of the medium could produce effective oligomers to react with natural fibers. The physical adsorption is formed by reactive monomers or oligomers and creates hydrogen bonds with hydroxyl groups in fiber surface. The chemically grafting occurs under elevated temperature. The formed hydrogen bonds are converted to Si-O-C bonds by removing water molecules

[148, 149]. Silylation process can further enhance the storage modulus of fiber reinforced composites [150].

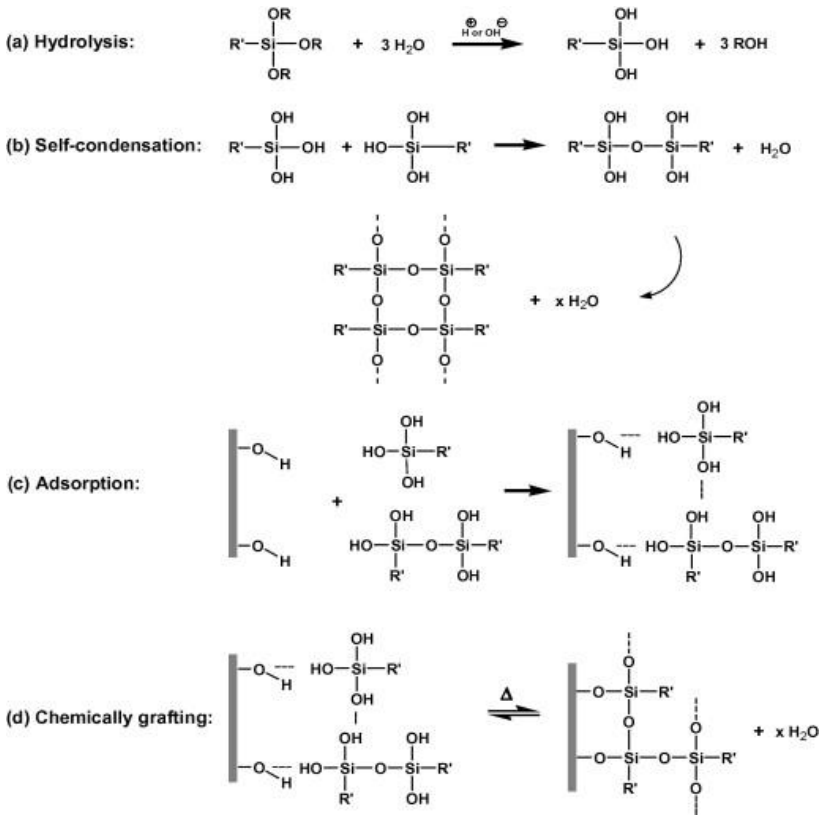

Figure 2.6: Interaction of silane with natural fibers by hydrolysis process *[148]*
Source: https://www.sciencedirect.com/science/article/pii/S1359835X10000850

The surface modification of microfibrillated cellulose by the silylation (chlorodimethyl isopropylsilane (CDMIPS)) results in the degree of surface substitution in between 0.6 and 1. Therefore, better dispersion of the fibrillated cellulose with non-flocculating manner can be obtained in the nonpolar medium. However, an excess of CDMIPS can partially dissolve fibrillated cellulose and as a result, the degree of surface substitution and the characteristics of the fibrillary structure are degraded [151]. As an advantage, the thermal stability of the NFC after the silylation process exhibit better enhancement.

Silylated NFC can be characterized using FTIR analysis. The characteristic Si-O bond has both symmetric and asymmetric stretching bands. The Si-O-Si band exists

in between 800 cm^{-1} – 690 cm^{-1} and both Si-O-C and Si-O-H bands are in between 930 cm^{-1} – 800 cm^{-1} [152, 153]. During the modification, hydroxyl groups present in the surface of the cellulose react and form Si-O-C bonds. Therefore, reduction of O-H stretching vibration intensity band between 3500 cm^{-1} – 3200 cm^{-1} indicates the success of surface modification. However, the samples should be dehydrated. If not O-H stretching vibrations of absorbed water (3400 cm^{-1} –3300 cm^{-1}) will provide incorrect measurements. Infrequently, small peaks present around 850 cm^{-1} and 765 cm^{-1} indicate the gathering of silane groups on cellulose (Si-C). Except to these characteristic peaks of silylation process, some other peaks may occur in the spectrum and those indicate the different functional groups present in the silane agent [154].

2.4.8.1.2 Acetylation

Esterification process of acetylation is frequently used method for nanocellulose and converts hydroxyl groups present in the surface of NFC to ester groups [155]. For the acetylation process, acetic anhydride is used as the main reagent. In addition, acetylation solution consists of toluene and a small amount of catalyst such as sulfuric or perchloric acid [44, 156]. The toluene is acting as a diluent which assists acetylated chain to remain insoluble in the medium. The degree of substitution is occurred in between 0.4-0.5 and the result is depending on the reaction time and temperature.

There are main three FTIR characteristic peaks for acetylation process. Those bands are present in between 1740 cm^{-1} – 1750 cm^{-1}, 1368 cm^{-1}, and 1230 cm^{-1} – 1240 cm^{-1} respectively to the C=O carbonyl stretching vibrations, C-H bending vibrations in –O(C=O)-CH_3 and C-O stretching vibrations of acetyl groups [157]. The intensities of the characteristic peaks are increased with time while an O-H stretching vibration of cellulose (3500 cm^{-1} – 3200 cm^{-1}) peak is decreased. Therefore, the results indicate the improvement of acetylation on the cellulose surface [158].

2.4.8.1.3 Graft copolymerization

Graft copolymerization is another chemical surface modification process which forms segmented polymers consisting with main polymer backbone and covalently bonded branched polymer with another composition [159]. The method can be categorized as homogeneous and heterogeneous according to the grafting medium used as well as depending on the attachment type of the polymer chain, the method can be classified as grafting from, grafting to and grafting through [160]. There are several mechanisms used to initiate the polymerization such as free radical polymerization [161, 162], controlled radical polymerization [163, 164] and coupling chemistries [165]. The Surface of the cellulose can be hydrophilic or hydrophobic depending on the monomer grafted. Hence, styrene, methyl methacrylate, acrylonitrile, butadiene, isobutyl vinyl ether, vinyl acetate etc. can be grafted onto the surface of cellulose to gain hydrophobic characteristics [159]. The commonly used grafting agent is maleic anhydride and the nonpolar synthetic polymers grafted maleic anhydride (ex: maleic anhydride polypropylene (MAPP/MAHgPP), ethylene/maleic anhydride (EMA) and styrene/maleic anhydride (SMA)). The copolymers indicate improved bonding properties and fiber dispersion within the matrix material [166].

2.4.8.2 Physical surface modification

Physical absorption of molecules onto nanocellulose surface is easy and more controllable process compared to chemical surface modifications. There are mainly two subcategories; surfactants and polyelectrolytes. However, physical surface modification methods are not highly effective for production of composites due to insufficient covalent bonding between reinforcement and the matrix [10]. Therefore, for composites, chemical surface modifications (notably derivatization methods) are more effective to modify the surface properties such as hydrophilicity, polarity, and density of nanocellulose [142].

2.4.8.2.1 Surfactants

Surfactants or surface active agents are the chemical compounds used to reduce surface tension. The structure of the surfactant contains hydrophilic head and hydrophobic tail [167]. If further applied the chemistry of the surfactant to the composite of nanocellulose and synthetic nonpolar matrix, the hydrophilic head groups of surfactant adsorb on to the nanocellulose surface while hydrophobic tails are extended into nonpolar matrix phase. Surfactants can be classified into four groups as cationic, anionic, nonionic and amphoteric (or zwitterionic) depending on the polarity of the head groups [168]. Most of the time anionic and nonionic surfactants are used for the surface modification of nanocellulose for nonpolar matrixes [169]. Among anionic surfactants, Alkyl sulfates, alkyl ethoxylate sulfates, and carboxylates are frequently used as well as sorbitan monostearate [170], polyoxyethylene(10)nonylphenyl ether [171] are used as nonionic surfactants for the surface modification of cellulose.

2.4.8.2.2 Polyelectrolytes

The polyelectrolyte is defined as homopolymer with several charged particles. Depends on the charge, the polyelectrolyte can be cationic or anionic. The addition of polyelectrolyte into a medium, the charged particles can attach to the opposite charges and adsorb to substrates [172]. The adsorption strongly affects to the wetting property of nanocellulose. Therefore, the method is frequently applied in pulp and paper industry and cationic polyelectrolytes such as polyacrylamides and polyethyleneimine [173]. However, Researchers have found, lignosulfonate is one of the best polyelectrolytes which can be used to improve the hydrophobicity of cellulose more than cationic polyacrylamide [174].

2.5 NFC reinforced polymer composites

To reduce environmental pollution, polymer-based researches can be done within two areas such as the production of bio-based completely biodegradable composites and production of synthetic based biodegradable composite materials. Therefore, extracted NFC can blend with another biopolymer or with a synthetic polymer. Bio-

based composites are produced by reinforcing NFC dominantly with natural, thermoplastic polylactic acid (PLA) [175, 176, 177] and starch [178, 179, 180]. In addition, biocomposites were produced by reinforcing nanocellulose in polyhydroxyalkanoate (PHA) [181], polyhydroxybutyrate (PHB) [182] and poly(3-hydroxybutyrate-co-3-hydroxyvalerate) (PHBV) [183] matrices produced by microorganisms. Nevertheless, the review is focused only on the production of NFC reinforced synthetic polymer composites.

Table 2.10: Modified nanofibrillated cellulose and microfibrillated cellulose (MFC) reinforcing various matrices for plastic composites

Type	Surface Modification/ Processing Aid	Matrix	Best Reinforcement (wt. %)	Processing Method	Ref.
NFC	MAPP	PP	6	Melt Processing (twin screw extruder)	[184]
	Anhydride modified HDPE	PP	2	Melt Processing (twin screw extruder)	[185]
	MAPP	PP/PC	1	Melt Processing (twin screw extruder)	[186]
	Silylation	PS	10	Melt Processing (twin screw extruder)	[149]
	PVA	PE	5	Melt Processing -injection molding	[187]
	MALDPE	LDPE/ Starch	6	Melt Processing -single screw extruder	[188]
	polyaniline	TPU	4	Melt Processing - screw extruder	[189]
MFC	Surfactant and MAPP	PP	10	Melt Processing - screw extruder	[171]
	Acetylation	PP	5	Melt Processing - screw extruder	[190]

Many synthetic thermoplastics are used in different industries. Among them, the most common types are polyethylene (PE), polypropylene (PP), polystyrene (PS) and some types of polyurethanes (PU). When producing NFC reinforced synthetic polymer composites, the natural hydrophilic surface of NFC should be changed to hydrophobic, if the matrix or reinforcing fibers are in different polarities. The table 2.10 contains different mixing ratios of fibrillated cellulose and synthetic thermoplastics as reinforcement and matrices respectively. Selecting the best weight

percentage range of reinforcement is very important because the low amount of reinforcement is not sufficient to obtain expected properties and an excessive amount of reinforcement may induce self-aggregation during the mixing. Therefore, according to the past studies, the best range of NFC as the reinforcement of the thermoplastic synthetic nanocomposite is less than 10% by weight.

2.5.1 Fabrication methods of Nanocomposite

Methods applied to the manufacturing process of nanocomposites can be classified into five approaches such as solvent processing, melt processing, electrospinning, in-situ polymerization and layer by layer assembly [191]. The early studies illustrated on the effect of processing approach to the ultimate properties of nanocellulose based composites. Among five methods, solvent processing and melt compounding are the most common methods used for fabrication of nanofibrillated cellulose reinforced nanocomposites. Unfortunately, only a few studies were reported on the electrospinning [192] and in-situ polymerization [193] methods for processing of nanocellulose reinforced nonpolar matrices nanocomposite due to the complexity of the processes. The layer-by-layer method or multilayer films method is used for the production of nanocomposites with polar matrices [194].

2.5.1.1 Solvent Processing

The wet process of solvent processing (or solvent intercalation/ solvent casting/ solution mixing) is defined as stabilization of polymer matrix in a solvent (such as toluene, chloroform, and dichloromethane) and homogeneously dispersion of the reinforcement (nanofillers) within the solvent [195]. Initially, nanofiller are allowed to agitate in the solvent within a certain temperature for a specific time period. To improve the dispersion, ultrasonication and less amount of selected surfactant can be added to the medium [196]. Then the matrix polymer (which is totally soluble in the solvent) is added and applied homogeneous mixing at a specific temperature. After that, the solvent is evaporated and the composite is placed for casting process [197]. The method is commonly used for nanocellulose reinforced composites because heavy duty equipment is not necessary; therefore, fewer amounts of capital cost and energy required as well as it produces good mechanical property materials with less

structural damages. However, the method produces low mechanical property materials due to the incomplete evaporation of solvent as well as not economically or industrially effective because of some limitations in the selection of polymer matrices. If further reveal, the matrix material is annon-water soluble polymer, an additional challenge would be added to the dispersion of nanocellulose in the selected solvent [142].

2.5.1.2 Melt Processing

The melt processing is the mixing or blending of a polymer matrix and nanofiller in the molten state of matrix material under high shear rate. Then the formed nanocomposite is subjected to extrusion or injection molding to obtain the final shape [198]. The process is more compatible and economical for industrial scale process because produced nanocomposite can be easily fabricated via molding. Compared to solvent processing method, melt processing method is more environmentally friendly due to less use of hazard chemicals [142]. During the processing of the nanocomposite, some researches are used extruders with a specially designed feeder to add the powdered form of NFC [199]. However, all types of extruders are not contained the special feeder. Therefore, some difficulties exit when feeding of NFC to the extruder and to obtain a uniform dispersion of NFC in the matrix because NFC is in a powder form and particles are lighter in weight. Furthermore, low amount of NFC is added as the reinforcement to achieve better properties in the nanocomposite. Therefore, to overcome the difficulties, NFC can be initially mixed with less amount of selected solvent and feed into the extruder after complete drying [200].

2.5.1.3 Electrospinning

In the electrospinning method, an electrostatic force is used to extrude a positively charged polymer solution. Therefore, the method is also called as electrostatic fiber spinning and due to the electrostatic force, fibers can be produced with a diameter ranging from few micrometers to nanometers [192]. However, dispersion of NFC within the matrix is difficult than solvent processing method due to numerous

concurrent phenomena generate during spinning. Addition of surfactants can improve the dispersion of nanocellulose. Selection of a suitable solvent (to dissolve the matrix and disperse the nanocellulose) and processing under the melting state are the major parameters of the process. Moreover, acetone, dichloromethane, and Tetrahydrofuran are frequently used as a solvent for nanocellulose based composites [200, 201].

2.5.1.4 In-situ Polymerization

Application of specific conditions for monomers to polymerize in the presence of nanofillers is defined as in-situ polymerization. Nanofillers are dispersed in a monomer solution and begin the polymerization by application of suitable initiator (such as heat, catalyst, and radiation) [195]. According to the previous studies, IR absorption bands of the nanocomposite were overlapped with the bands of the pure matrix and reinforced nanocellulose. Therefore, it can be concluded that the polymerization of the matrix material occurs on the surface of nanocellulose. The method has an ability to manufacture nanocomposites with uniformly dispersed nanoparticles. However, it is difficult to control the agglomeration during the processing. Based on the SEM and TEM analysis of polyaniline/ nanocellulose nanocomposite, agglomerations in some areas were identified because of the high percentage of monomer cause more intensive polymerization [202].

2.5.2 Bonding mechanism of NFC and matrix

During the fabrication process, surface modified NFC is compounded together with matrix molecules by different bonding mechanisms. The bonding mechanisms are determined by the NFC surface modification methods, additives, and conditions applied to the fabrication process [26]. Among all surface modification methods of NFC (hydrophilic to hydrophobic), the most common, simple and effective modification methods are silylation, acetylation and graft copolymerization (using MAPP).

2.5.2.1 Interfacial adhesion – NFC modified by the silylation process

In the fabrication process, radical molecules can be formed due to thermal degradation during mixing and compression molding. As a result of the reaction (Figure 2.7), chemical bonds are formed between the matrix and modified fibers and it leads to accelerates the interfacial adhesion [203].

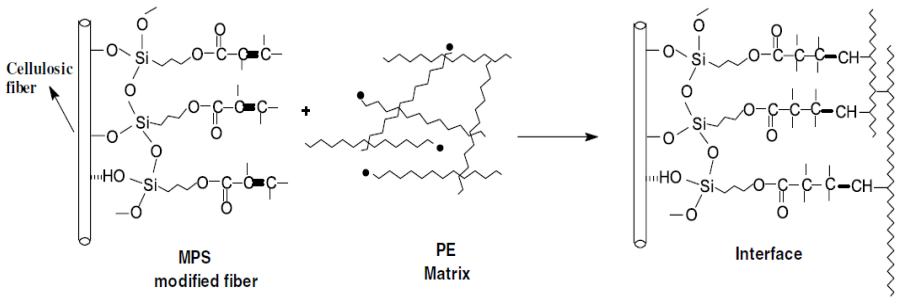

Figure 2.7: Schematic illustration of the interfacial zone in LDPE-based composites containing modified cellulose fibers [203]

To improve the efficiency of the reaction, peroxide initiators (R-O-O-R) such as benzoyl peroxide and dicumyl peroxide can be used. The peroxide initiators form oxy radicals at high temperature and the radicals react with both thermoplastic main chain and silane agent (vinyl silane) and produce vinyl radicals (Figure 2.8). The formed vinyl radical then attack to the other molecules in the same manner to propagate the free radical reaction or can combine with the thermoplastic matrix to improve the interfacial adhesion [148].

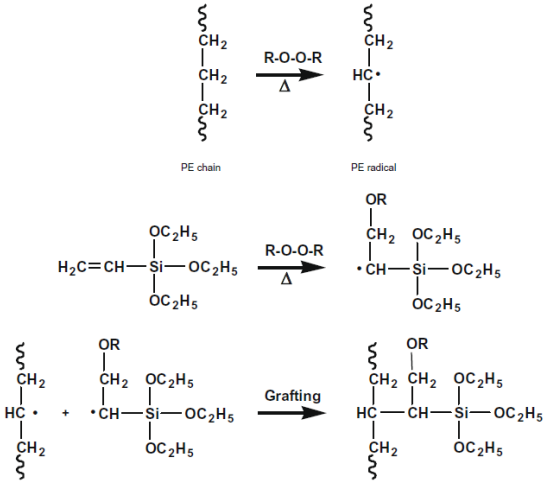

Figure 2.8: Radical grafting of vinylsilane onto polyethylene matrix [148]

2.5.2.2 Interfacial adhesion – NFC modified by MAPP

Maleic anhydride grafted polypropylene (MAPP/ MAHgPP) surface modifier can improve the interfacial adhesion by acting as a compatibilizer between polar NFC and nonpolar matrix material. According to the Figure 2.9, polypropylene chain of MAPP is diffused into the matrix (especially PP) by creating interchain entanglements. The maleic anhydride present in the modified NFC surface can be created both ester bonds (chemical) and hydrogen bonds (physical) with the matrix molecules. Therefore, MAPP modified NFC can form better adhesion between fiber and the matrix [204].

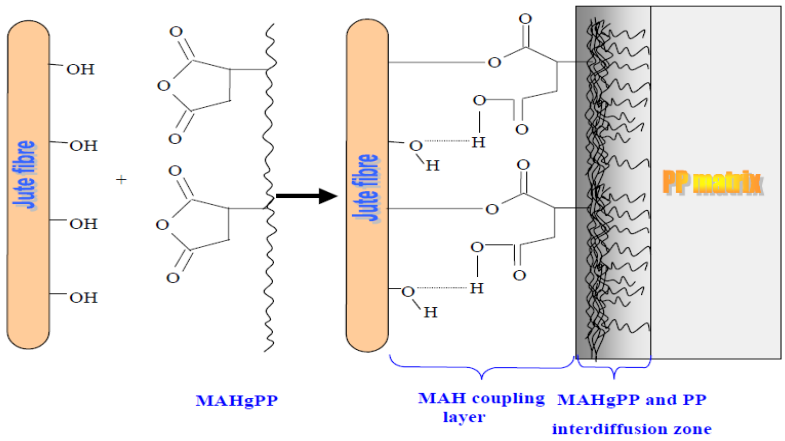

Figure 2.9: Schematic illustration of the interfacial adhesion between PP matrix MAHgPP and cellulose fibers [204]

Source: http://article.sapub.org/10.5923.j.textile.20120106.05.html

2.5.3 Fabrication Parameters of Nanocomposite

When fabricating the nanocomposite, the major components are matrix material, reinforcement, the surface modifier and the other additives. Therefore, the adding ratios of each component have a large affection on the properties of the ultimate product. In general, reinforcement amounts differ from one research to another depending on the matrix, fabrication method and aspect ratio, as well as the amount of the surface modifier, depends on its composition and matrix-filler compatibility. Therefore, selecting the best reinforcement and a surface modifier can be improved the properties of the new composite than the neat matrix material. During the surface modification process, minimal amounts of initiators, inhibitors, antioxidants,

stabilizers, plasticizers and other processing aids should be included to the blends to obtain better performance of the nanocomposite [145].

After selecting the best materials and amounts, the next step is to the formation of "master batch" or all additives optimally dispersed in a highly concentrated material. Then the master batch is diluted with the matrix polymer and extrusion process can be carried out to produce the sample batches. After that, the extruded composite is pelletized and dry before use [185]. Masterbatch preparation is a significant step for researches based on nanocomposites. When compounds are used in mini scale, the solvent processing method could use for fabrication of nanocomposite. However, the melt processing is better to obtain homogeneous samples with uniform thickness. Therefore master batches produce by solvent casting would further process by melt processing [175].

When processing the nanocomposite, the other most important parameters are the applied conditions such as temperature, pressure, time and other instrumental condition for instant rotation speed and fill factor. These are directly influenced to the action of the surface modifier and indirectly change the performance of the composite [205]. Usually, mixing temperature of less than 200 ^{0}C is preferred to avoid the degradation of natural fibers and some thermoplastic matrix material [206]. In addition, the fill factor of the mixing machine should be higher than 0.8 to acquire uniform distribution. Furthermore, both time and rotation speed are influenced on the dispersion of the filler in the matrix and it was reported that the use of the moderate process is the best option to improve the effectiveness [207].

After the mixing, the composite is fabricated using different methods and the thickness of the nanocomposite becomes a more important parameter for many properties. According to the ASTM D3039, the standard test method for tensile properties of polymer composite materials, the thickness of the specimen is recommended to maintain the in-between 1mm and 2 mm for 0^0 and 90^0 unidirectional respectively and 2.5 mm for both balanced systematic and random discontinuous fiber orientation composites. However, the specimen thickness

tolerance specified as ± 4 % of the thickness. Based on the past studies, researchers were used different specimen thicknesses and the values are in between 0.1 – 2.5 mm because of the thickness of a specimen depends on the ultimate application of the produced nanocomposite.

2.5.4 Analysis of nanocomposite

A nanocomposite with optimum properties can be used to produce a new product or replace an existing product with better performance. Variations of rheological, mechanical, water absorption and biodegradable properties of a nanocomposite were studied with various NFC weight percentages (0, 6, 8, 9, 10, 11, 12 and 14) and constant amount of matrix (LDPE/starch) and processing aid (MALDPE). According to the rheological studies, melt flow index (MFI) was decreased slightly from 0 to 10 wt.% of NFC. The outcome may arise due to the improvement of the melt stability by the addition of NFC. Then the MFI values were reduced gradually from 11 to 14 wt.% because the further addition of NFC reduced processability of the nanocomposite. The formation of a chemical and physical interaction between the high amount of hydroxyl groups present in NFC and processing aid lead to caused agglomeration. The tensile properties of the nanocomposites also reduced with an increment of NFC level. Compared to the neat matrix, the tensile strength of 6% NFC was reduced by 23% because the low interaction between NFC and matrix and the ability of NFC to form cracks were improved with the addition of more NFC. However, mechanical properties of nanocomposite with 6% to 10% NFC have slight variation. Noticeably, composites with higher NFC contents are more favorable for water [188].

Another study was done by using the weight amount of both NFC and processing aid (PVA) as variables and matrix (PE) amount as a constant while maintaining the total weight of the nanocomposites as 100 g [187]. In respect to the neat polymer, thermal properties of composites are slightly reduced due to the low thermal stability of PVA. However, mechanical properties of composite unexpectedly increased by 25% with the addition of NFC and PVA up to 5%. In other words, the same percentage of

PVA can enhance the compatibility and load transferring properties of the nanocomposite.

Moreover, it has been investigated under different amount of surface modifier (0%, 0.1%, 0.5% and 1%) and a fixed amount of NFC (2%) and matrix. As a consequence, tensile strength (19.99 MPa) and modulus (1.067 GPa) of nanocomposite reinforced with 0.1% maleic anhydride grafted HDPE modified NFC is better than neat polypropylene (14.45 MPa and 0.570 GPa respectively) [185]. However, depends on the type and the grades of the polypropylene neat values may change. Therefore, another composite of polypropylene reinforced with maleic anhydride grafted polypropylene (2%) modified NFC (6%) has improved properties of tensile strength (32.8 MPa), tensile modulus (1.94 GPa), flexural strength (50.1 MPa), flexural modulus (1.63 GPa) and impact strength (3.8 kJ m^{-2}) with respect to the neat polypropylene (29.5 MPa, 1.43 GPa, 46.9 MPa, 1.35 GPa and 3.1 kJ m^{-2}). The improved percentages of the properties are 36%, 11%, 21%, 7% and 23% respectively [184]. Both types of research are based on same matrix and slightly different NFC modifiers. When comparative to MAHDPE, MAPP has better compatibility with polypropylene matrix. Therefore, improved amount of MAPP grafted NFC reinforcement displays better mechanical properties.

In addition, mechanical properties were compared with neat and silylated NFC reinforced polystyrene under different loadings of NFC (0%, 0.5%, 1%, 5% and 10%) and processing techniques. According to the results, both tensile strength and elastic modulus were improved with increasing NFC loading (10%) under dual heat process. Percentage values of ultimate tensile strength and modulus are approximately two and nine times, respectively higher than the neat polymer with single heat processing. The results imply the dual heat process can be improved linear arrangement of NFC and enhance the load convey properties and compatibility with the matrix [149].

2.5.5 Applications

Recent years, science and technology researches are based on the development of composite materials with enhance properties by utilizing natural waste materials. The main reason is the worldwide plastic production has instance growing and exceeding 300 million tons in the year 2015 includes plastic materials of thermoplastics and polyurethanes, thermosets, adhesives, coatings and sealants [208]. Therefore, nanofibrillated cellulose is a good alternative solution to reduce the use of hazardous petroleum-based synthetic polymers.

Surface modified or non-modified NFC can be used to produce polymer composites with both thermoplastic and thermosetting polymers. Predominantly, the produced NFC reinforced synthetic polymer composite can be used for packaging applications. Since plastic packaging items have a large share in the global plastic market and compare to paper packaging, less amount of plastic can be recycled [209]. In addition, NFC based composites are possible to use for biomedical applications such as dialysis membranes, catheters, containers, surgical meshes and blood bags because of the biodegradability, biocompatibility and rheological characteristics [210].

Contrast to the neat synthetic polymers, NFC reinforced nanocomposites are lighter in weight. Therefore, the product is suitable for automotive, aerospace, construction and also furniture industries. Addition of NFC to the thermoplastic polymers such as PU and PVA can improve the thermal stability of composites. Therefore, the composite has an ability to absorb ultraviolet light with moderate transparency as well as the composite films can be used for future optical applications [211]. Moreover, NFC and synthetic polymer blends are possible to produce new kind of textile fibers and new membranes.

3 MATERIALS AND METHODOLOGY

3.1 Raw materials

100 g of nanofibrillated cellulose and 5 kg of Polypropylene homopolymer (TASNEE PP H4260M) were supplied by the process development center of the University of Maine, USA in the form of a spray-dried powder (CAS Number: 9004-34-6) and by the National Petrochemical Industrialization Marketing Cooperation, Saudi Arabia, respectively (Figure 3.1).

Figure 3.1: Raw materials (a) Nanofibrillated Cellulose (b) Polypropylene

3.1.1 Characterization and analysis of raw materials

3.1.1.1 SEM

Scanning electron microscope or SEM (ZEISS EVO 18 Research) was used to investigate the morphology of NFC. Initially, the NFC powder was sonicated in distilled water for 5 min. Then the film was produced after drying the suspension drop on a graphite plate.

3.1.1.2 FTIR

FTIR spectra of the NFC and PP were obtained by KBr and ATR techniques respectively using BRUKER Alpha-E spectrometer. A total of 24 cumulative scans were taken, with a resolution of 4 cm^{-1}, in absorption mode under the frequency range of 4000-500 cm^{-1}.

3.1.1.3 TGA and DTA

Thermogravimetric analysis (TGA) and differential thermal analysis (DTA) of samples were conducted at the temperature between 25 °C - 600 °C under 10 °C min^{-1} constant heating rate using TA Instruments-SDT Q600 machine.

3.1.1.4 X-ray Diffraction

The X-ray diffraction (XRD) patterns were measured for the raw materials by X-ray diffractometer (BRUKER D8 ADVANCE Eco), using CuK-α. Scattered radiation was detected in the range of $2\theta = 5–80^{\circ}$ with 2 s step time.

3.1.1.5 Ash Content

Ash content of NFC was measured according to the standard test method for ash in biomass (ASTM E1755 – 01) at 575 °C for 3 hours in GALLENKAMP Model 5723 muffle furnace. Four replicates were used to calculate the average ash content.

3.2 Surface modification of NFC

The surface modification of NFC was done by silylation process and Si-69 (Bis [3-(triethoxysilyl)propyl] tetrasulfide) was used as the silane coupling agent. 50 g of NFC was mixed with 1:10 weight ratio of 85% ethanol (500 g) and the mixture was sonicated for 40 minutes. While sonicating, 30 wt.% Si-69 (15 g) was added to another 500 g of ethanol and the mixture was placed 10 min for hydrolysis and silanol formation. After that, the two separate mixtures were added together and again sonicated for 40 min. Afterward, the solution was heated to 70 °C for 2 hours using magnetic stirrer. Then the concentrated solution was transferred to a flat ceramic plate and oven dried for 1 hour at 70 °C. Ultimately, surface modified or silylated NFC was collected after the complete evaporation of ethanol [212].

3.2.1 Characterization and analysis of surface modified NFC

Successfully surface modified NFC was characterized by SEM, FTIR, TGA, DTA and XRD analysis methods.

3.3 Composite Fabrication

Silane-modified and unmodified NFC was mixed with a homopolymer of polypropylene with different loadings of NFC (0-5 wt.% by adding 0.5 wt.% per sample) through melt processing method. Initially, PP was added to internal mixing machine (CT Internal Mixer MX300) and was mixed 5 min at 180 °C (Banbury type rotors, speed – 65 revs/min). Then, the specific amount of surface modified NFC was added to the polypropylene (to obtain the sample total weight as 150 g) and the sample was further mixed at the same temperature for another 3 min. Afterward, the sample was compressed to produce temporary plates (Figure 3.2 (a)). All 21 different samples (Pure PP, 0.5-5 wt. % 10 unmodified NFC and 10 silane-modified NFC added composites) were prepared by following the same procedure. After that, the prepared batch samples were separately molded at 180 °C for 8 min, with 0.5 Ton/inch pressure. Ultimately, the samples were placed to cool down and sheets were separated from the molds after 25 min (Figure 3.2 (b)).

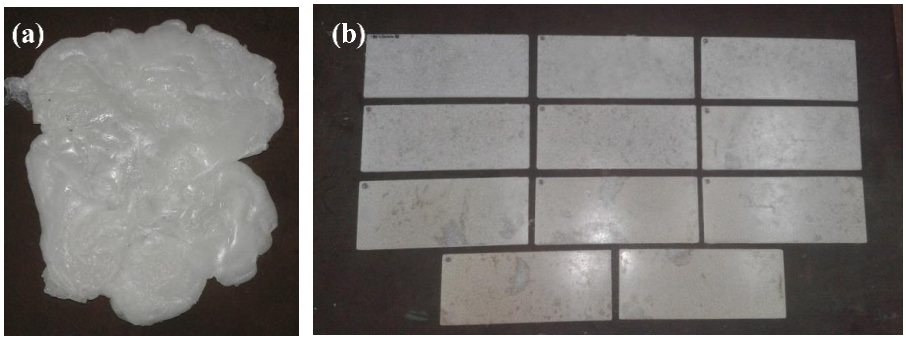

Figure 3.2: (a) Temporary composite plates (b) Molded composites

3.3.1 Characterization and analysis of composite samples

The 21 different fabricated composite samples were analyzed through SEM, FTIR, water absorption test, TGA, DTA, melt flow index (MFI) and mechanical tests of tensile, impact and hardness.

3.3.1.1 Tensile test

The test was conducted according to the standard test method for tensile test of plastics (ASTM D 638) and five replicates of each sample were used to calculate the average value (Figure 3.3). Initially, the thickness, width, and length of each sample were measured and applied load, extension, strain rate and, gauge length were entered to universal testing machine (HTE Hounsfield) as 1 kN, 400 mm, 10 mm/min and 30 mm respectively at room temperature. Then the tensile forces and elongation percentage at break of each sample were measured using the machine.

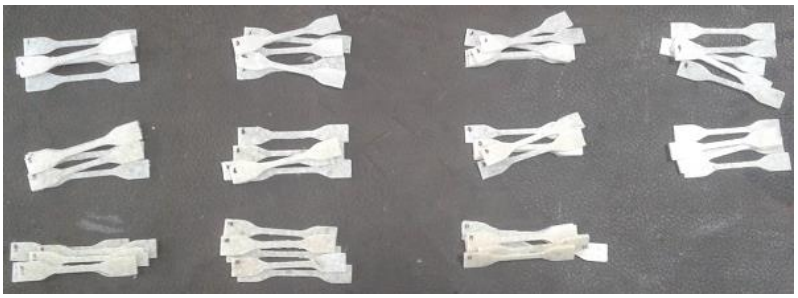

Figure 3.3: Tensile test samples

3.3.1.2 Impact test

Five samples of each composite were prepared to correspond to the standard method of determination of Izod impact strength of plastics (ISO 180:2000). Therefore, the length, width and thickness of the samples were used as 80 mm, 10 mm and 2 mm respectively (Figure 3.4). Furthermore, the notch of each sample was prepared in 2 mm depth. Consequently, the remaining width at notch base was estimated as 8 mm. then the surfaces of all samples were smoothly ground using hand grinder (METASERV) to obtain uniform dimensions. Finally, the impact angle was measured using Izod impact testing machine (HUNG TA HT-8041B) and the value was converted to energy lost per unit cross-sectional area at the notch (kJ/m^2).

Figure 3.4: Impact test samples

3.3.1.3 Hardness test

The standard test method of the hardness of plastics (ASTM D2240) was measured using D type shore durometer and several points of each sample were used to obtain hardness values (Figure 3.5).

Figure 3.5: Hardness test sample

3.3.1.4 Water absorption test

Three specimens of each sample were cut according to ASTM D 570 standard test method (30x28x3 mm^3) as mentioned in Figure 3.6. At the beginning of the test, the initial weight of each specimen was measured and then the samples were soaked in distilled water at room temperature for 24 hours. After the specific time period, the samples were reweighted the water absorption percentage was calculated.

Figure 3.6: Water absorption test samples

3.3.1.5 Melt flow index (MFI)

ASTM D1238 – 79, the standard test method for the flow rate of thermoplastics by extrusion plastometer was conducted using CSI melt flow indexer (model: Mfi2-115). Initially, the samples were cut into small, equal sized pieces and then were placed in the indexer. The temperature and the load were used as 230 °C and 2.06 kg, respectively as stated in the condition "L" of the ASTM method and 5 replicates of each sample were tested to calculate the average MFI value.

4 RESULTS AND DISCUSSION

4.1 Characterization of raw materials

4.1.1 Morphological analysis

SEM observations of pure NFC have indicated a compact structure of original nanofibers and most of the fibers were in nanometer scale. The nanofibers in Figure 4.1 appeared in different length and diameters. Therefore, the aspect ratio of NFC is comparatively high. According to SEM image, the original fibers form a compact structure because initially liquid medium was used to observe SEM images of NFC and nanoparticle can be aggregated due to high aspect ratios [213]. To reduce the attraction, electrostatic repulsion can be generated between nanoparticles. However, ultra-sonication is a common way to avoid nanoparticles aggregation.

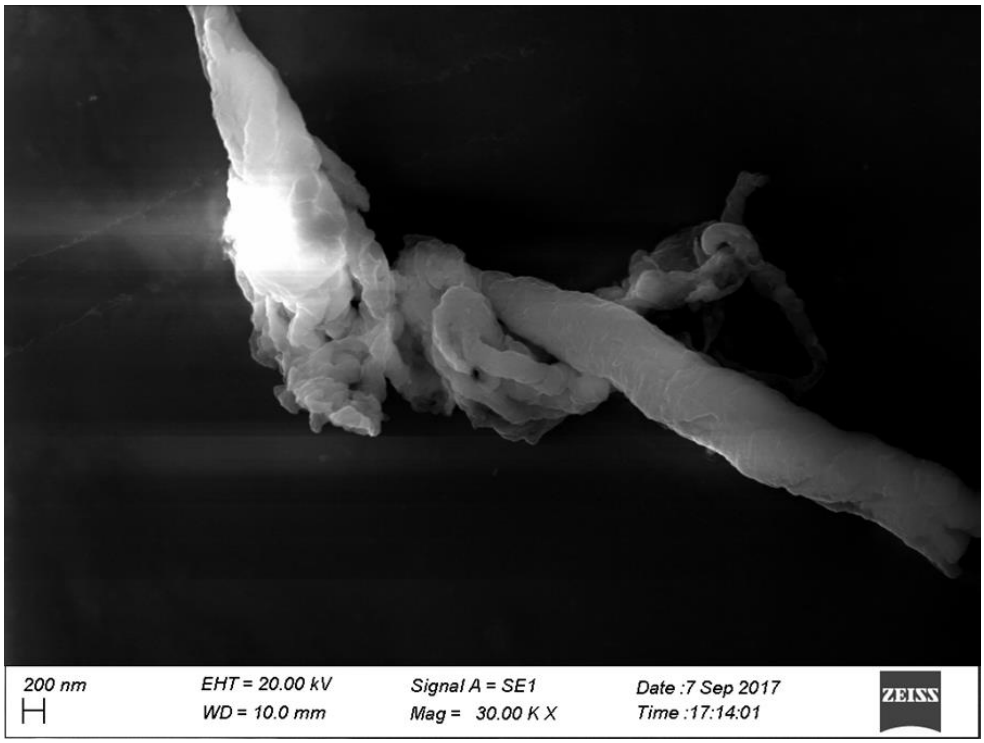

Figure 4.1: SEM image of spray dried NFC

4.1.2 FTIR

Generally, FTIR transmittance spectrum can be divided into 3300–3600 cm^{-1}, 2800–3000 cm^{-1} and the region in between 500–1750 cm^{-1}. Notable spectral band at 3419.89 cm^{-1} of NFC spectrum explains the O-H stretching vibrations of the sample (Figure 4.2). And also the peak at 2916.86 cm^{-1} confirms C-H stretching vibrations. This band has also shifted to high values from 2900 cm^{-1} which further proves the presence of an amorphous structure of nanocellulose. In addition, nanofibrillated cellulose contains not only the amorphous regions but also crystalline regions. As a result, there are some significant absorption bands present in the region between 1500-900 cm^{-1}. The peak at 1430.51 cm^{-1} is responsible for symmetric bending vibrations of $–CH_2$ and 1374.41 cm^{-1} represents the C-H vibrations in pyranose ring. In the fingerprint region (800-1200 cm^{-1}), the presence of both primary and secondary alcoholic C-O stretching vibrations in cellulose is evident by the peaks of 1113.67 cm^{-1} and 1163.81 cm^{-1}, respectively. Other than that, the absorption bands at 897.16 cm^{-1} and 1058.97 cm^{-1} appeared can be assigned to C–O–C stretching at glycosidic linkages and within pyranose ring, respectively. Except for all the peaks, another particular peak is present at 1634.74 cm^{-1}. This absorption band confirms the H-O-H bending of water which can be appeared in between 1620-1642 cm^{-1} [214].

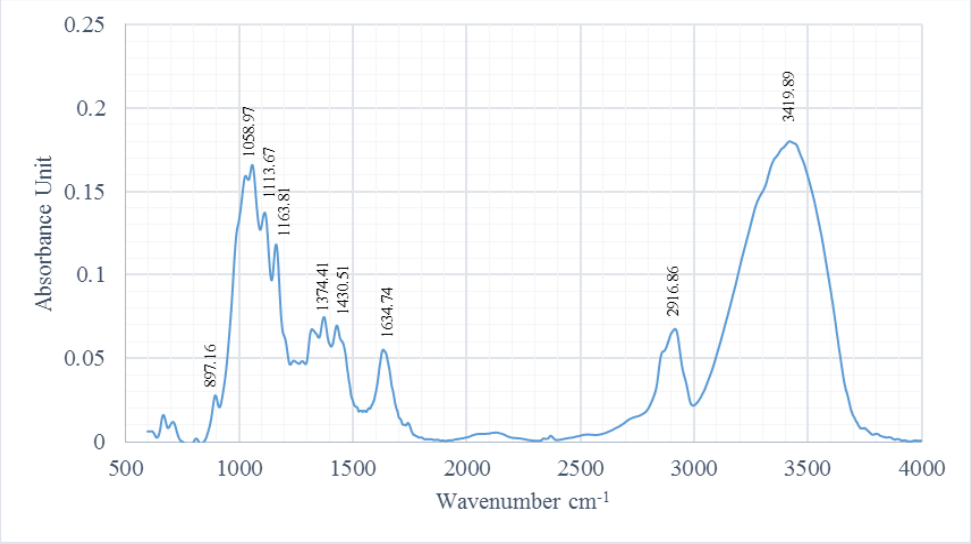

Figure 4.2: FTIR spectrum of NFC

Four large characteristic peaks of pure PP were identified in the ATR-FTIR spectrum at the region between 3000–2800 cm^{-1} (Figure 4.3). The peaks at 2953.12 cm^{-1} and 2873.99 cm^{-1} represent the asymmetric and symmetric stretching vibrations of $–CH_3$ group. In addition to that, the peaks at 2916.94 cm^{-1} and 2838.02 cm^{-1} attributes to asymmetric and symmetric stretching vibrations of $–CH_2$ main chain [215]. Other significant peaks of 1455.5 cm^{-1} and 1374.42 cm^{-1} assign to symmetrical bending vibrations of $-CH_2$ and $–CH_3$ respectively [216].

Base on the tacticity, isotactic polypropylene (iPP) has the highest energy values due to the steric repulsion of side groups present on the same side. Therefore, to become stable, iPP produce stable helix structure along with one repeating unit by turning one out of three repeating units. The unique structure of iPP is called as 3_1 helix [217]. According to the literature, there are several additional bands may appear in the region between 800-1200 cm^{-1} for isotactic polypropylene. Most importantly, the peaks present at 998.82 cm^{-1} and 843.36 cm^{-1} are responsible for the 3_1 helix. The peak 998.82 cm^{-1} corresponding to the bending, wagging and rocking frequencies of $–CH$, $-CH_2$ and $–CH_3$ [218]. Therefore, based on the ATR-FTIR spectrum the pure PP can be identified as isotactic polypropylene.

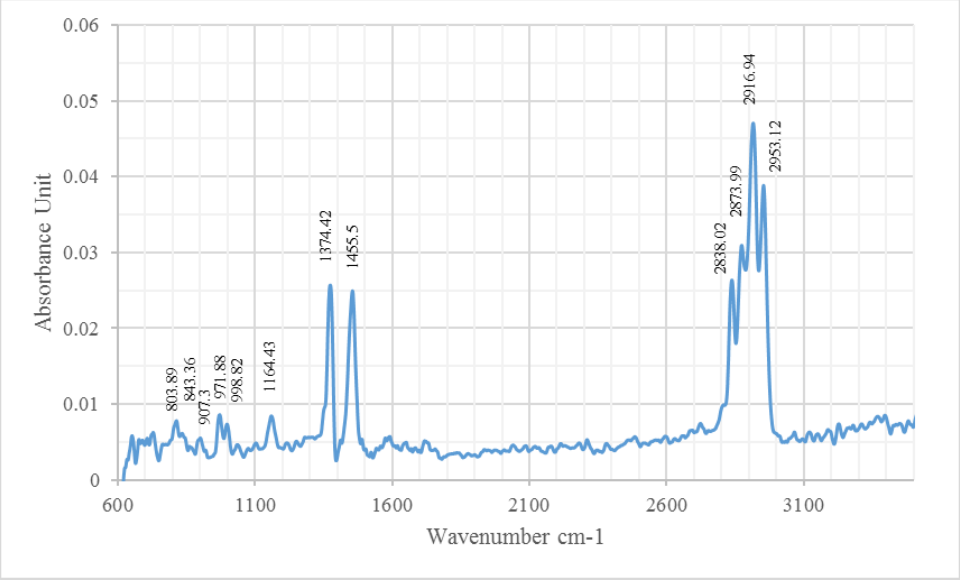

Figure 4.3: ATR-FTIR spectra of pure PP

4.1.3 TGA and DTA

Based on TGA thermogram (Figure 4.4) of NFC, weight loss observed in three different temperature regions of 25-200 °C, 200-375 °C and 375-600 °C and the percentages of weight loss are 6.5%, 70%, and 7.5% respectively. The first region 6.5% weight loss indicates the evaporation of adsorbed water. Then the maximum weight loss of 70% was given by the second region and it can be explained as thermal depolarization and cleavage of glycosidic bonds of cellulose.

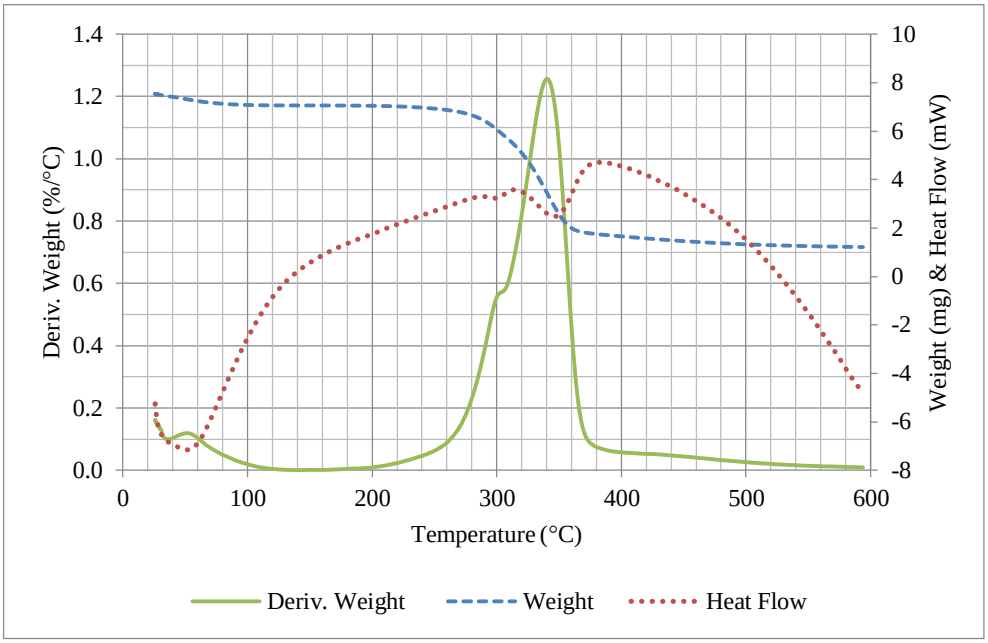

Figure 4.4: TGA and DTA graphs of spray dried NFC

According to the original DTA curve (Figure 4.4) of NFC, one large exothermic peak between 40-60 °C and another two closely merged exothermic peaks between 250-350 °C can be observed. Therefore, the baseline correction was done using a data analysis and graphing software to generate better predictions (Figure 4.5). In general, the first exothermic peak related to the energy absorption to initiate water evaporation. The two merge exothermic peaks can be identified as the decomposition points of amorphous and crystalline regions of NFC because the peaks are related to the onset of the large weight loss in the regular derivative curve. Therefore, the amorphous and crystalline decomposition points of pure NFC are approximated as 300 °C and 335 °C, respectively. At the decomposition point, a huge amount of

energy is needed to cleave the strong glycodicid bond in NFC main chain. Therefore, high amount of energy is absorbed to breaks the molecular structure.

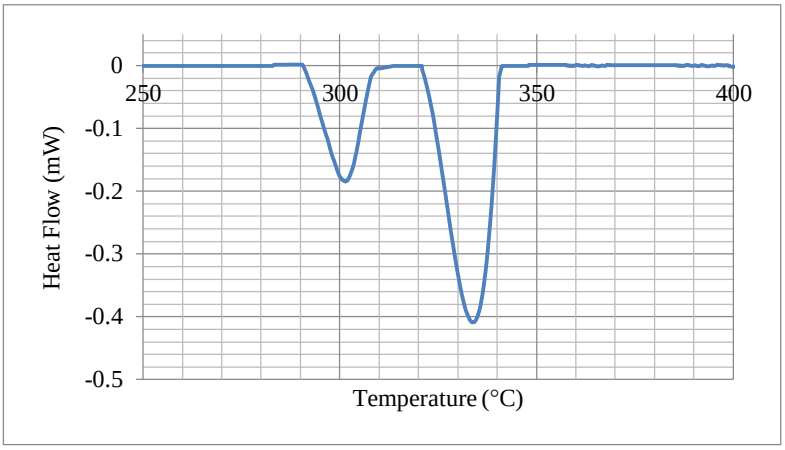

Figure 4.5: Baseline corrected DTA graph of spray dried NFC

In relation to the Figure 4.6, weight loss of pure polypropylene from room temperature to 380 ^{0}C is 0.89% and the value is ignorable compared to the initial weight of the sample. The results make evidence to the high thermal stability of polypropylene because Initial and final decomposition temperature of PP matrix have been observed at 380 ^{0}C and 480 ^{0}C.

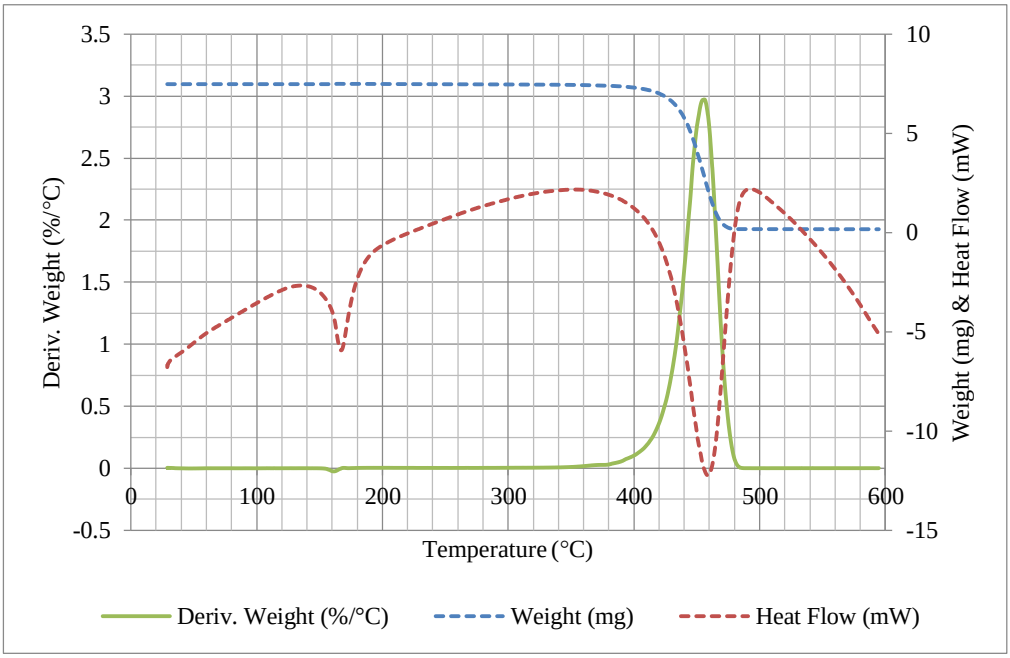

Figure 4.6: TGA and DTA graphs of pure PP

The baseline corrected DTA curve of pure PP (Figure 4.7) was indicated the melting and decomposition temperatures of PP at around 165 ^{0}C and 455 ^{0}C, respectively.

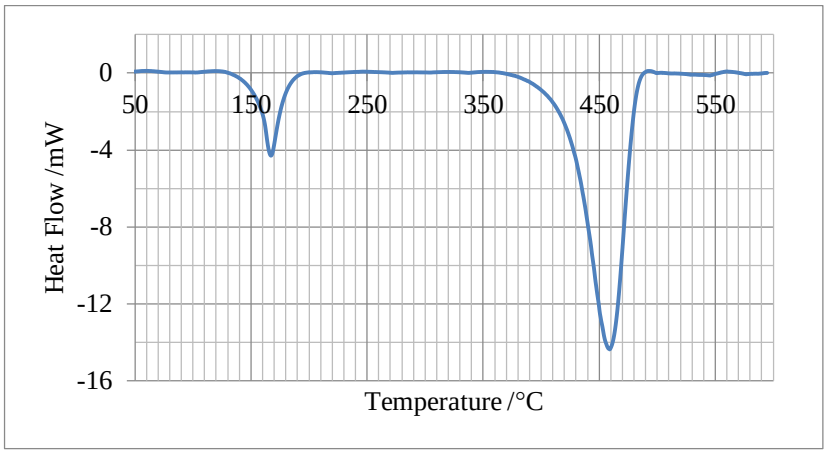

Figure 4.7: Baseline corrected DTA graph of pure PP

4.1.4 XRD

The diffractogram of NFC (Figure 4.8) indicated notable peaks at (2θ) 14.9° 16.4°, 22.5° and 34.6° and the peaks correspond to the planes of (1$\bar{1}$0), (110), (200) and (004) of native cellulose, respectively [219, 220]. More intensity and sharpness of 22.5° peak confirms that the sample has high crystalline regions [221].

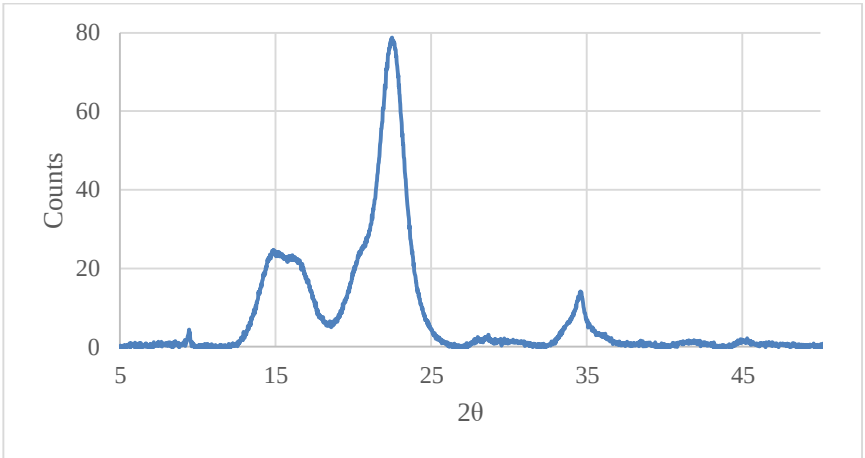

Figure 4.8: X-ray diffractogram of pure NFC

The native cellulose (cellulose I) has two different crystal structures; I_α and I_β and differ mainly in the packing arrangement of their hydrogen-bonded sheets. Cellulose I_α and I_β contain triclinic and monoclinic unit cell structures, respectively. Therefore, (110) plane is the characteristic plane for I_α and (200) plane for I_β [222]. However, both structures are co-occurring in nature with different ratios; though, nanofibrilated cellulose has higher percentage of I_β [223]. According to the XRD pattern, it is proved that NFC sample contains more I_β as well as the instrumental analysis was extremely matched with native cellulose with monoclinic unit cell structure and the crystallinity of NFC was given as 74.5%.

Based on the crystal structure, isotactic polypropylene can be divided into three groups; α (monoclinic), β (hexagonal), and γ (triclinic). These three types of crystal structures and the mesophase could be coexisted in one product especially injected molded products [224]. The three crystal structures have different characteristic crystal planes in XRD patterns. For instances, (110), (040) and (130) planes of α phase has 2θ value in 14^0, 16.7^0 and 18.4^0 as well as (300) and (301) planes for β phase has 2θ values around 16 and 21^0 respectively. In addition to the peaks close to 14^0 and 16.5^0, the γ phase has unique (117) plane 2θ value in between 19.2-20.5º. Except for the characteristic peaks, there are some significant peaks appeared in the XRD spectrum of pure PP (Figure 4.9). Therefore, 21.055^0 and 21.768^0 could be (111) and (041) plane of α-iPP. [225, 226].

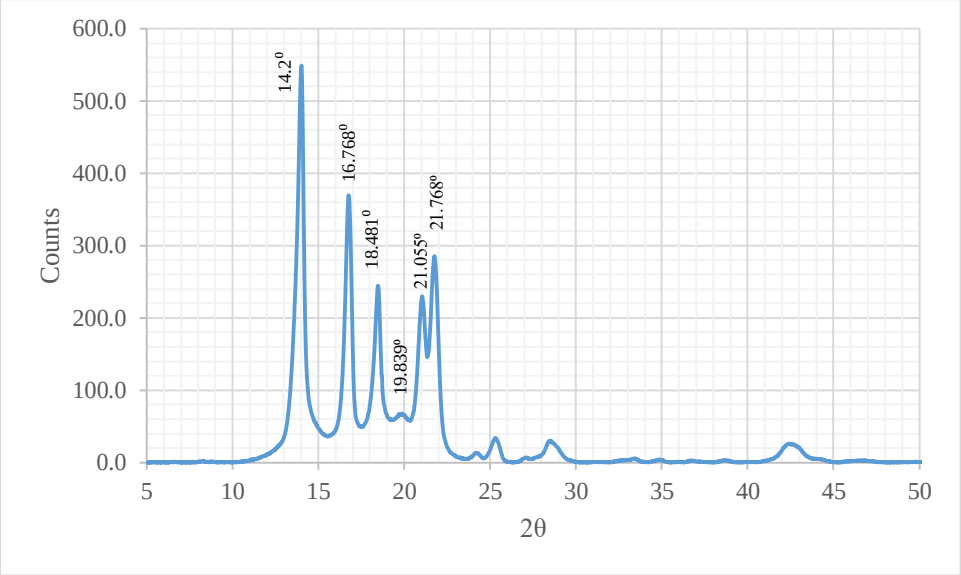

Figure 4.9: X-ray diffractogram of pure PP

Relating to the XRD spectrum (Figure 4.9), the pure polypropylene is further clarified to iPP with both α and γ phases. The real portion of α and γ phases (ex: K_γ) can be estimated by adding the intensity values of characteristic peaks to equation 1. Therefore, the sample contains approximately 22% γ -iPP and 78% α-iPP. Additionally, the crystallinity of polypropylene sample was given as 80% by the XRD instrument.

$$K_\gamma = \frac{I_{\gamma(117)}}{I_{\gamma(117)} + I_{\alpha(130)}} \times 100 \quad (1)$$

4.1.5 Ash content

Ash content of biomass defined as the amount of inorganic compounds presence as the structural or extractable amount with respect to the total biomass [227]. Average ash percentage of NFC was calculated as 0.48 wt.%. Theoretically, NFC is an organic material and completely converts to CO_2 and H_2O at high temperatures. Therefore, the inorganic mater presence as ash can be concluded as impurities, mineral acids or high-temperature stable chemicals which were added during the processing of NFC [77].

4.2 Characterization of surface modified NFC

4.2.1 Morphological analysis

According to the Figure 4.10 (a), a smoothly covered layer around the NFC particles was observed. The Figure 4.10 (b) was obtained by further zooming the micrograph of separated NFC particles. Therefore, it can be clearly seen a smoothly covered layer around the particles and there should be Si-O-C bonds on the NFC surface. However, some coagulation of nanoparticles was also identified.

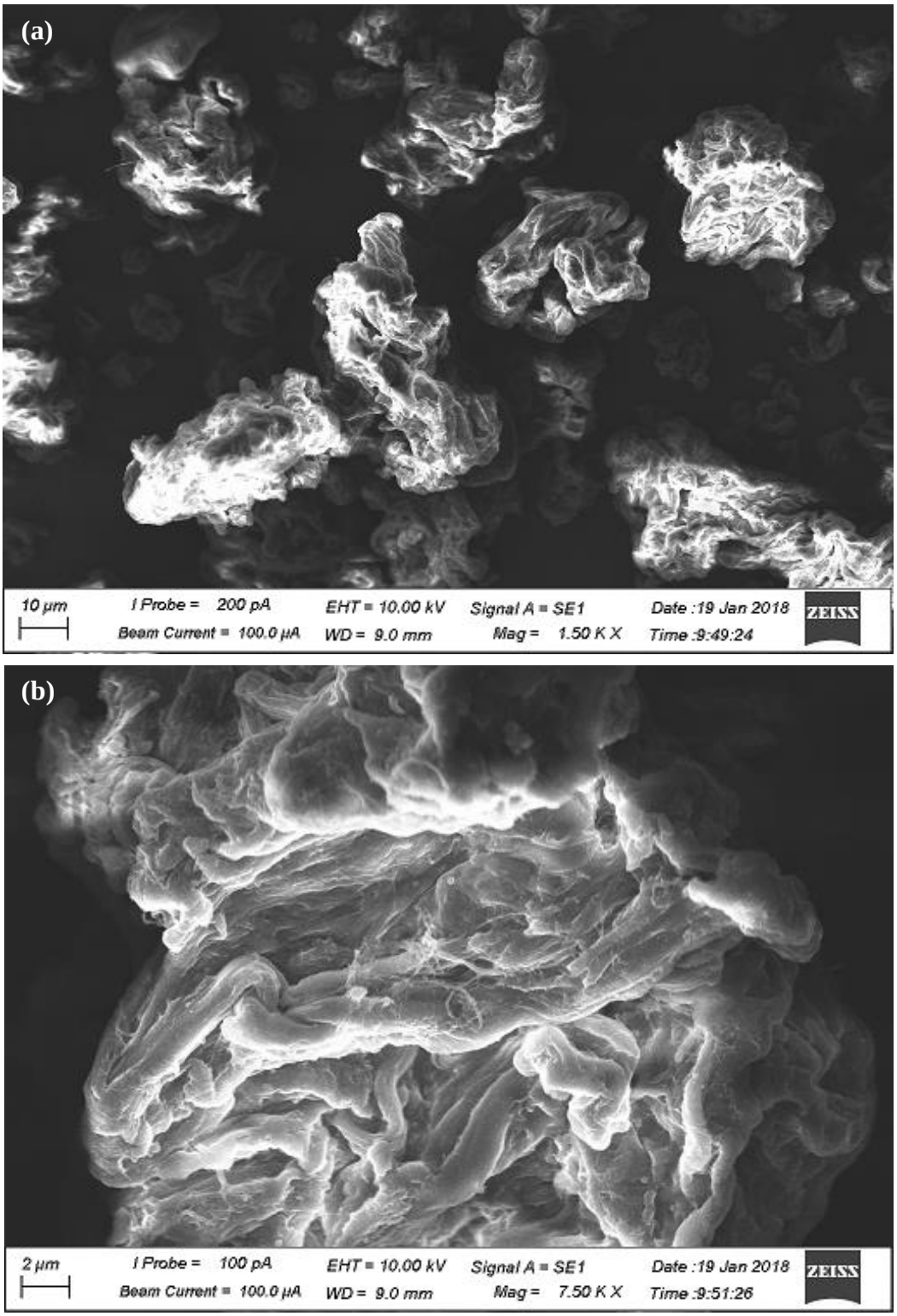

Figure 4.10: SEM Image of (a) surface modified NFC (b) magnified image of surface modified NFC

4.2.2 FTIR

The FTIR spectrum was used to study the main functional groups present in surface modified NFC (Figure 4.11). There are four new peaks identified. The absorption band in around 788 cm^{-1} corresponds to the Si–C symmetric stretching bonds and the band at 670 cm^{-1} indicates the Si–O–Si symmetric stretching. Other than that, a minor peak near to the major band in 964.58 cm^{-1} was notified. According to the literature, the peak could be regarded as the presence of the asymmetric stretching of Si–O–Si and/or Si–O–C bonds [228]. Moreover, a significant absorption band approximately present at 1242 cm^{-1} is associated with the Si–O–C bond. Based on the previous studies shoulder peaks at 964.58 cm^{-1} and 1242.4 cm^{-1} are the characteristic peaks for –Si–O–C– bond [229] and it confirms the reaction between the hydrolyzed silane and the nanocellulose. Therefore, these peaks can prove the existence of bonds between nanocellulose and silane groups and favorably prove the surface modification of NFC.

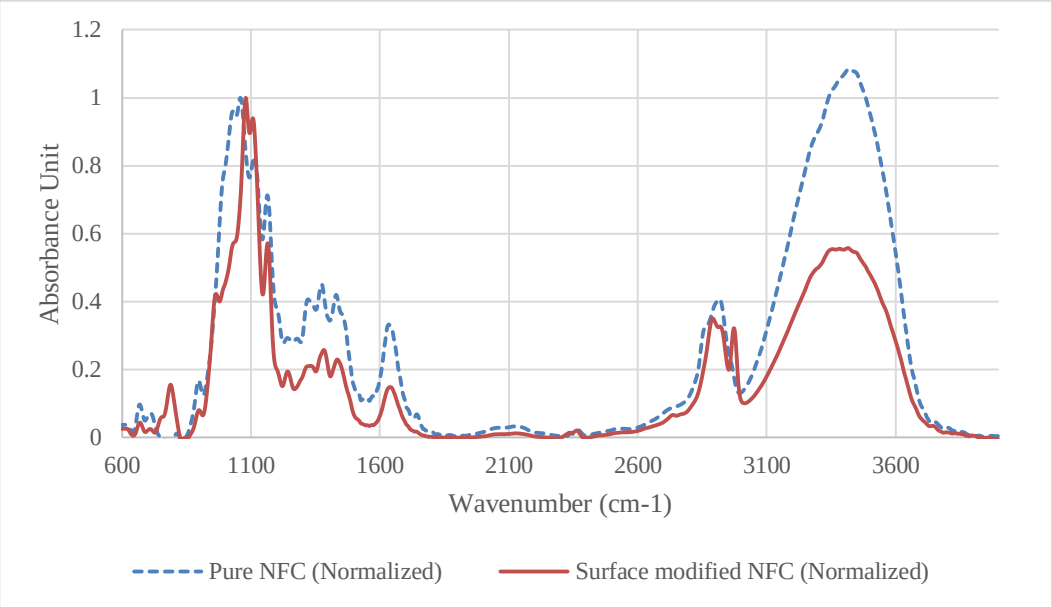

Figure 4.11: Normalized FTIR graphs of pure NFC and surface modified NFC

Furthermore, to compare the FTIR spectra of pure and surface modified NFC, the graphs were normalized using the peak of C–O–C stretching vibration peak within pyranose ring because; it considers that there is no structural change within the

polymer chain during the surface modification process. As shown in (Figure 4.11), the O-H stretching vibration peak of pure NFC graph has been reduced in respect to C-H peak of surface modified NFC graph and it also leads to prove the surface modification on the NFC polymer chains.

4.2.3 TGA and DTA

According to the Figure 4.12, the TGA thermogram of surface modified NFC has shifted to the high-temperature range in relation to that of the pure NFC. A drastic weight loss can be identified in the temperature range of 250 - 350 °C. At this temperature region, the solid polysaccharide structures of NFC converted to CO_2 and H_2O and release from the system. Therefore, the total weight is dramatically reduced and ultimately the system contains inorganic residuals which were added to the system during the processing.

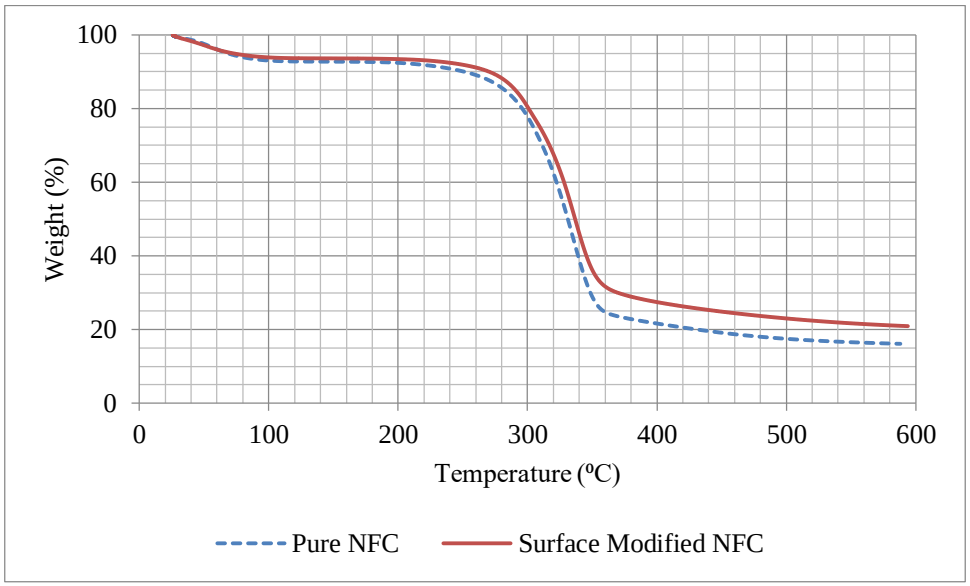

Figure 4.12: Comparison between TGA graphs of pure and surface modified NFC

The thermogram of the surface modified NFC shows a low rate of initial weight loss compared to that of pure NFC and the final weight of the system is higher than the pure NFC. Therefore, it confirms that the surface modifier is remaining in the system

at higher temperatures. These results imply the improvement of thermal stability after surface modification because the functional groups attached to the surface directly affect the thermal degradation of material [230]. Therefore, Si-69 surface modification provides better thermal stability for NFC and due to the better surface modification, the agglomeration and aggregation of nanoparticle get reduced and improve the nano-effect to obtain better properties.

As illustrated in Figure 4.13, the baseline corrected DTA curve of surface modified NFC was shifted to the high-temperature region. Therefore, the melting and decomposition temperatures of surface modified NFC can be evaluated as 310 ^{0}C and 355 ^{0}C respectively. In addition, the depths of the two exothermic peaks of surface modified NFC were increased in respect to pure NFC. The area below the DTA curve represents the enthalpy or the energy requirement to rupture the unit cell [231]. Therefore, surface modified NFC signifies the enhancement of heat stability than pure NFC because the energy needs to break the long chain macromolecular structure of nanocellulose is higher due to the formation of silylated cover around NFC.

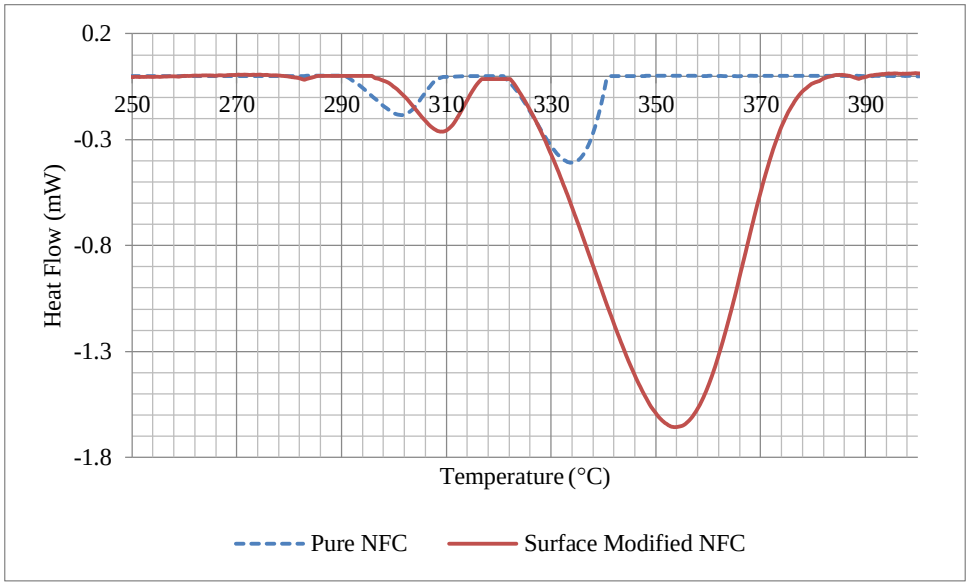

Figure 4.13: Comparison between baseline corrected DTA graphs of pure NFC and surface modified NFC

4.2.4 XRD

The Figure 4.14 shows the comparison between XRD graphs of pure NFC and surface modified NFC. All peak intensities of surface modified NFC was reduced in respect to pure NFC. Most importantly, the peak 22.5^0 intensity was reduced after the surface modification process. In addition, the instrumental value of crystallinity was turned down from 74.5% to 70.2%. The reduction of crystalline percentage may be happened due to the addition of silane coupling agents to crystalline regions of NFC. During the modification process, large silane groups replace the small –OH groups present in the NFC surface. Due to the addition of large groups to the surface, the distance between molecules in the main would increase [232]. Therefore, the separation could be affected by the reduction of the crystalline percentage of NFC after the surface modification.

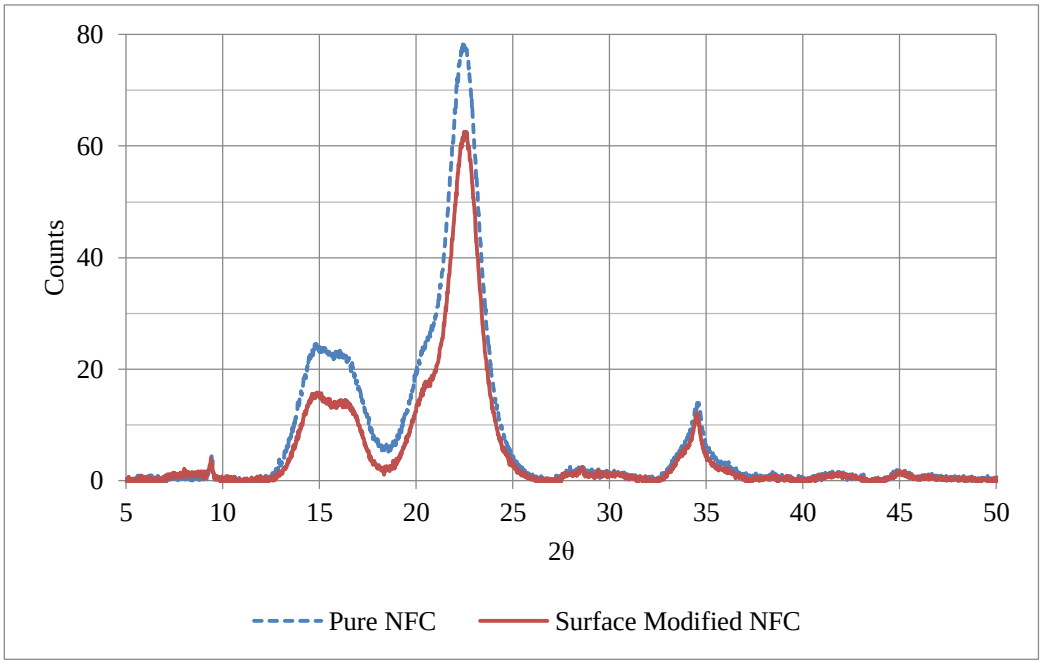

Figure 4.14: Comparison between X-ray diffractograms of pure NFC and surface modified NFC

4.3 Characterization and analysis of composite samples

4.3.1 Morphological analysis

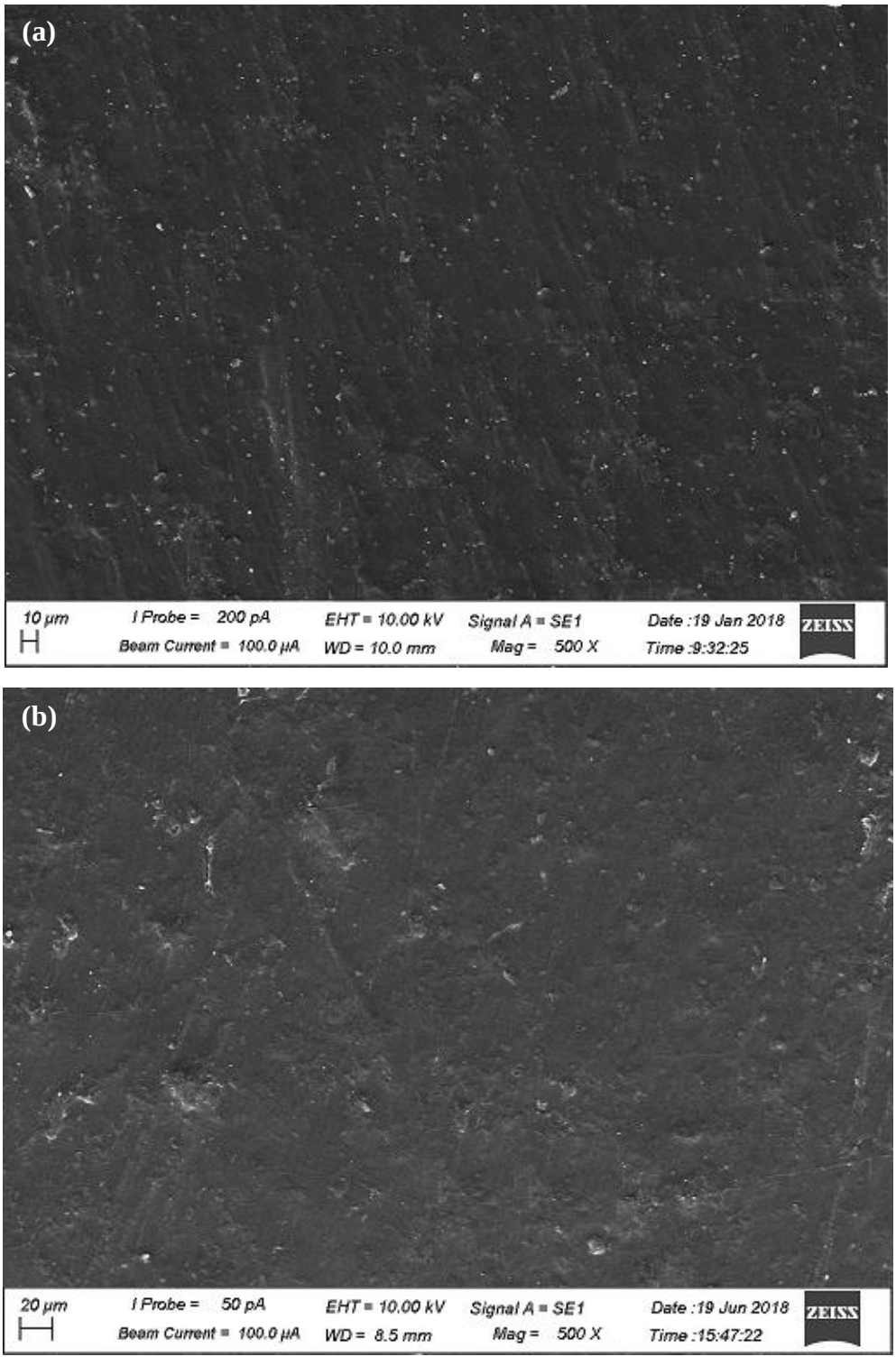

Figure 4.15: SEM images of (a) molded pure PP sample (2 KX magnification) and (b) 0.5% unmodified NFC reinforced composites (500X magnification)

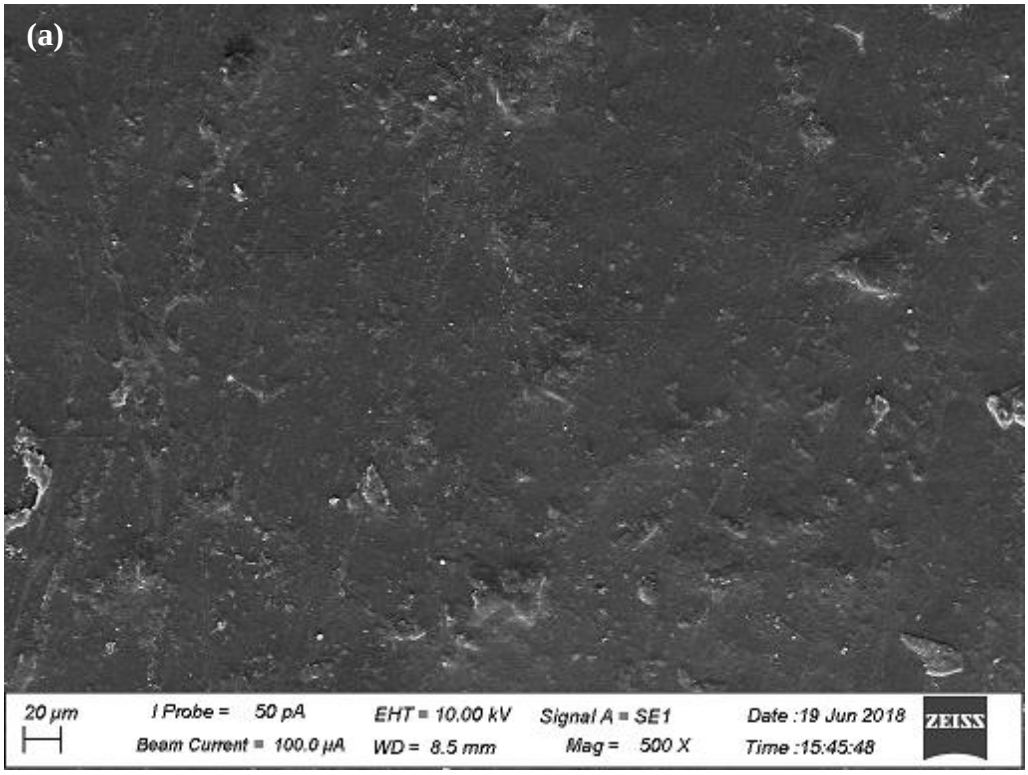

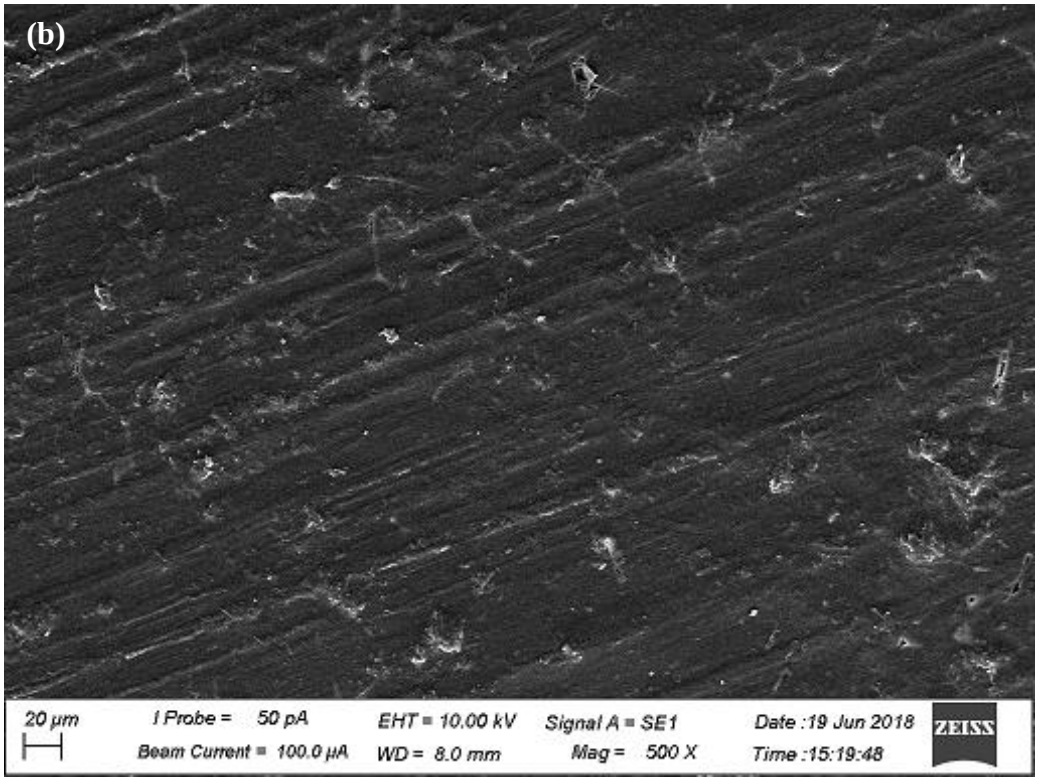

Figure 4.16: 500X magnified SEM images of composites (a) 1.0 % and (b) 1.5 % unmodified NFC reinforced composites

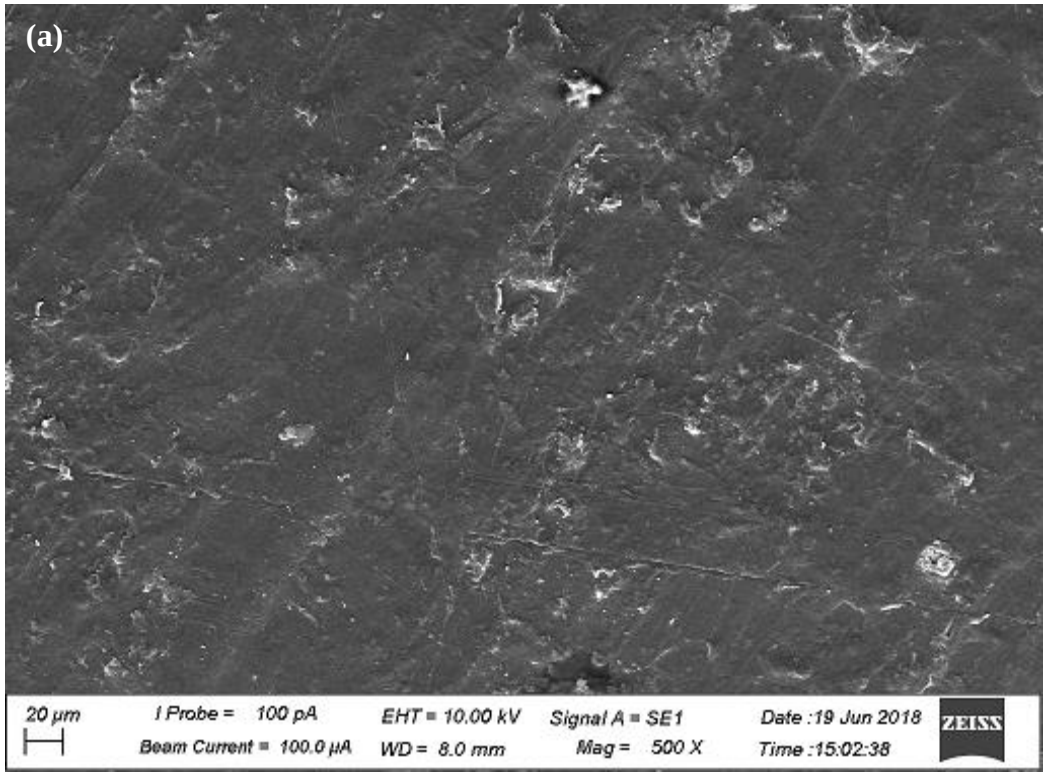

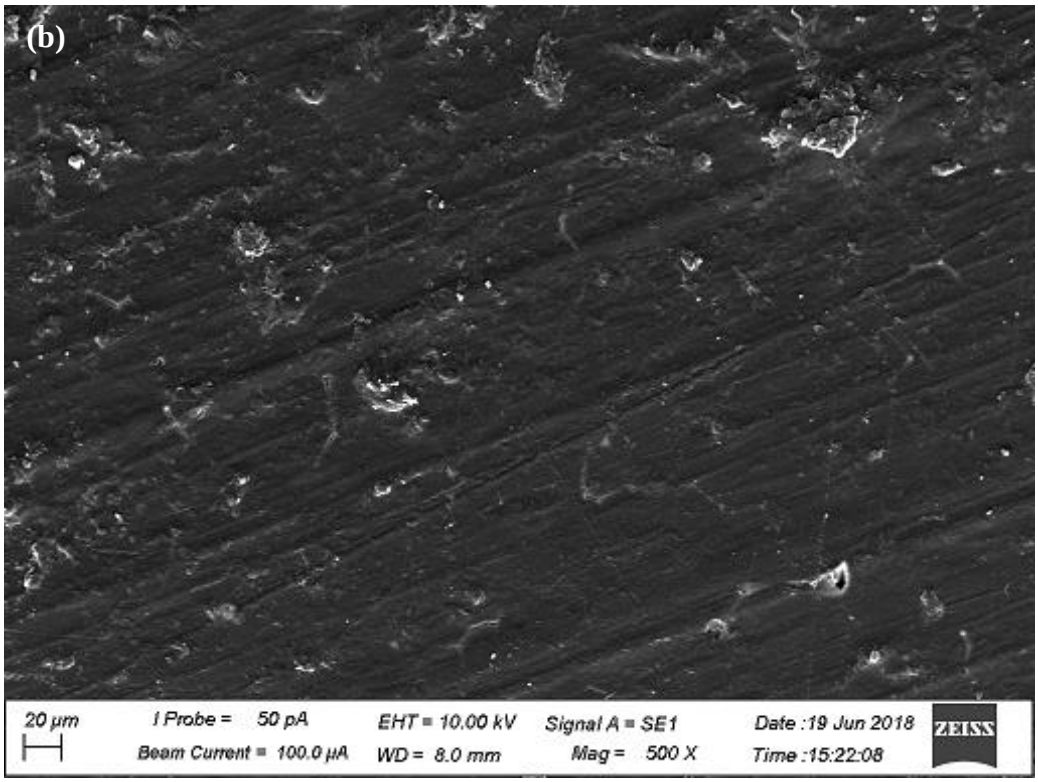

Figure 4.17: 500X magnified SEM images of composites (a) 2.0 % and (b) 2.5 % unmodified NFC reinforced composites

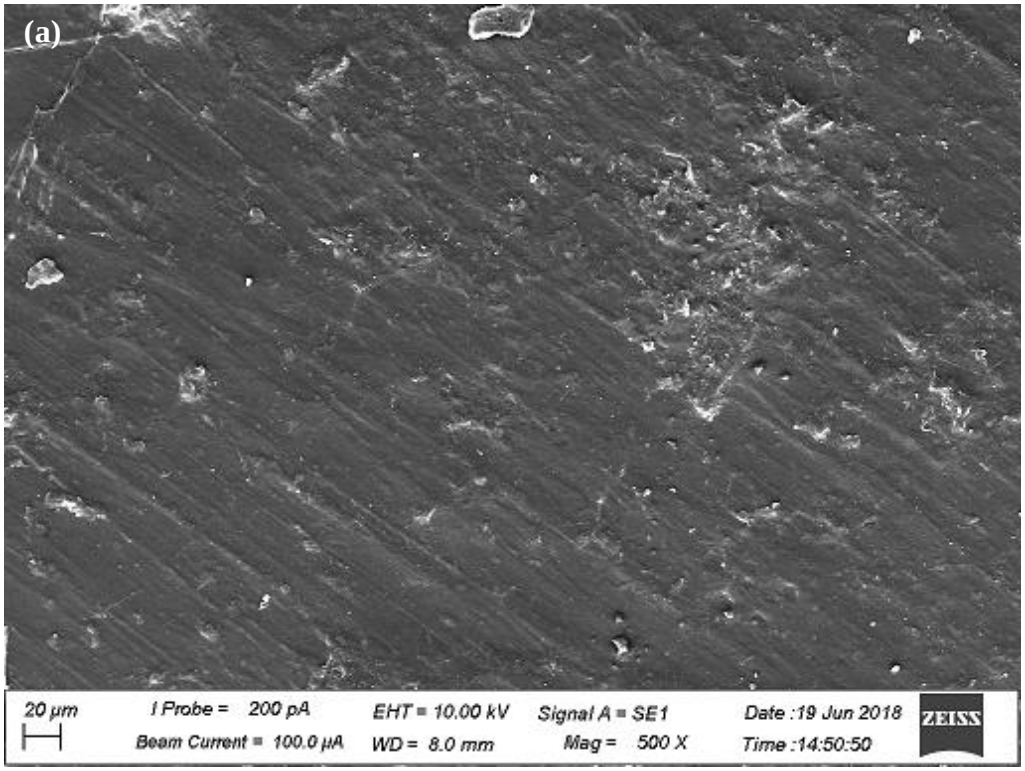

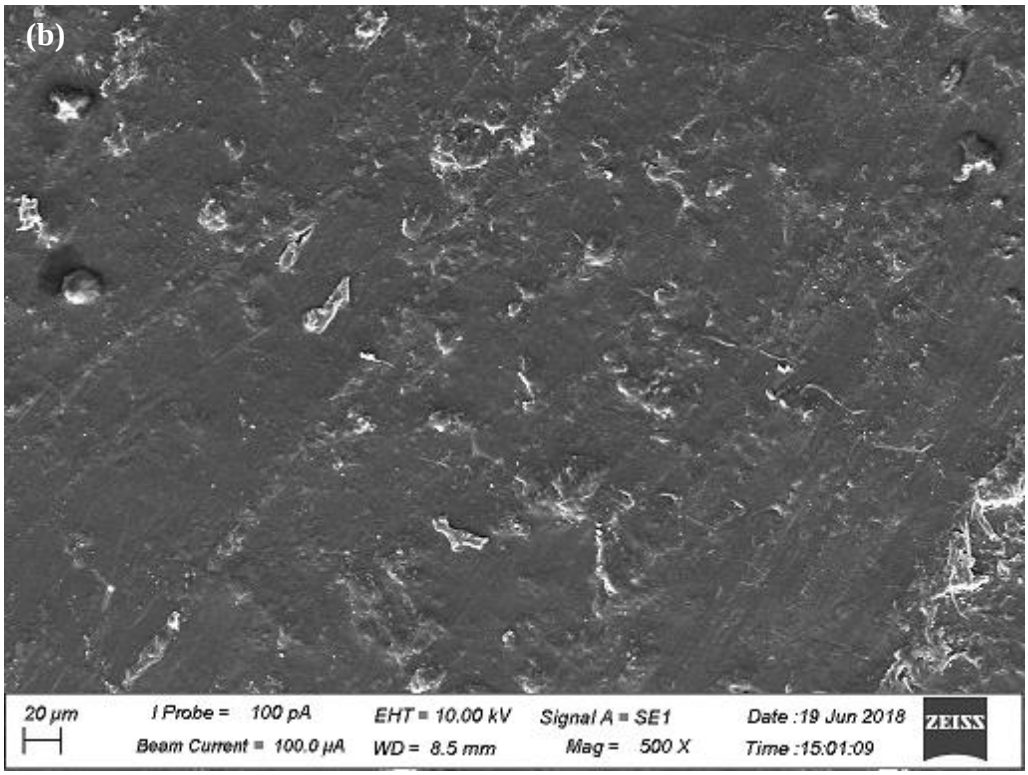

Figure 4.18: 500X magnified SEM images of composites (a) 3.0 % and (b) 3.5 % unmodified NFC reinforced composites

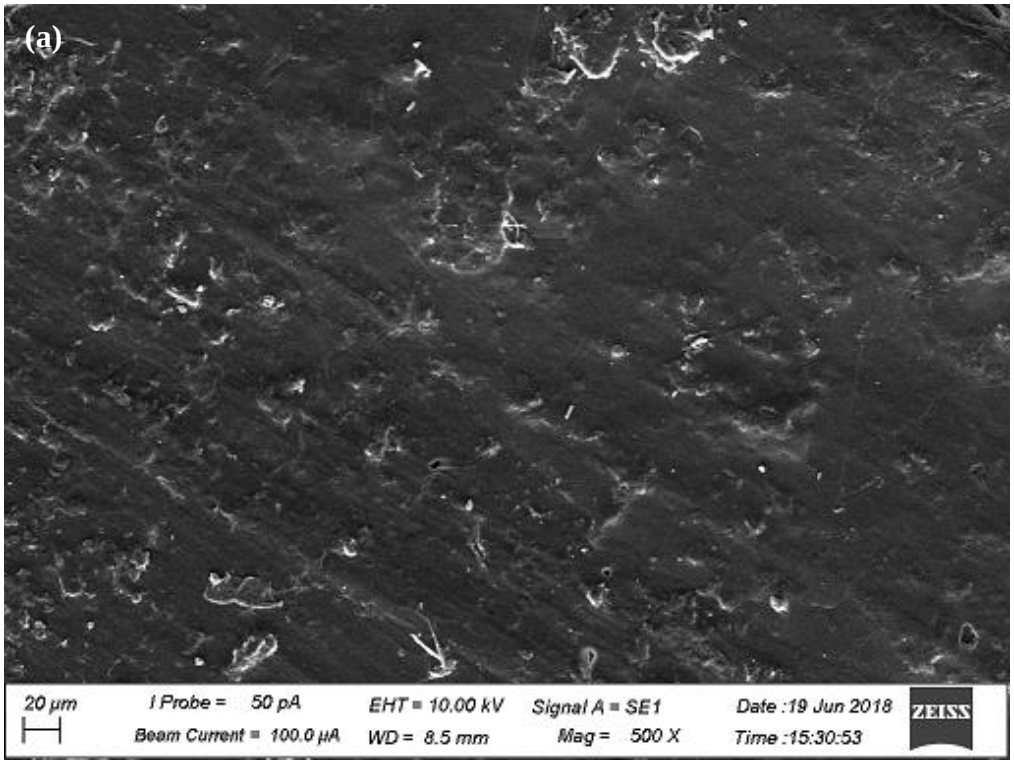

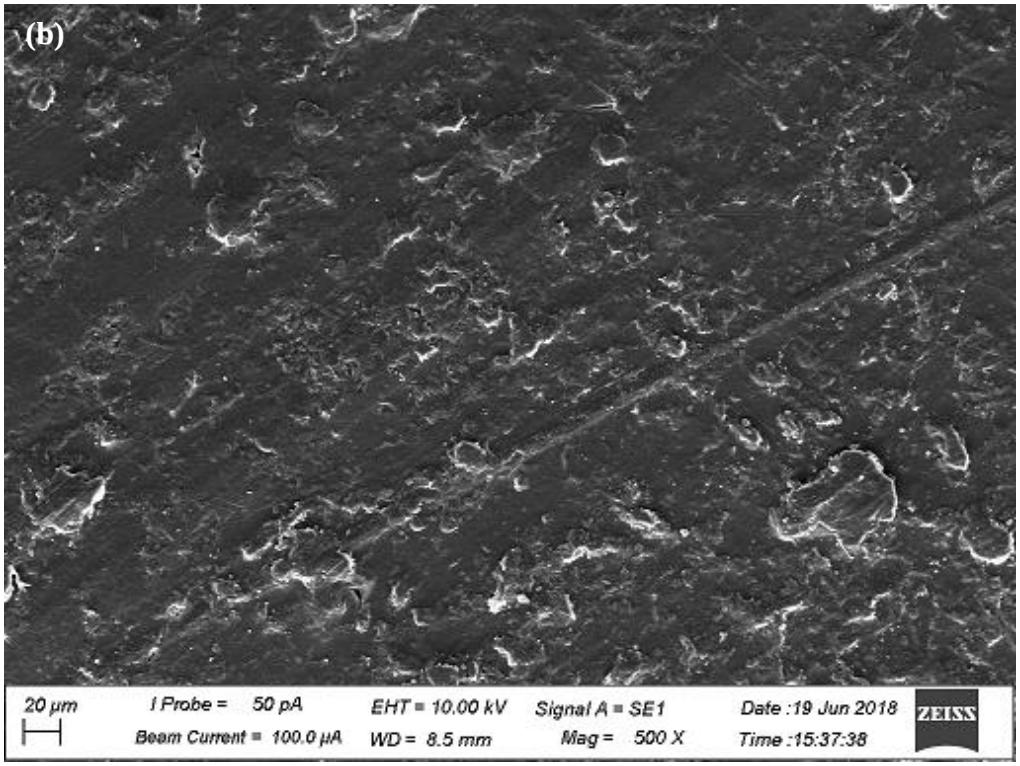

Figure 4.19: 500X magnified SEM images of composites (a) 4.0 % and (b) 4.5 % unmodified NFC reinforced composites

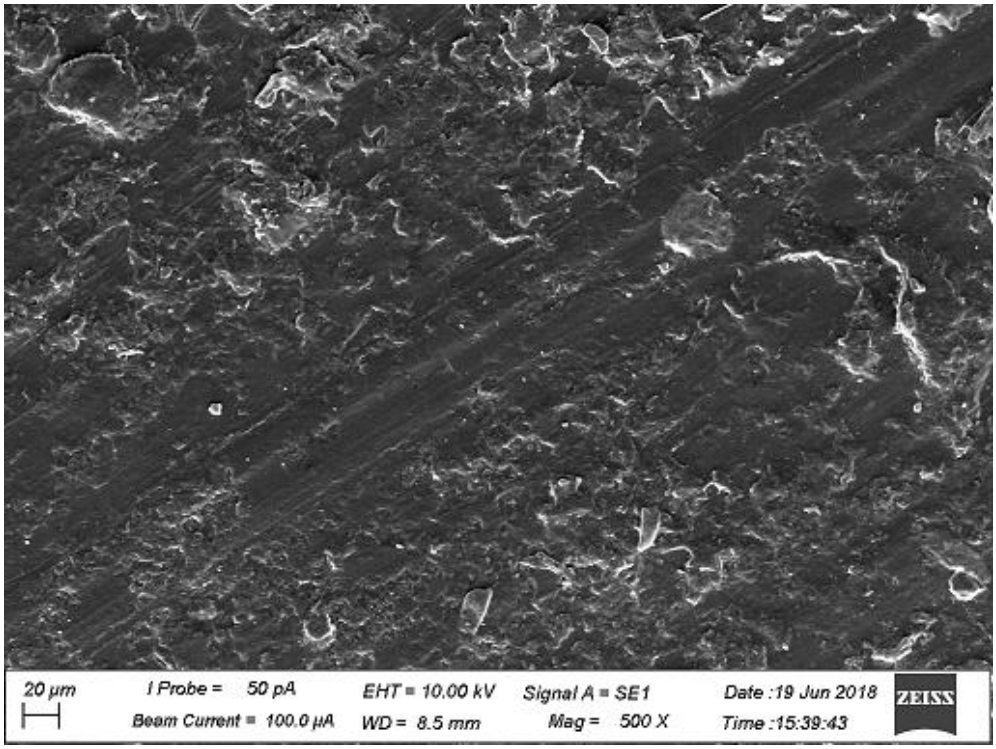

Figure 4.20: 500X magnified SEM image of composites 5.0 % unmodified NFC reinforced composites

The morphology of the pure polypropylene and ten unmodified composite samples were observed after the molding process. SEM image of pure PP (Figure 4.15 (a)) indicated clearer surface than composites because the sample completely contains one material with better crystallinity. With the addition of unmodified NFC content, uniformity of the surfaces are drastically reduced and significant coagulations are present beyond 1.5% unmodified NFC reinforced composite (Figure 4.17 (a)(b), Figure 4.18 (a)(b), Figure 4.19 (a)(b) and Figure 4.20) due to the attractive forces between nanofibers.

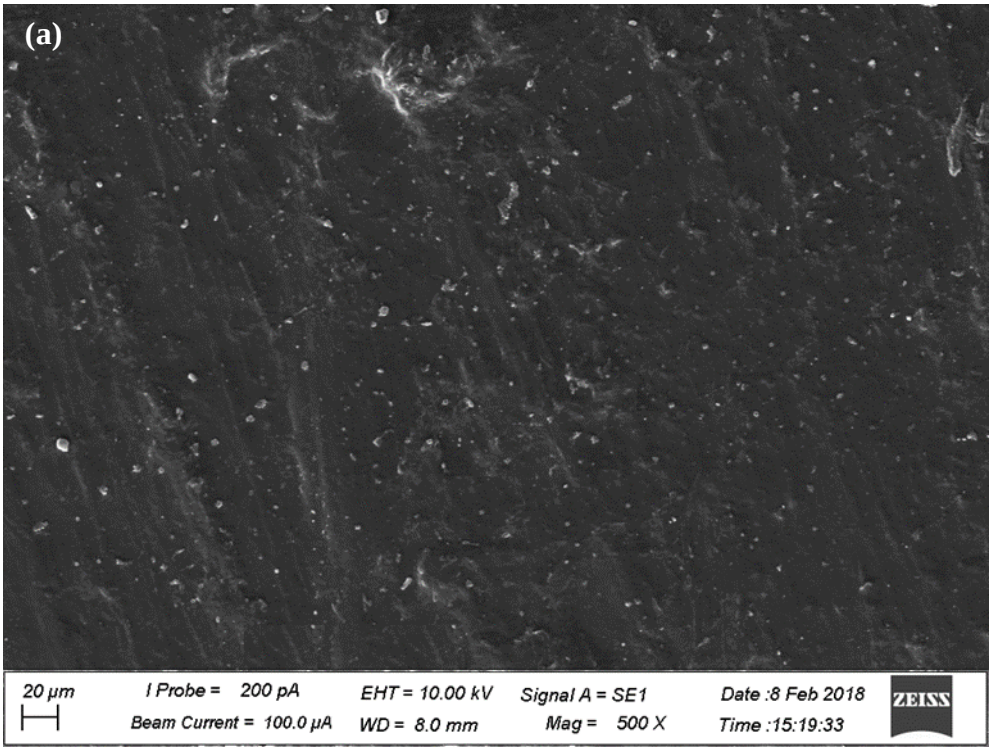

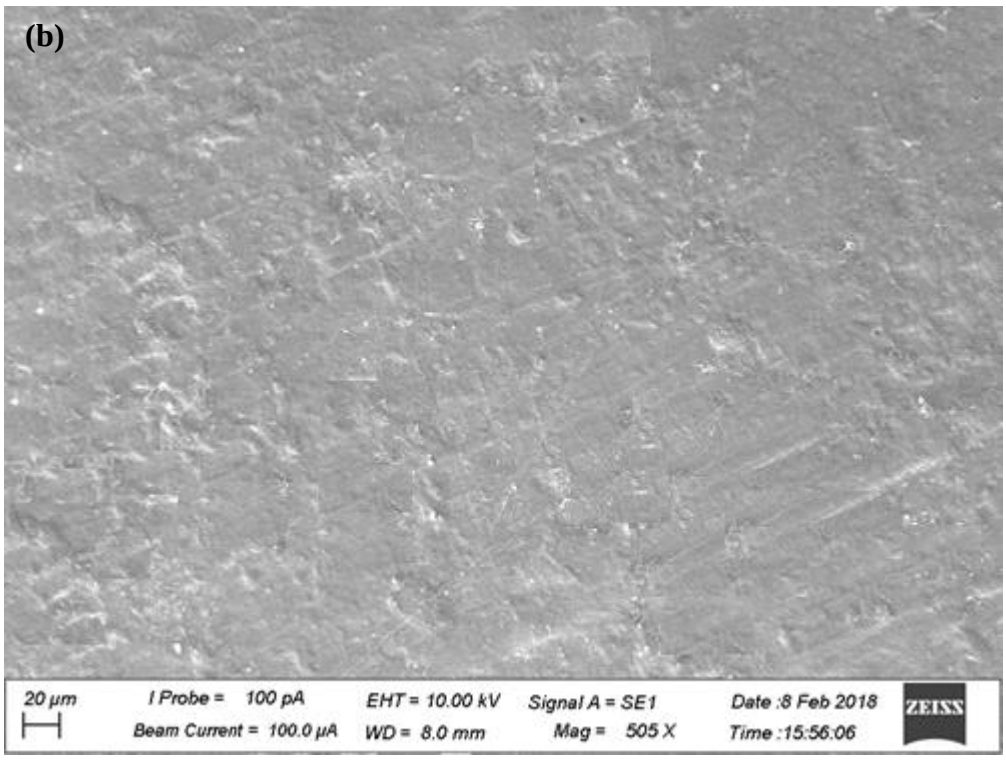

Figure 4.21: 500X magnified SEM images of composites (a) 0.5 % and (b) 1.0 % silane-modified NFC reinforced composites

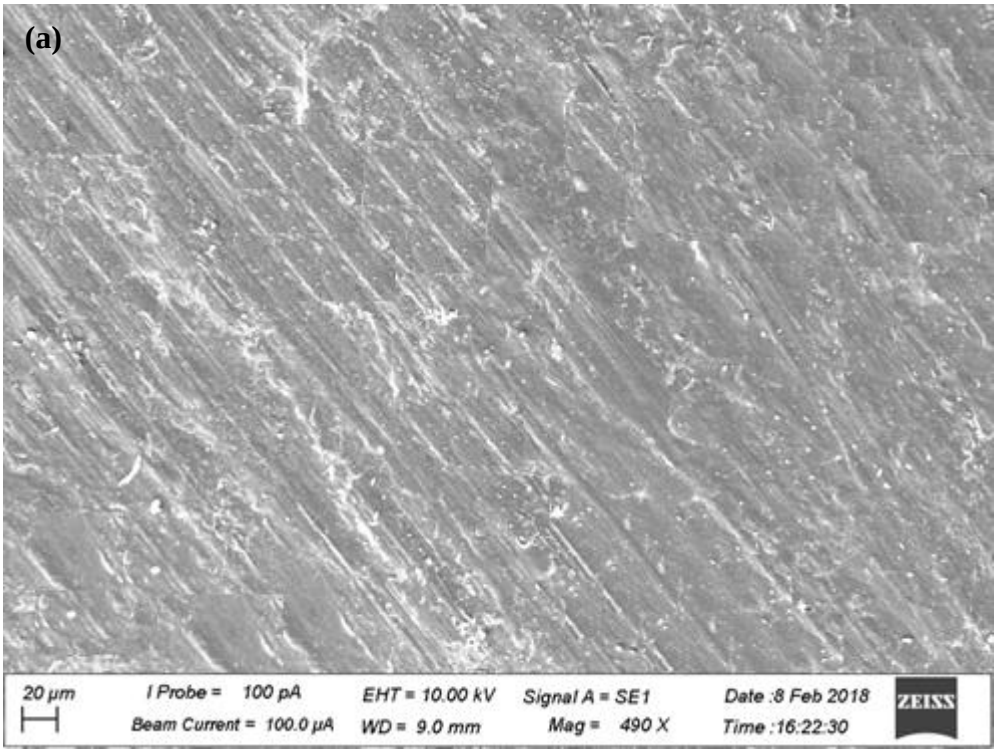

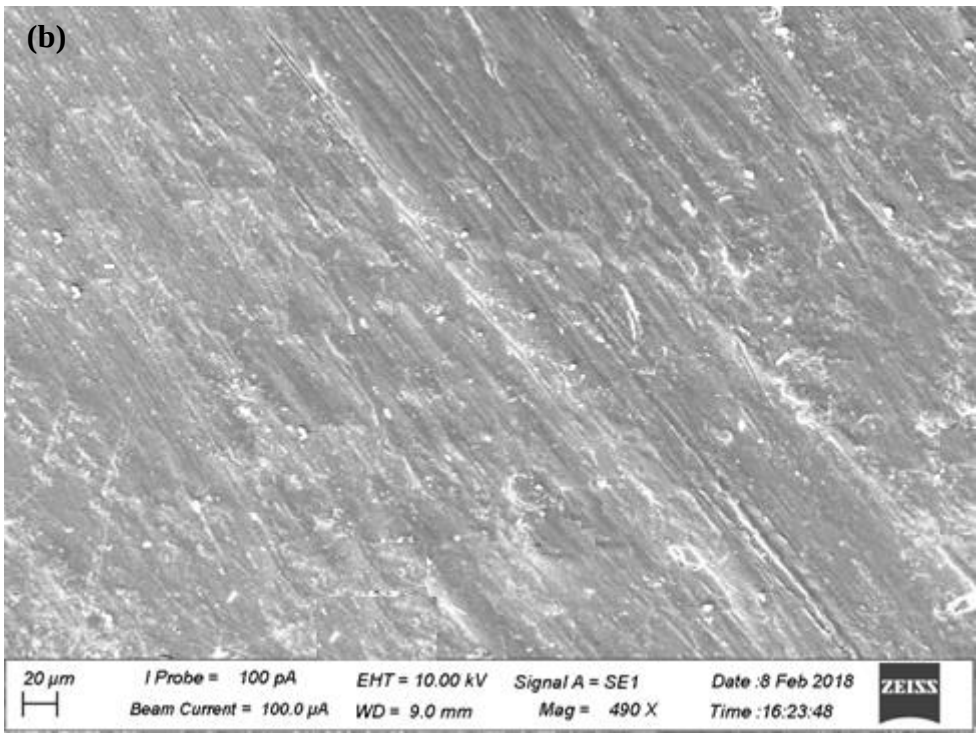

Figure 4.22: 500X magnified SEM images of composites (a) 1.5 % and (b) 2.0 % silane-modified NFC reinforced composites

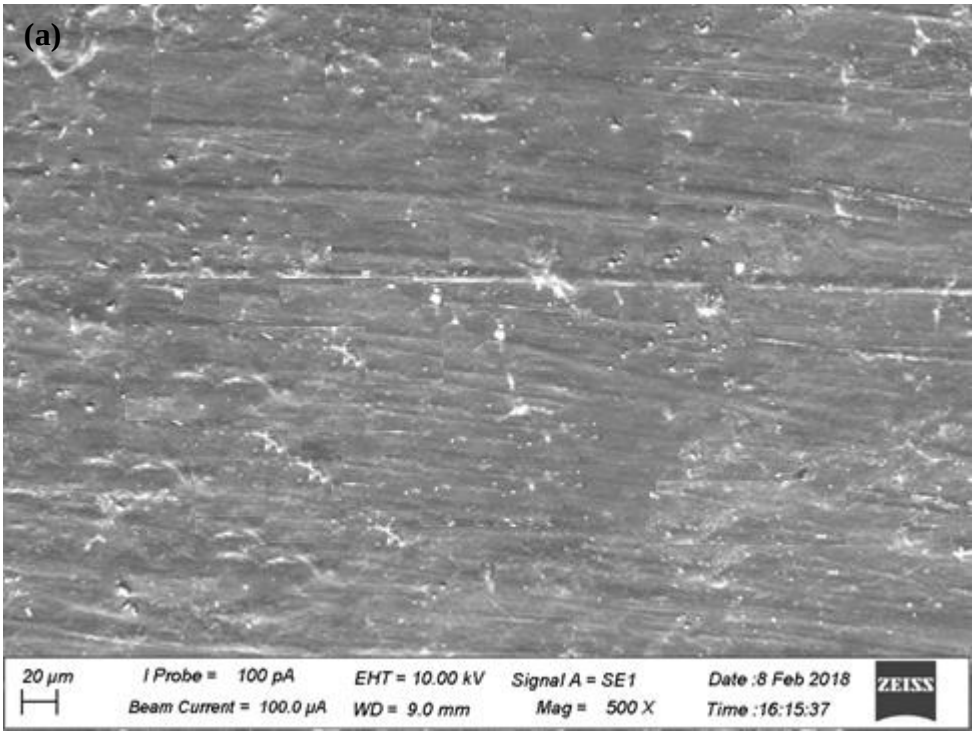

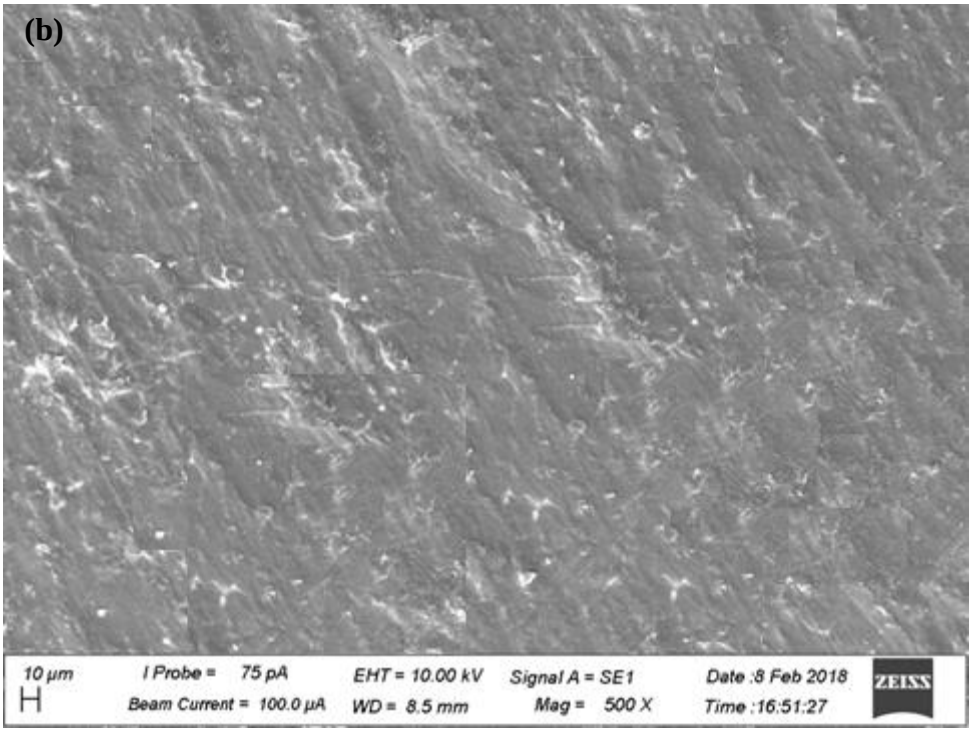

Figure 4.23: 500X magnified SEM images of composites (a) 2.5 % and (b) 3.0 % silane-modified NFC reinforced composites

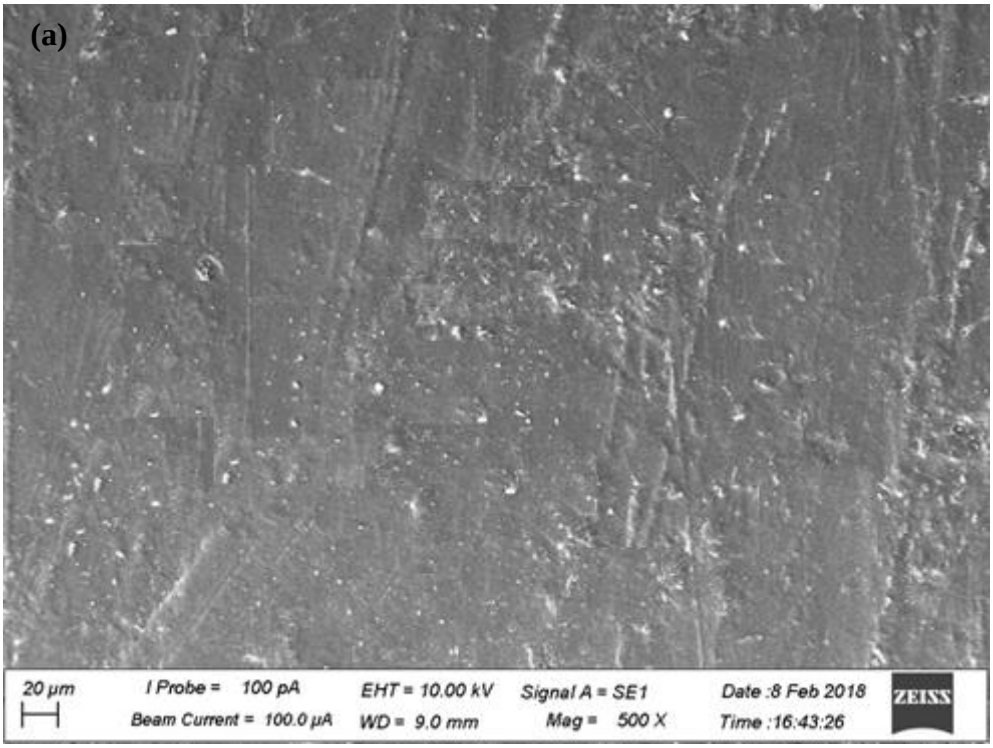

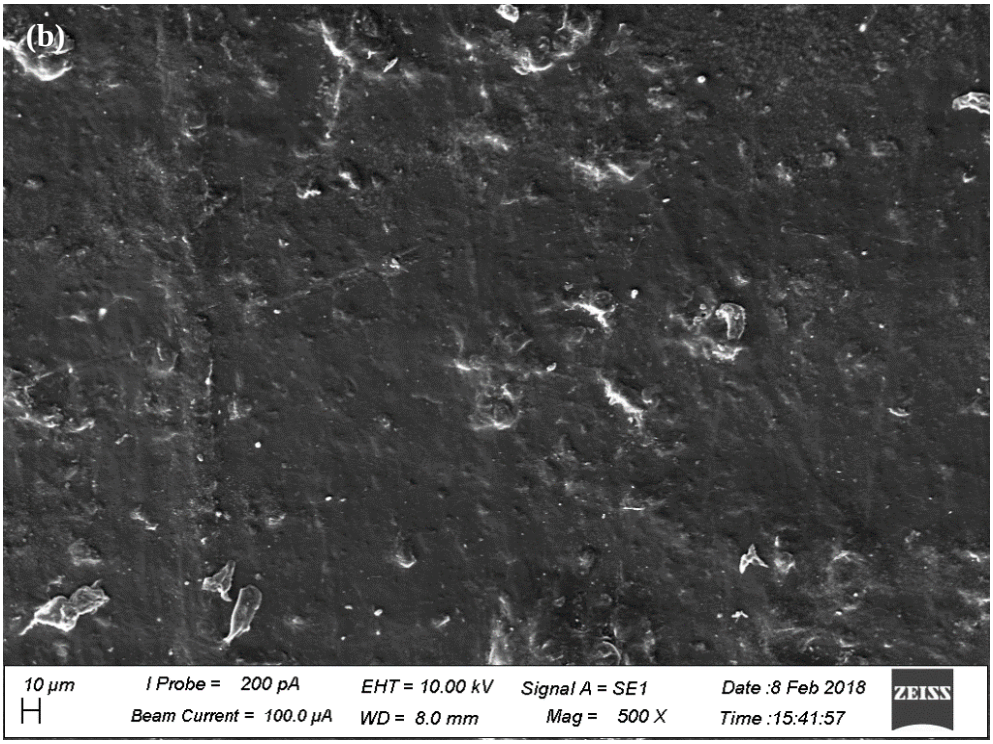

Figure 4.24: 500X magnified SEM images of composites (a) 3.5 % and (b) 4.0 % silane-modified NFC reinforced composites

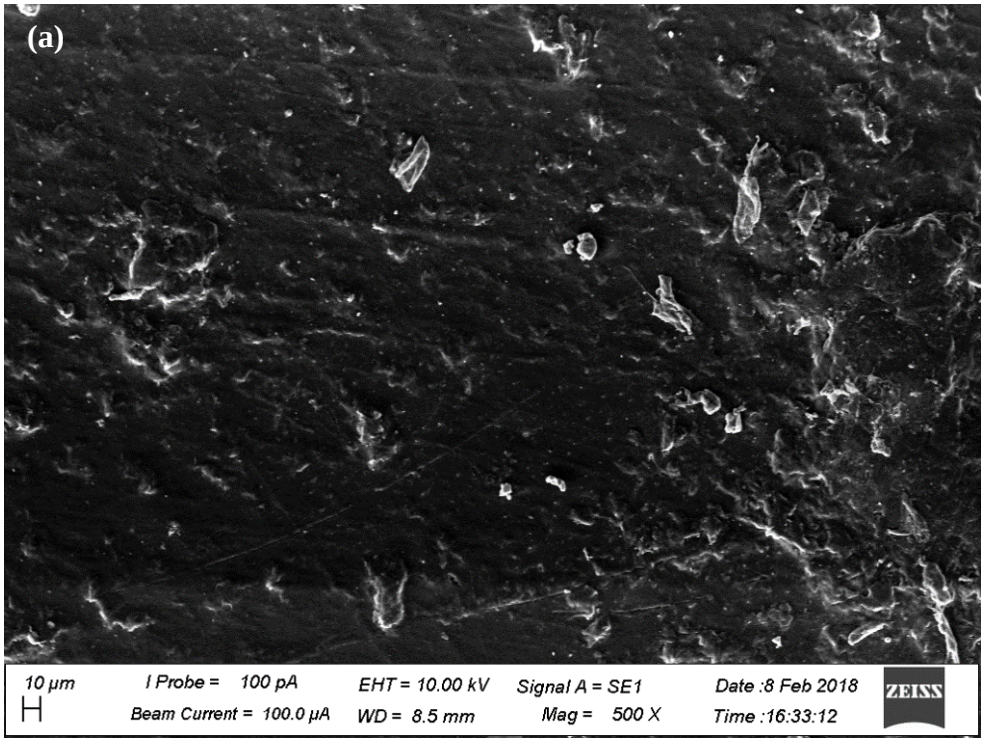

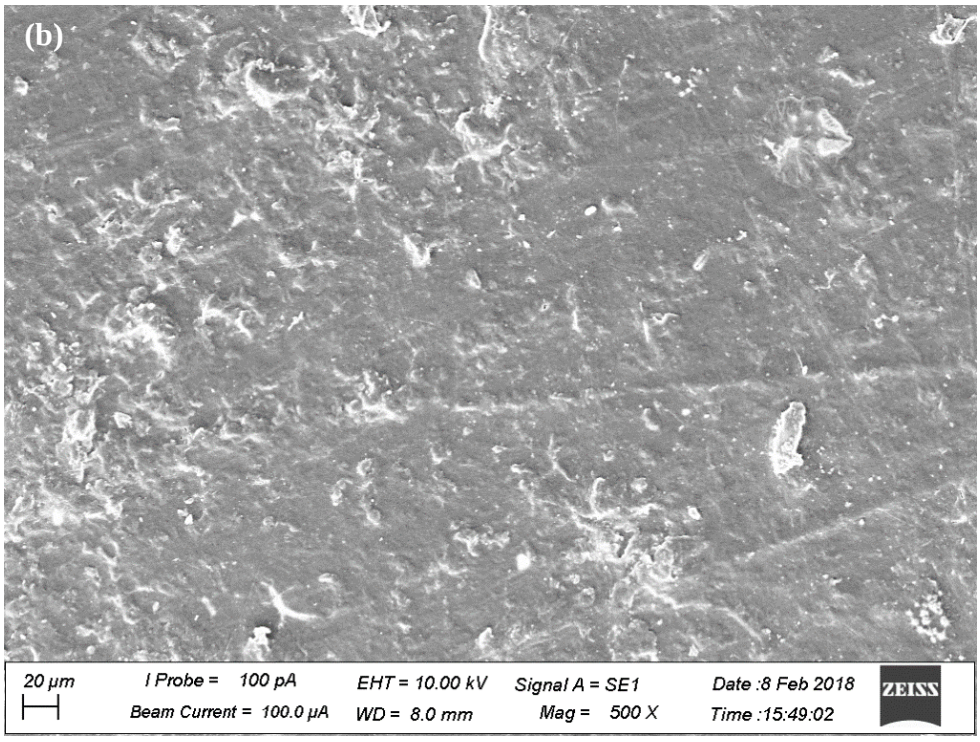

Figure 4.25: 500X modified SEM images of composites (a) 4.5 % and (b) 5.0 % silane-modified NFC reinforced composites

Silane-modified NFC reinforced composites have better morphological characteristics as far as 3.5% NFC loading. Further magnification of the Figure 4.24 (a) to 10 KX and 25 KX (Figure 4.26 (a) and (b)) can be clearly identified satisfactory amount of individualized nanoparticles of cellulose within the matrix. Therefore, the results imply a better reinforcement and it would lead to improve the properties of the 3.5% loaded NFC composite than the rest.

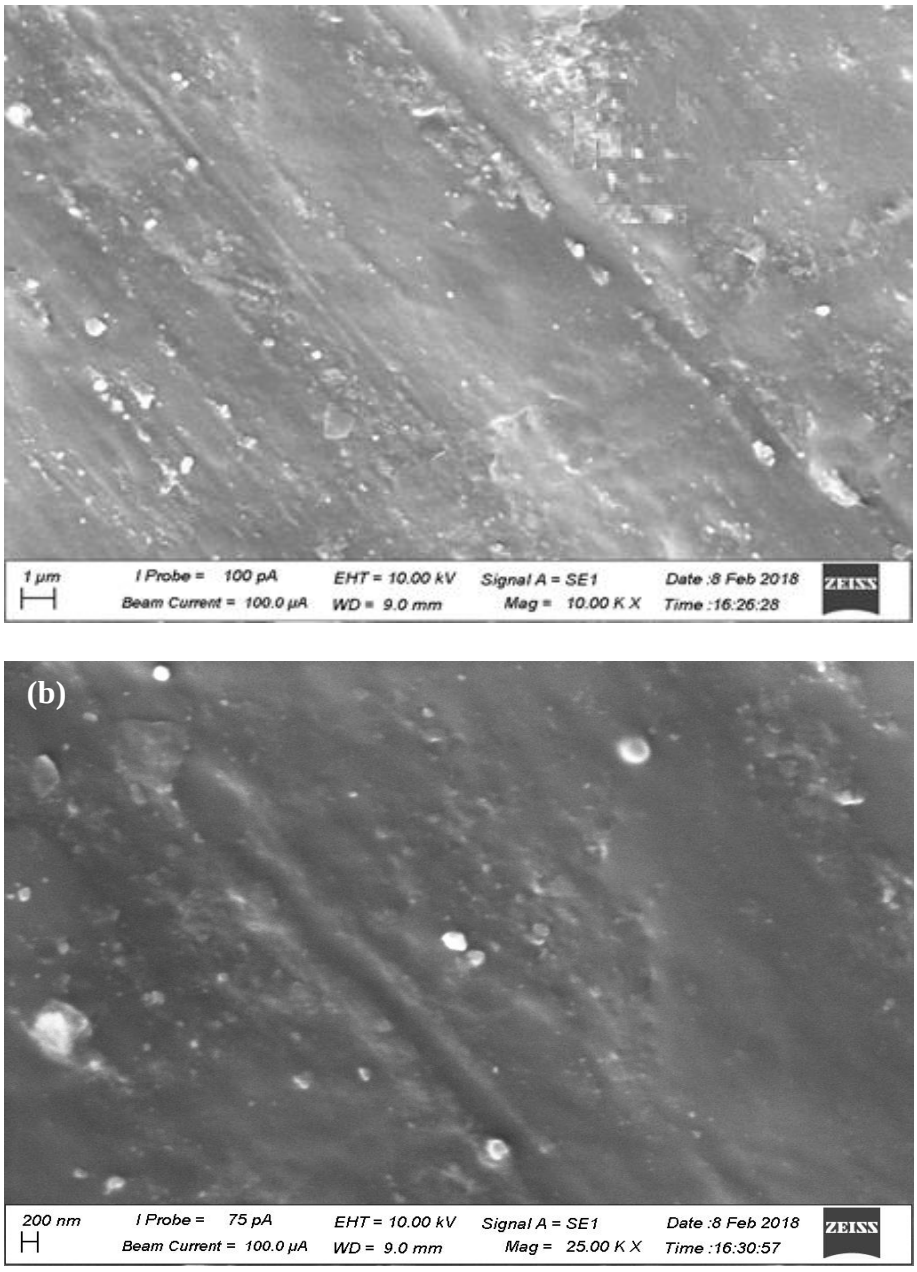

Figure 4.26: Magnified SEM images of 3.5% silane-modified NFC reinforced composites (a) 10 KX magnification (b) 25 KX magnification

However, a greater addition of silane-modified NFC to PP matrix accelerates the formation of NFC aggregates due to the reduction of favorable regions in the matrix. Therefore, Figure 4.24(b), Figure 4.25 (a) and (b) exhibit more clusters and the increase of aggregation of NFC content. The high magnification level of 5% NFC loaded sample (Figure 4.27) provides evidence for aggregation of nanocellulose particles.

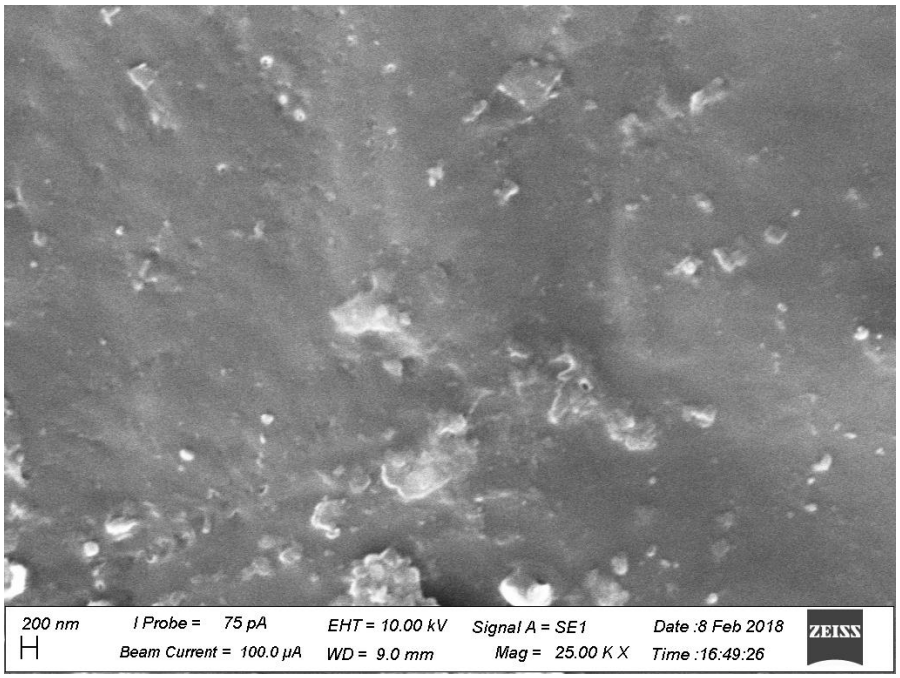

Figure 4.27: 25 KX magnified SEM image of 5% silane-modified NFC reinforced composites

4.3.2 FTIR

The normalized FTIR spectra comparison between pure PP and unmodified NFC (Appendix A) and silane-modified NFC (Appendix B) reinforced composite samples were most likely overlapped due to the presence of high amount of PP, however; a significant peak in between 1000-1100 cm^{-1} can be found only in composite materials. The peak intensity in unmodified NFC reinforced composites is higher than the same NFC percentage in modified NFC composites. The peak would be the

C-O-C stretching vibrations within the pyranose ring (1058.97 cm^{-1}). Therefore, the peak confirms the presence of NFC in the composites without changing the chemical structure. In addition, silane-modified NFC composites have improved intensities at low wavenumbers due to the presence of Si-O-C, Si-C and Si-O-Si bonds.

When comparing the two series of unmodified and silane-modified NFC reinforced composites together, 2.0% and 3.5% NFC reinforced composites are given the minimum absorbance of the four large PP characteristic peaks present in the wavenumber range 3000–2800 cm^{-1}, respectively (Appendix A and B). The Figure 4.28 shows the clear comparison between the normalized 2.0% unmodified and 3.5% silane-modified NFC composites in respect to surface modified NFC and pure PP. The composite samples contain characteristic peaks of PP and stretching vibrations C-O-C bond around 1060 cm^{-1}. However, the silane-modified NFC reinforced composite has low intensity at C-O-C stretching vibrations due to the restriction produce by the added large silane groups. In addition, the composite samples do not contain the -OH band. The results imply that the amount of –OH bonds present in the composites are comparatively very low in respect to -CH bonds.

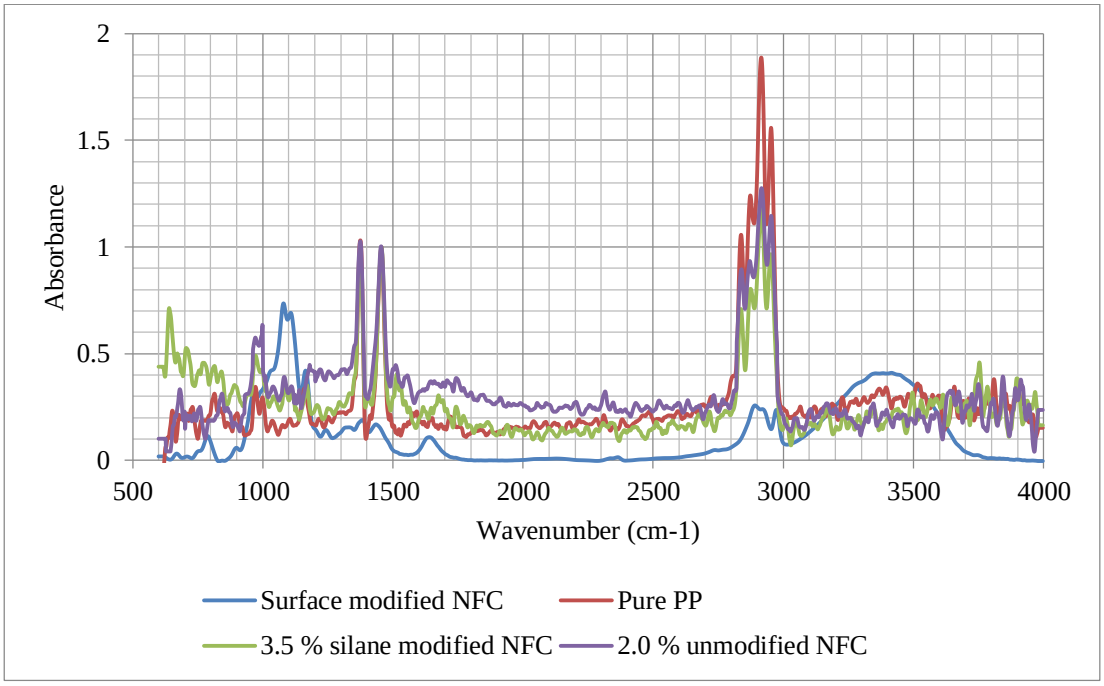

Figure 4.28: Comparison of FTIR spectra of normalized PP, silane-modified and unmodified 3.5 % NFC reinforced composites and surface modified NFC

4.3.3 Tensile strength

The tensile strength of pure PP and different ratios of surface modified and unmodified NFC reinforced PP composites are shown in Figure 4.29. In reference to the tensile strength of pure PP (24.7 MPa), all the composite samples with silane surface modification demonstrate high values. NFC reinforced composites from 0.5% to 3.5% NFC loadings indicate improved tensile strength and 3.5% NFC composite achieve the maximum amount of 27.8 MPa. After that, the tensile strength of samples decreases to 25.2 MPa (5% NFC sample). However, unmodified NFC reinforced composite series show a moderate reduction with the improvement of NFC percentage and the maximum value.

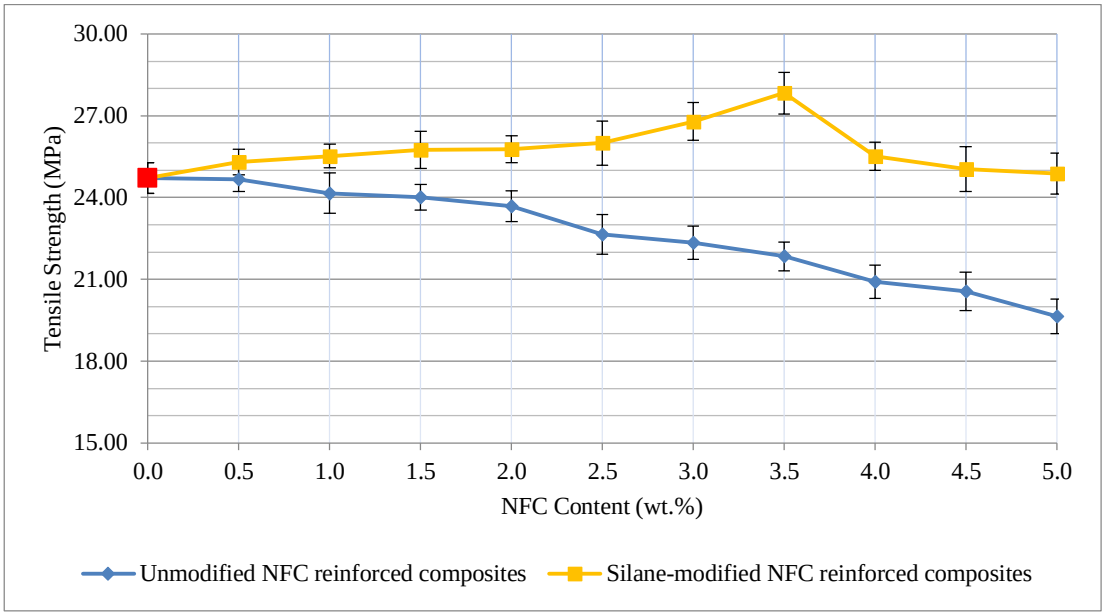

Figure 4.29: Comparison of the tensile strength of silane-modified and unmodified NFC reinforced composites

The improvement of the tensile strength of all the samples in the surface modified NFC composite series, prove the better adhesion between NFC and polypropylene matrix. Naturally, NFC is hydrophilic material because –OH groups present in the surface. The matrix PP is completely hydrophobic. Therefore, the surface modification of NFC, replace –OH groups in the NFC surface by adding hydrophobic silane groups. If the attachment is more powerful, NFC is acting as reinforcement to PP matrix and performs better than the pure PP. Therefore, the

results strongly imply that the surface modifier or Si-69 is acting as a compatibilizer and improve the compatibility between hydrophilic reinforcement and the hydrophobic matrix up to the addition of 3.5% of NFC. Then the tensile strength of higher reinforcement composites (4% to 5%) indicated slight decrement due to the agglomeration of NFC as a result of the reduction of hydrophobic silane groups in the surface.

The reduction of the tensile strength of all samples in unmodified NFC series emphasis the weak interfacial bonding between the filler and matrix. In addition, the formation of large NFC agglomerates due to the filler-filler interaction can be lead to reduce the mechanical properties because these agglomerates can act as stress raisers and begin to form cracks [233].

4.3.4 Elongation at break

Compared to pure PP, the addition of both modified and unmodified NFC to PP matrix reduce the material elongation percentage at break (Figure 4.30) because the addition of rigid filler can act as a barrier for dislocation motion. At higher loadings of NFC, reduce the distance between fillers and enhance the interaction with each other. Therefore, the elongations at break of high amount of unmodified NFC loaded samples are reduced as the increase of aggregation of rigid fillers. Further, the reduction of elongations at break for silane-modified NFC reinforced composites are comparatively higher than that of unmodified NFC composite series. The results suggest that increase of silane-modified NFC amount in PP matrix resulted in the reduction of ductility or the improvement of brittleness of composites. The outcome confirms the strong interfacial bonding between reinforcement and the matrix. Therefore, the silane-modification could create rigid interphase between the NFC and PP. Further, strong adhesion could bond more amounts of stiff filler to the matrix and indirectly, it would lead to increase the rigidity of the composite [234].

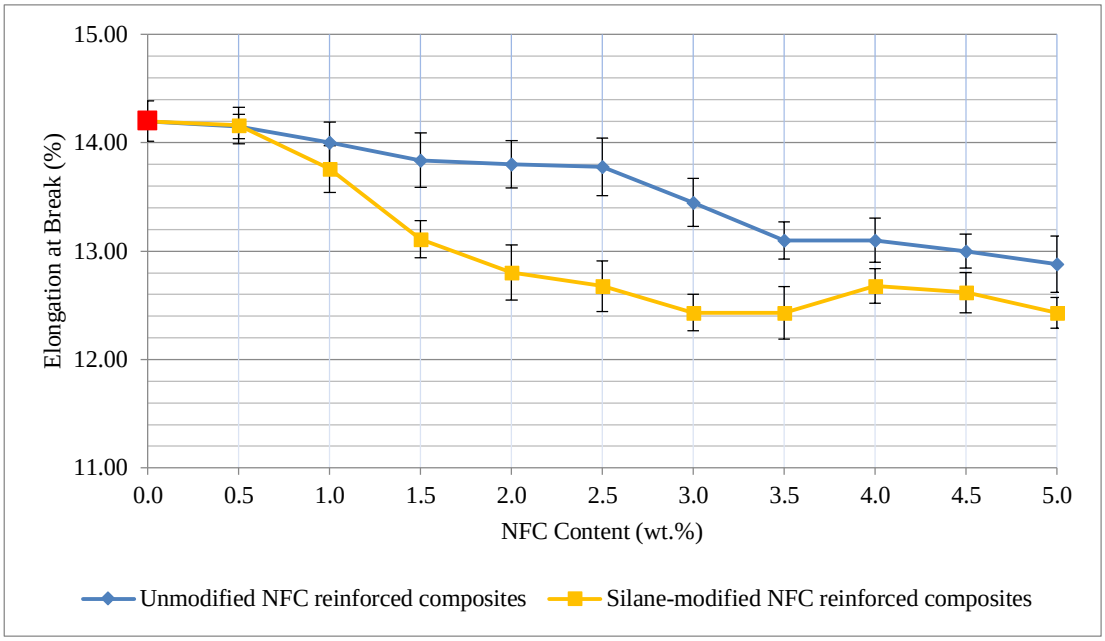

Figure 4.30: Comparison of elongation at break of silane-modified and unmodified NFC reinforced composites

4.3.5 Impact strength

Impact strength is the capability of a material to withstand a maximum sudden load could be applied without failure and is defined in terms of energy [235]. In respect to the impact strength of pure PP (2.16 kJ m^{-2}), a significant improvement was shown by the silane-modified NFC series than that of untreated NFC reinforced composites (Figure 4.31). The unmodified NFC composites have a slight improvement in low NFC loadings whereas less ability to absorb energy at higher NFC loadings because of the formation of aggregates. The maximum value (4.67 kJ m^{-2}) was achieved by the 5.0 % silane-modified NFC reinforced composite and it is more than two times higher than that of pure PP. The results clearly verified that Si-69 is acting as a perfect compatibilizer and create better interaction between hydrophobic PP matrix and hydrophilic NFC. The properties of a composite material are not only depending on fiber and matrix properties but also the interfacial bonds between fiber–matrix [236]. As the reason of formation of appreciable interfacial bonds, Si-69 is acting as a better load transferring material from matrix to fiber.

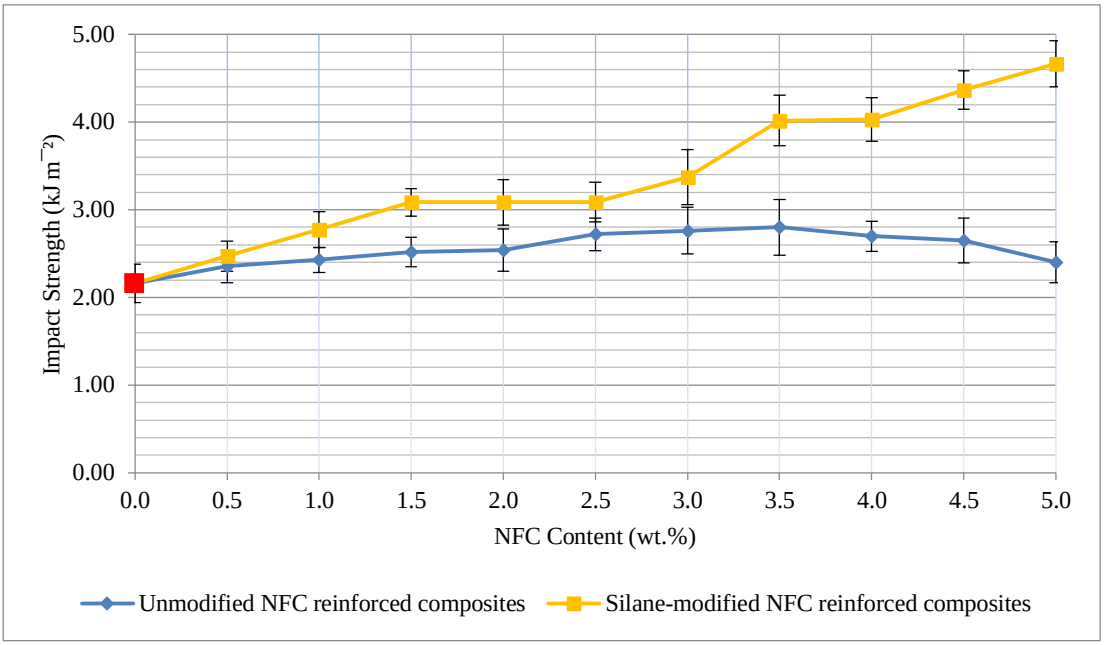

Figure 4.31: Comparison of Impact strength of silane-modified and unmodified NFC reinforced composites

4.3.6 Hardness

The hardness of a material generally defined as resistance to plastic deformation. All average hardness values of two composite series are higher than that of pure PP (Figure 4.32). Incorporation of NFC to the matrix improves the hardness of the material, however; untreated NFC reinforced series has slight improvement due to the incompatible nature. The addition of silane-modified NFC to PP matrix shows a considerable increase of the hardness up to 3.5% of NFC content and after that, a slight reduction was observed. Initially, the hardness value increased with an increase in modified NFC content due to the better interaction between NFC and PP matrix. The FTIR and XRD analysis prove that the matrix and reinforcement contain same crystallographic structures (monoclinic and triclinic). Therefore, NFC could be nicely packed within PP and improve the mechanical properties. However, the slight reduction of hardness at higher NFC loadings was observed. Beyond 3.5 wt.% of NFC incorporation may lead to improve the agglomeration in PP matrix and become difficult to achieve a homogeneous dispersion. In addition, silane-modified NFC reinforced composites are also sensitive for water molecules and may form

microcavities during the processing. Other than that, 3.5 wt.% may be the maximum percentage of fiber volume fraction witch interact with the matrix.

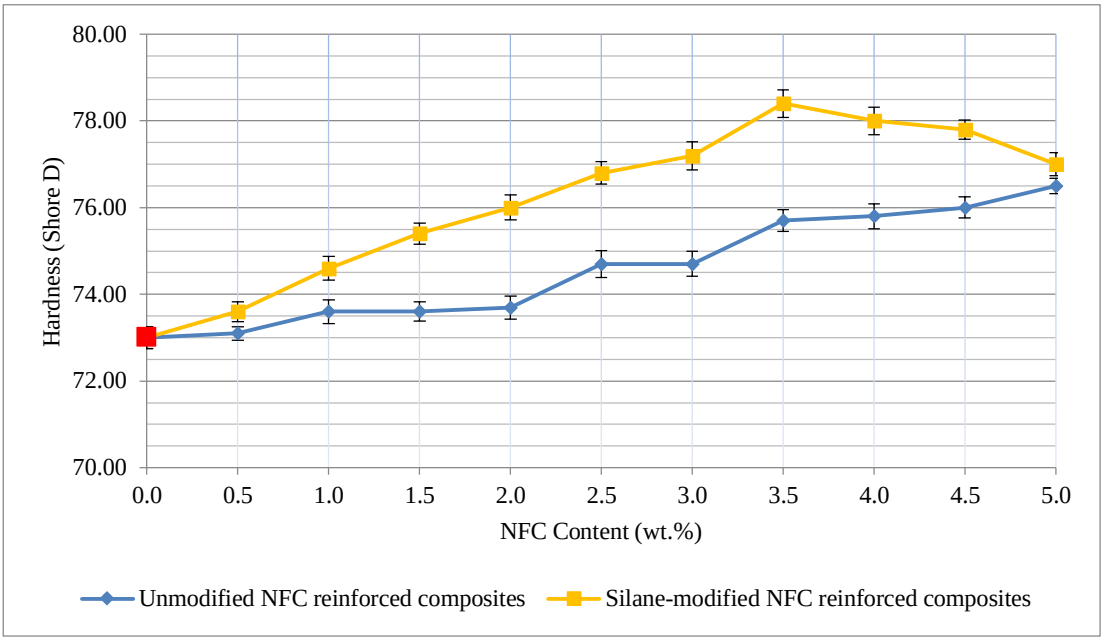

Figure 4.32: Comparison of the hardness of silane-modified and unmodified NFC reinforced composites

4.3.7 Water Absorption

Water absorption amount of silane-modified and unmodified NFC reinforced composites were shown in Figure 4.33. Out of the 20 samples, pure PP has the lowest level of water absorption (0.03%) due to the hydrophobic nature of the material. Nevertheless, the water absorption of silane-modified NFC composite series is lower than that of untreated NFC series because the hydrophilic characteristic of NFC was reduced by the replacement of –OH from silane groups. Practically, 100% of replacement could not be achieved and the surface modified NFC contains some water favorable –OH groups also. Therefore, the addition of modified NFC to pure PP leads to improve the water absorption. The analysis of water absorption is very important for dimensional stability as well as biodegradability. If the water absorption level is high means the dimensional stability is becoming low and biodegradability of the material is getting high because the presence of water creates low interfacial adhesion between fiber and matrix and then

the fibers become the food source of microbes in soil improve the biodegradability [237]. Therefore, it can be estimated that the 5.0 % untreated NFC loaded composite have the maximum biodegradable properties with low dimensional stability.

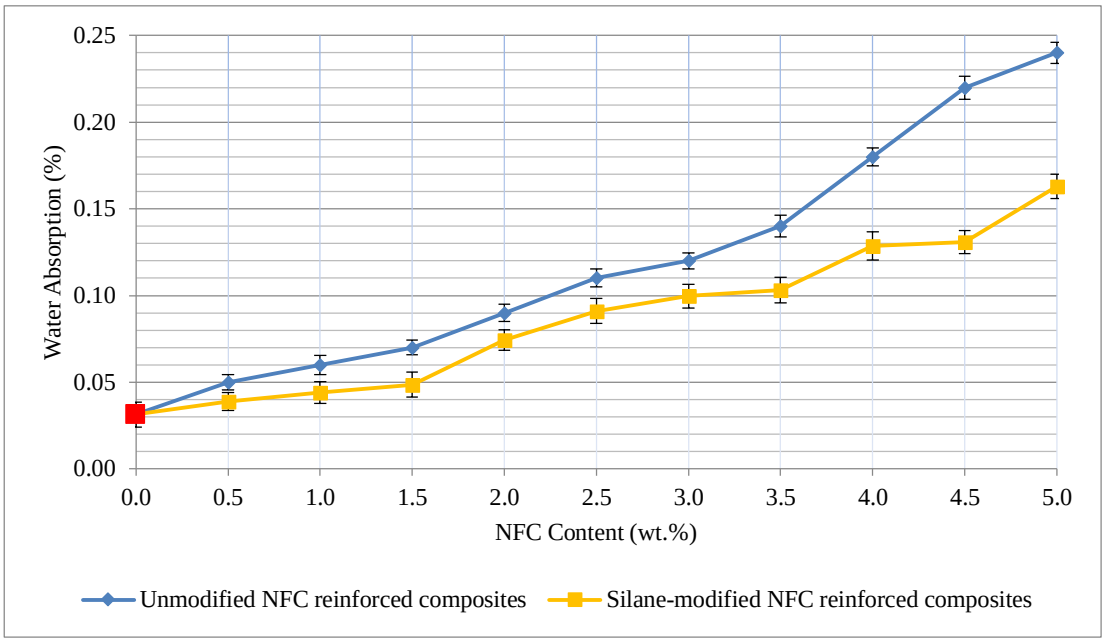

Figure 4.33: Comparison of water absorption percentage of silane-modified and unmodified NFC reinforced composites

4.3.8 TGA and DTA

Comparison between the TGA curves of pure PP and the two composite series samples are recorded in the appendix C and D and the curves were apparently overlapped except the 300-450 °C region. The results appeared due to the degradation of the reinforcement; because the degradation temperatures of unmodified and silane-modified NFC were identified in between 300-360 °C. Figure 4.34 provides evidence that degradation points of pure NFC lay in the same temperature of the onset as mass reduction of the composite materials.

In respect to pure PP, all the silane-modified NFC reinforced composites have improved thermal stability and the unmodified NFC reinforced composite series has a reduction of the thermal stability with improvement of NFC percentage because the surface modifier can act as a protective layer around NFC and prevent the thermal

energy and mass transfer between reinforcement and the melted matrix [238]. However, there is a slight reduction in thermal resistance at higher loadings of NFC due to the decline of interfacial interaction between the matrix and reinforcement. Therefore, the maximum thermal stability given by 3.5 % silane-modified NFC composite is significantly higher than the highest thermal stability represented by the 0.5 % unmodified NFC reinforced composite (Figure 4.34).

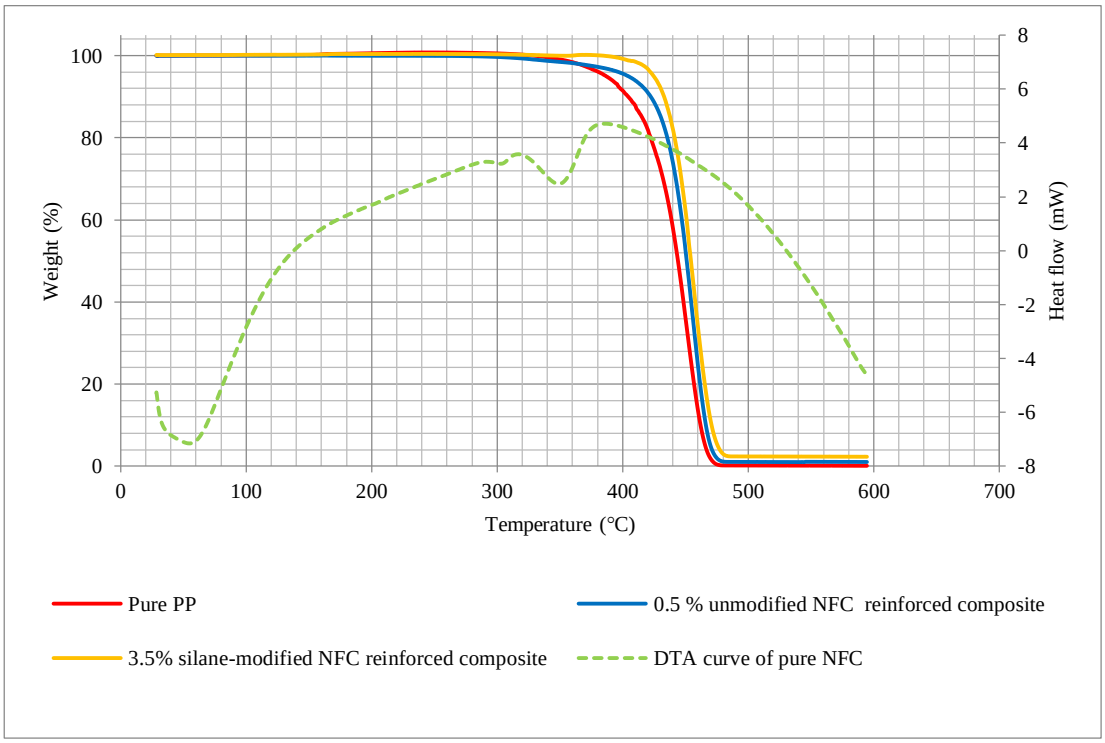

Figure 4.34: Comparison between the TGA graphs of pure PP, 0.5 % unmodified and 3.5% silane-modified NFC composites and the DTA curve of pure NFC

Moreover, the DTA curves of all samples (Appendix E and F) state some facts to prove the advancement of thermal resistance of some composite samples than the pure PP. There is no direct relationship between the melting point and thermal stability; however, enthalpy or the area beneath the exothermic peak high means the improvement of heat stability. Figure 4.35 focus on the calculated decomposition point area of all DTA curves in two series and the highest enthalpy of untreated NFC reinforce composites given by 0.5% loading of NFC which is significantly lower than then maximum enthalpy of 3.5 % silane-modified NFC composite. Therefore,

3.5% NFC composite express the maximum thermal resistance and further proves the thermal stability induce by the silane Si-69 surface modifier.

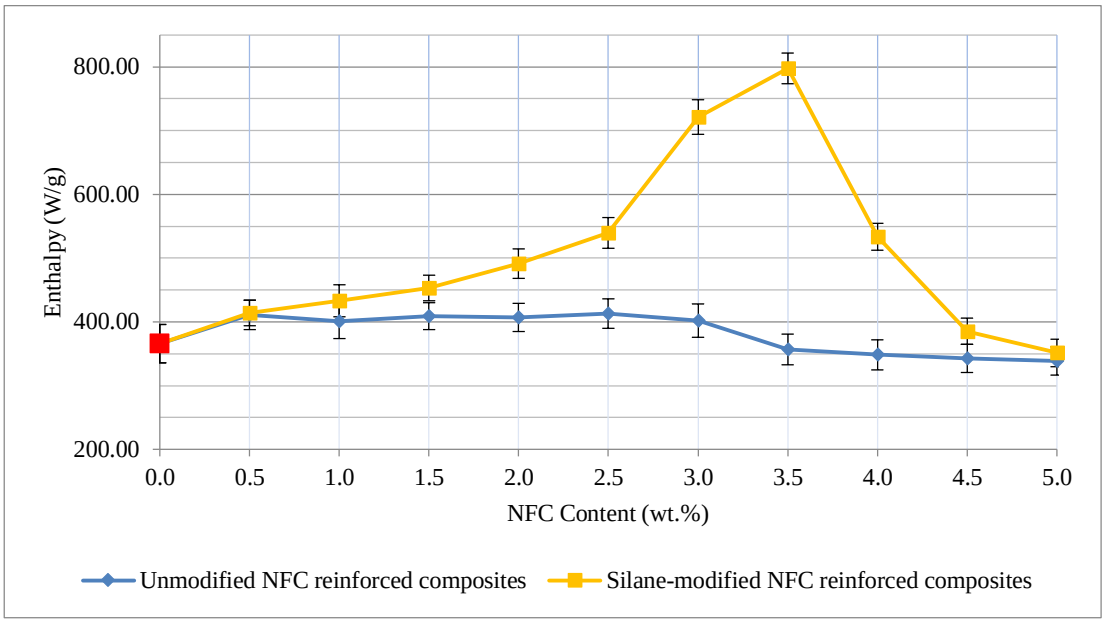

Figure 4.35: Comparison of Enthalpy of silane-modified and unmodified NFC reinforced composites

4.3.9 Melt flow index

Melt flow index (MFI) measures the flow properties of polymeric materials at processing temperature under standard load. The MFI is indirectly proportional to the viscosity and molecular weight of the material [239]. The high MFI values imply the low viscosity, therefore; energy needed to process a material is low. Economically it is good; however, mechanical properties of the final product may reduce due to the reduction of molecular weight. Furthermore, materials with very low MFI values are worthless because of the requirement of a high amount of energy in the processing. Therefore, it is very important to select a material with better MFI value, which should be high enough to easily flow and low enough to better mechanical properties.

According to the Figure 4.37, increase of both unmodified and silane-modified NFC amount in the composite; lead to reduce the MFI values. The test was carried at 230 ^{0}C and the melting point of pure PP is 165 ^{0}C. Therefore, it can be assumed that at 230 ^{0}C, pure PP is completely in the melting state whereas NFC is in the solid phase.

Therefore, NFC contains strong internal bonds with respect to matrix PP molecules and surface modified NFC has even more thermal stability due to the silane cover around particles. As a result of that, MFI of silane-modified NFC reinforced composites slightly improves the viscosity and reduces the MFI value. However, the variation between MFI values of pure PP and composites are low. Therefore, the addition of both modified and unmodified forms of NFC to pure PP were not given a significant change in the processing of the material.

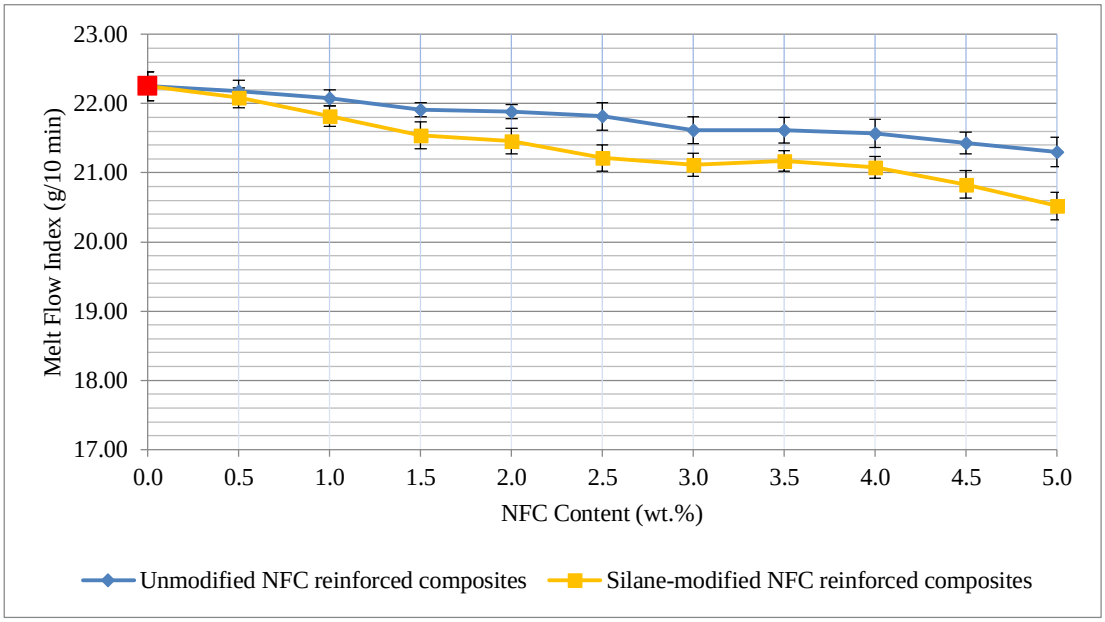

Figure 4.36: Comparison of melt flow index of silane-modified and unmodified NFC reinforced composites

5 CONCLUSIONS

The research is focused to improve the properties of pure polypropylene by producing a composite material reinforcing with NFC. The two different series of composites were used to compare the effect of surface modification of NFC on the properties. In respect to the properties of pure PP, the experimental results emphasis the wide improvement of mechanical and thermal properties with extremely narrow reduction of water absorption and processability of silane surface modified NFC based polypropylene than that of untreated NFC reinforced composites. It explains that the silane surface modification crate better interaction between NFC and matrix. The 3.5 wt.% silane-modified NFC reinforced PP sample showed the uniform distribution of reinforcement in the PP matrix with highest thermal resistance and mechanical properties including tensile strength (27.8 MPa) and hardness (78.4 shore D) with moderate impact strength (4.02 kJ m^{-2}) and average level of water absorption (0.1%) and processability (21.1 g/10 min). Therefore, 3.5 wt.% of silane Si-69 surface modified NFC was given the optimum level of reinforcement for isostatic polypropylene matrix.

References List

[1] D. Ndiaye and A. Tidjani, "Physical changes associated with gamma doses on Wood/ Polypropylene composites," in *2014 Global Conference on Polymer and Composite Materials: Materials Science and Engineering*, 2014.

[2] J. Pritchard, "Introduction to Polyolefins," in *Polyolefin Reaction Engineering*, Wiley-VCH Verlag GmbH & Co. KGaA, 2012, pp. 1-13.

[3] D. N. Bikiaris, G. Z. Papageorgiou, E. Pavlidou, N. Vouroutzis, P. Palatzoglou and G. P. Karayannidis, "Preparation by melt mixing and characterization of isotactic polypropylene/SiO2 nanocomposites containing untreated and surface-treated nanoparticles," *Applied Polymer Science,* vol. 100, no. 4, p. 2684–2696, 2006.

[4] A. H. W. O. Sandaruwan and A. M. P. B. Samarasekara, "Preparation of biodegradable polymer materials using agricultural waste," in *International forestry and environment symposium*, 2012.

[5] A. M. P. B. Samarasekara and E. A. P. C. D. Jayasuriya, "Synthesis of biodegradable polyolefines based polymer composites using degradable natural materials," in *International forestry and environment symposium*, 2014.

[6] S. Umadaran, P. Somasuntharam and A. M. P. B. Samarasekara, "Preparation and characterization of cellulose and hemicellulose based degradable composite material using sugarcane waste," in *Moratuwa Engineering Research Conference*, 2016.

[7] K. D. H. N. Kahawita and A. M. P. B. Samarasekara, "Extraction and characterization of cellulose fibers form sawmill waste," in *Moratuwa Engineering Research Conference*, 2016.

[8] M. Nanayakkara, W. G. A. Pabasara, A. M. P. B. Samarasekara, D. A. S. Amarasinghe and L. Karunanayake, "Synthesis and characterization of cellulose from lacally available rice straw," in *Moratuwa Engineering Research Conference* , 2017.

[9] D. R. Paul and L. M. Robeson, "Polymer nanotechnology: Nanocomposites," *Polymer,* vol. 49, no. 15, pp. 3187-3204, 2008.

[10] K. Missoum, M. N. Belgacem and J. Bras, "Nanofibrillated Cellulose Surface Modification: A Review," *Materials* , vol. 6, no. 5, pp. 1745-1766, 2013.

[11] Y. Habibi, "Key advances in the chemical modification of nanocelluloses," *chemical society reviews* , vol. 43, pp. 1519--1542, 2014.

[12] "Manufacturing: Materials and Processing," in *Polymer Science and Engineering: The Shifting Research Frontiers*, Washington, The National

Academies Press, 1994, pp. 65-115.

[13] M. Ghanta, D. Fahey and B. Subramaniam, "Environmental impacts of ethylene production from diverse feedstocks and energy sources," *Applied Petrochemical Research,* vol. 4, no. 2, p. 167–179, 2014.

[14] "Material Properties of Plastics," in *Laser Welding of Plastics*, Wiley-VCH Verlag GmbH & Co. KGaA, 2011, pp. 3-69.

[15] J. Jancar, "Structure-property relationships in thermoplastic matrices," in *Mineral Fillers in Thermoplastics I: Raw Materials and Processing*, New York, Springer, 1999, pp. 1-65.

[16] A. Farshi, "Propylene Production Methods And FCC Process Rules In Propylene Demands," in *12th chemical engineering conference*, Iran, 2008.

[17] L. A. Castonguay and A. K. Rappe, "Ziegler-Natta catalysis. A theoretical study of the isotactic polymerization of propylene," *Journal of the American Chemical Society,* vol. 114, no. 14, p. 5832–5842, 1992.

[18] H. A. Maddah, "Polypropylene as a Promising Plastic: A Review," *American Journal of Polymer Science,* vol. 6, no. 1, pp. 1-11, 2016.

[19] R. Crawford and J. L. Throne, "Rotational Molding Polymers," in *Rotational Molding Technology*, New York, William Andrew publishers, 2002, pp. 19-65.

[20] J. M. Garcia-Martinez, S. Areso, J. Taranco and E. P. Collar, "Atactic polypropylene from industrial by-Product to high added value material for advanced application through chemical modification processes," in *1st Spanish National Conference on Advances in Materials Recycling and Eco – Energy* , Madrid, 2009.

[21] R. Shanks, "Technology of polyolefin film production," in *Handbook of Plastic Films*, E. M. Abdel-Bary, Ed., Rapra Technology Limited, 2003, pp. 5-38.

[22] J. A. Brydson, Plastics Materials, 6 ed., Oxford: Butterworth-Heinemann , 1995.

[23] X. Zhang and G. Shi, "Effect of converting the crystalline form from α to β on the mechanical properties of ethylene/propylene random and block copolymers," *Polymer,* vol. 35, no. 23, pp. 5067-5079, 1994.

[24] D. Chandramohan and K. Marimuthu, "A Review on Natural Fibers," *International Journal of Recent Research and Applied Studies,* vol. 8, no. 2, pp. 194-206, 2011.

[25] M. J. John and S. Thomas, "Biofibres and biocomposites - A Review," *Carbohydrate Polymers,* vol. 71, p. 343–364, 2008.

[26] K. L. Pickering, M. G. A. Efendy and T. M. Le, "A review of recent developments in natural fibre composites and their mechanical performance," *Composites Part A: Applied Science and Manufacturing,* vol. 83, pp. 98-112, April 2016.

[27] B. H. Davison, J. Parks, M. F. Davis and B. S. Donohoe, "Plant Cell Walls: Basics of Structure, Chemistry, Accessibility and the Influence on Conversion," in *Aqueous Pretreatment of Plant Biomass for Biological and Chemical Conversion to Fuels and Chemicals*, C. E. Wyman, Ed., New York, Wiley, 2013, pp. 23-26.

[28] J. Perez, J. Munoz-Dorado, T. D. L. Rubia and J. Martinez, "Biodegradation and Biological Treatments of Cellulose, Hemicellulose and Lignin," *International Microbiology,* vol. 5, pp. 53-63, April 2002.

[29] "Chemical Composition and Structure of Natural Lignocellulose," in *Biotechnology of Lignocellulose: Theory and Practice* , Beijing, Chemical Industry press , 2014, pp. 25-71.

[30] T. Heinze, "Cellulose: Structure and Properties," in *Cellulose Chemistry and Properties: Fibers, Nanocellulose and Advanced Materials*, O. J. Rojas, Ed., Springer, 2015, pp. 1-52.

[31] H. A. Krässig, Cellulose: structure, accessibility and reactivity, Amsterdam: Gordon and Breach Science, 1996.

[32] H. Krässig, J. Schurz, R. G. Steadman, K. Schliefer, W. Albrecht, M. Mohring and H. Schlosser, "Cellulose," in *Ullmann's Encyclopedia of Industrial Chemistry*, John Wiley & Sons, 2004.

[33] D. Lavanya, P. K. Kulkarni, M. Dixit, P. K. Raavi and L. N. V. Krishna, "Source of Cellulose and Their Applications - A Review," *International Journal of Drug Formulation and Research,* vol. 2, no. 6, pp. 19-38, December 2011.

[34] D. Klemm, D. Schumann, U. Udhardt and S. Marsch, "Bacterial synthesized cellulose - artificial blood vessels for microsurgery," *Progress in Polymer Science,* vol. 26, pp. 1561-1603, 2001.

[35] I. M. Saxena and R. M. Brown, "Cellulose Biosynthesis: Current Views and Evolving Concepts," *Annals of Botany,* vol. 96, pp. 9-21, May 2005.

[36] M. Hummel, A. Michud, M. Tanttu, S. Asaadi, Y. Ma, L. K. J. Hauru, A. Parviainen, A. W. T. King, I. Kilpelainen and H. Sixta, "Ionic Liquids for the Production of Man-Made Cellulosic Fibers: Opportunities and Challenges," in *Advances in Polymer Science*, Cham, Springer International Publishing, 2015, pp. 133-168.

[37] J. Roesler, H. Harders and M. Baeker, Mechanical Behaviour of Engineering

Materials: Metals, Ceramics, Polymers and Composites, 1 ed., New York: Springer, 2007.

[38] D. Hayes, Fwbruary 2010. [Online]. Available: http://www.carbolea.ul.ie/wood.php.

[39] T. Heinze, "Cellulose: Structure and Properties," in *Advances in Polymer Science*, cham, Springer International Publishing, 2016, pp. 1-52.

[40] N. E. El-Naggar, S. Deraz and A. Khalil, "Bioethanol Production from Lignocellulosic Feedstocks Based on Enzymatic Hydrolysis: Current Status and Recent Developments - Review Article," *Biotechnology,* vol. 13, no. 1, pp. 1-21, 2014.

[41] S. Kavesh and J. M. Schultz, "Meaning and Measurement of Cystallinity in Polymers: A Review," *Polymer Engineering and Science,* vol. 9, no. 5, pp. 331-338, 1969.

[42] R. J. Moon, A. Martini, J. Nairn, J. Simonsenf and J. Youngblood, "Cellulose nanomaterials review: structure, properties and nanocomposites," *The royal society of chemistry,* vol. 40, p. 3941–3994, 2011.

[43] J. L. Wertz and O. Bédué, Lignocellulosic Biorefineries, Lausanne: EPEL press, 2013.

[44] A. K. Bledzki, A. A. Mamun, M. Lucka-Gabor and V. S. Gutowski, "The effects of acetylation on properties of flax fibre and its polypropylene composites," *Express Polymer Letters,* vol. 2, no. 6, pp. 413-422, 2008.

[45] T. Saito, R. Kuramae, J. Wohlert, L. A. Berglund and A. Isogai, "An Ultrastrong Nanofibrillar Biomaterial: The Strength of Single Cellulose Nanofibrils Revealed via Sonication-Induced Fragmentation," *Biomacromolecules,* vol. 14, no. 1, p. 248–253, 2013.

[46] D. J. Gardner, G. S. Oporto, R. Mills and M. A. S. A. Samir, "Adhesion and Surface Issues in Cellulose and Nanocellulose," *Adhesion Science and Technology,* vol. 22, p. 545–567, 2008.

[47] M. P. Ansell and L. Y. Mwaikambo, "The structure of cotton and other plant fibers," in *Handbook of Textile Fibre Structure,* Washington, CRC press, 2009, pp. 62-94.

[48] S. Iqbal and Z. Ahmad, "Impact of Degree of Polymerization of Fiber on Viscose Fiber Strength," The swedish school of textiles, University of Boras, Gothenburg, 2011.

[49] N. Shiraishi, "Wood Plasticization," in *Wood and Cellulosic Chemistry,* D. N. S. Hon and N. Shiraishi, Eds., New York, CRC, 2000, pp. 655-700.

[50] M. V. Ramiah, "Thermogravimetric and differential thermal analysis of cellulose, hemicellulose and lignin," *Applied Polymer Science,* vol. 14, no. 5, p. 1323–1337, May 1970.

[51] M. V. Ramiah and D. A. I. Goring, "The thermal expansion of cellulose, hemicellulose, and lignin," *Journal of Polymer Science: Polymer Symposia,* vol. 11, no. 1, p. 27–48 , 1965.

[52] L. Szczes, A. Rachocki and J. Tritt-Goc, "Glass transition temperature and thermal decomposition of cellulose powder," *Cellulose,* vol. 15, p. 445–451, 2008.

[53] J. H. Kwon, S. B. Park, N. Ayrilmis, S. W. Oh and N. H. Kim, "Effect of carbonization temperature on electrical resistivity and physical properties of wood and wood-based composites," *Composite: Part B,* vol. 46, pp. 102-107, 2013.

[54] G. I. Torgovnikov, Dielectric Properties of Wood and Wood-Based Materials, T. E. Timell, Ed., New York: Springer-Verlag, 1993.

[55] B. Ellis and R. Smith, Eds., Polymers: A Property Database, New York: CRC press, 2009.

[56] H. P. S. A. Khalil, Y. Davoudpour, M. N. Islam, A. Mustapha, K. Sudesh, R. Dungani and M. Jawaid, "Production and madification of nanofibrillated celllulose using various mechanical processes: A Review," *Carbohydrate Polymers,* pp. 649-665, 2014.

[57] R. Anderson, J. W. Owens and C. W. Timms, "The toxicity of purified cellulose in studies with laboratory animals," *Cancer Letters,* vol. 63, no. 2, pp. 83-92, April 1992.

[58] S. Kalia, B. S. Kaith and I. Kaur, "Pretreatments of natural fibers and their application as reinforcing material in polymer composites—A review," *Polymer Engineering Science,* vol. 49, no. 7, p. 1253–1272, 2009.

[59] A. Dufresne, "Nanocellulose: a new ageless bionanomaterial," *Materials Today,* vol. 16, no. 6, pp. 220-227, June 2013.

[60] L. Nielsen, S. Eyley, W. Thielemans and J. Aylott, "Dual Fluorescent Labelling of Cellulose Nanocrystals for pH sensing," *chemical communications,* vol. 46, no. 47, p. 8929–8931, 2010.

[61] L. Zhang, Q. Li, J. Zhou and L. Zhang, "Synthesis and Photophysical Behavior of Pyrene-Bearing Cellulose Nanocrystals for Fe3+ Sensing," *Macromolecular Chemistry and Physics,* vol. 213, no. 15, p. 1612–1617, 2012.

[62] X. Du, Z. Zhang, W. Liu and Y. Deng, "Nanocellulose-based conductive materials and their emerging applications in energy devices - A review," *Nano*

Energy, vol. 35, pp. 299-320, 2017.

[63] Y. Zhou, T. Khan, J.-C. Liu, C. Fuentes-Hernandez, J. Shim, E. Najafabadi, J. Youngblood, R. Moon and B. Kippelen, "Efficient recyclable organic solar cells on cellulose nanocrystal substrates with a conducting polymer top electrode deposited by film-transfer lamination," *Organic Electronics,* vol. 15, pp. 661-666, 2014.

[64] L. Hu, N. Liu, M. Eskilsson, G. Zheng, J. McDonough, L. Wågberg and Y. Cui, "Silicon-conductive nanopaper for Li-ion batteries," *Nano Energy,* vol. 2, no. 1, p. 138–145, 2013.

[65] Y. Jung, T. Chang, H. Zhang, C. Yao, Q. Zheng, V. Yang, H. Mi, M. Kim, S. Cho, D. Park, H. Jiang, J. Lee, Y. Qiu, W. Zhou, Z. Cai, S. Gong and Z. Ma, "High-performance green flexible electronics based on biodegradable cellulose nanofibril paper," *Nature Communication,* vol. 6, pp. 1-11, 2015.

[66] J. Huang, H. Zhu, Y. Chen, C. Preston, K. Rohrbach, J. Cumings and L. Hu, "Highly transparent and flexible nanopaper transistors," *ACS Nano,* vol. 7, no. 3, p. 2106–2113, 2013.

[67] H. Yagyu, T. Saito, A. Isogai, H. Koga and M. Nogi, "Chemical Modification of Cellulose Nanofibers for the Production of Highly Thermal Resistant and Optically Transparent Nanopaper for Paper Devices," *ACS Applied Materials and Interfaces,* vol. 7, no. 39, p. 22012–22017, 2015.

[68] H. Oulachgar, M. Bolduc, G. Chauve, Y. Desroches, P. Beaupre, J. Bouchard and P. Galarneau, "Fabrication and Electro-Optical Characterization of a Nanocellulose-Based Spatial Light Modulator," *Biomaterials and Softmaterials,* vol. 1, no. 10, pp. 631-637, 2016.

[69] Y. Okahisa, A. Yoshida, S. Miyaguchi and H. Yano, "Optically transparent wood–cellulose nanocomposite as a base substrate for flexible organic light-emitting diode displays," *Composites Science and Technology,* vol. 69, no. 11–12, pp. 1958-1961, 2009.

[70] R. Sabo, A. Yermakov, C. T. Law and R. Elhajjar, "Nanocellulose-Enabled Electronics, Energy Harvesting Devices, Smart Materials and Sensors: A Review," *Journal of Renewable Materials* , vol. 4, no. 5, pp. 297-312, 2016.

[71] R. Sabo, J. H. Seo and Z. Ma, "Cellulose nanofiber composite substrates for flexible electronics," in *2012 TAPPI International Conference on Nanotechnology for Renewable Materials*, Montreal, 2012.

[72] S. Couderc, O. Ducloux, B. J. Kim and T. Someya, "A mechanical switch device made of a polyimide-coated microfibrillated cellulose sheet," *Journal of Micromachanics and Microengineering,* vol. 19, no. 5, 2009.

[73] H. Koga, T. Saito, T. Kitaoka, M. Nogi, K. Suganuma and A. Isogai,

"Transparent, Conductive, and Printable Composites Consisting of TEMPO-Oxidized Nanocellulose and Carbon Nanotube," *Biomacromolecules,* vol. 14, no. 4, p. 1160–1165, 2013.

[74] Q. Li, "Nanocellulose: Preparation, Characterization, Supramolecular Modelling, and its Life Cycle Assesment," Virginia, 2012.

[75] I. Sakurada, Y. Nukushina and T. Ito, "Experimental Determination of Elastic Moduli of the Crystalline Regions in Oriented Polymers," *Journal of Polymer Science,* vol. 57, no. 165, pp. 651-660, March 1962.

[76] V. K. Rastogi and P. Samyn, "Bio-Based Coatings for Paper Applications," *Coatings,* vol. 5, pp. 887-930, November 2015.

[77] H. V. Lee, S. B. A. Hamid and S. K. Zain, "Conversion of Lignocellulosic Biomass to Nanocellulose: Structure and Chemical Process," *The Scientific World Journal,* pp. 1-20, August 2014.

[78] L. Brinchi, F. Cotana, E. Fortunati and J. M. Kenny, "Production of Nanocrystalline Cellulose from Lignocellulosic Biomass: Technology and Applications," *Carbohydrate Polymer,* vol. 94, no. 1, pp. 154-169, April 2013.

[79] Y. W. Chen, T. H. Tan, H. V. Lee and S. B. A. Hamid, "Easy Fabrication of Highly Thermal-Stable Cellulose Nanocrystals Using Cr(NO3)3 Catalytic Hydrolysis System: A Feasibility Study from Macro to Nano Dimentions," *Materials,* vol. 10, no. 42, pp. 1-24, January 2017.

[80] S. Schubert, K. Schlufter and T. Heinze, "Configurations, Structures and Morpologies of Cellulose," in *Polysaccharides in Medicinal and Pharmaceutical Applications*, V. Popa, Ed., shropshire, iSmithers, 2011, pp. 1-56.

[81] R. Weishaupt, G. Siqueira, M. Schubert, P. Tingaut, K. Maniura-Weber, T. Zimmermann, L. Thöny-Meyer, G. Faccio and J. Ihssen, "TEMPO-Oxidized Nanofibrillated Cellulose as a High Density Carrier for Bioactive Molecules," *Biomacromolecules,* vol. 16, p. 3640−3650, 2015.

[82] M. Ioelovich, "Characterization of Various Kinds of Nanocellulose," in *Handbook of Nanocellulose and Cellulose Nanocomposites*, H. Kargarzadeh, I. Ahmad, S. Thomas and A. Dufresne, Eds., John Wiley & Sons, 2017, pp. 51-100.

[83] K. Karimi and M. J. Taherzadeh, "A critical review of analytical methods in pretreatment of lignocelluloses: Composition, imaging, and crystallinity," *Bioresource Technology,* vol. 200, p. 1008–1018, January 2016.

[84] I. Siró and D. Plackett, "Microfibrillated cellulose and new nanocomposite materials: A review," *Cellulose,* vol. 17, no. 3, p. 459–494, June 2010.

[85] L. P. Ramos, "The Chemistry Involoved in the Steam Treatment of Lignocellulosic Materials," *Química Nova,* vol. 26, no. 6, pp. 863-871, 2003.

[86] G. Yu, S. Yano, H. Inoue, S. Inoue, T. Endo and S. Sawa, "Pretreatment of rice straw by a hot-compressed water process for enzymatic hydrolysis," *Applied Biochemistry and Biotechnology,* vol. 160, no. 2, p. 539–551, 2010.

[87] F. Teymouri, L. Laureano-P´erez, H. Alizadeh and B. E. Dale, "Ammonia fiber explosion treatment of corn stover," *Applied Biochemistry and Biotechnology,* vol. 119, no. 3, p. 951–963, 2004.

[88] Y. Sun and J. Cheng, "Hydrolysis of lignocellulosic materials for ethanol production: A review," *Bioresource Technology,* vol. 83, no. 1, pp. 1-11, 2002.

[89] J. Zheng and L. Rehmann, "Extrusion pretreatment of lignocellulosic biomass: A review," *International Journal of Molecular Sciences,* vol. 15, p. 18967–18984, 2014.

[90] S. &. S. M. Janardhnan, " Isolation of cellulose microfibrils – An enzymathic approach," *Bioresources,* vol. 1, no. 2, p. 176–188., 2006.

[91] M. Ahmad, C. R. Taylor, D. Pink , K. Burton, D. Eastwood, G. D. Bending and T. D. Bugg, "Development of novel assays for lignin degradation: comparative analysis of bacterial and fungal lignin degraders," *Molecular bioSystems,* vol. 6, no. 5, pp. 815-821, May 2010.

[92] N. Vigneshwaran and P. Satyamurthy, "Nanocellulose Production Using Cellulose Degrading Fungi," in *Advances and Applications Through Fungal Nanobiotechnology*, R. Prasad, Ed., Springer International Publishing, 2016, pp. 321-331.

[93] Z. Sun, V. Tang, T. Iwanaga, T. Sho and K. Kida, "Production of fuel ethanol frombamboo by concentrated sulfuric acid hydrolysis followed by continuous ethanol fermentation," *Bioresource Technology,* vol. 102, no. 23, p. 10929–10935, 2011.

[94] J. C. L´opez-Linares, C. Cara, M. Moya, E. Ruiz, E. Castro and I. Romero, "Fermentable sugar production from fromrapeseed straw by dilute phosphoric acid pretreatment," *Industrial Crops and Products,* vol. 50, p. 525–531, 2013.

[95] M. Taherdanak and H. Zilouei, "Improving biogas production from wheat plant using alkaline pretreatment," *Fuel,* vol. 115, p. 714–719, 2014.

[96] G. Brodeur, E. Yau, K. Badal, J. Collier, K. B. Ramachandran and S. Ramakrishnan, "Chemical and Physicochemical Pretreatment of Lignocellulosic Biomass: A Review," *Enzyme Research,* pp. 1-17, 2011.

[97] S. Hina, Y. Zhang and H. Wang, "Role of Ionic Liquids in Dissolution and Regeneration of Cellulose," *Reviews on advanced materials science,* vol. 40,

pp. 215-226, 2015.

[98] R. P. Swatloski, S. K. Spear, J. D. Holbrey and R. D. Rog, "Dissolution of Cellose with Ionic Liquids," *Journal of American Chemical Society,* vol. 124, pp. 4974-4975, April 2002.

[99] A. Pinkert, K. N. Marsh, S. Pang and M. P. Staiger, "Ionic Liquids and Their Interaction with Cellulose," *Chemical Reviews,* vol. 109, p. 6712–6728, 2009.

[100] J. L. Espinoza-Acosta, P. I. Torres-Chavez, E. Carvajal-Millan, B. Ramirez-Wong, L. A. Bello-Perez and B. Montan-Leyva, "Ionic Liquids and Organic Solvents for Recovering Lignin from Lignocellulosic Biomass," *BioResources,* vol. 9, no. 2, pp. 3660-3687, 2014.

[101] X. Zhao, K. Cheng and D. Liu, "Organosolv pretreatment of lignocellulosic biomass for enzymatic hydrolysis," *Applied Microbiology and Biotechnology,* vol. 82, no. 5, p. 815–827, 2009.

[102] E. C. Bensah and M. Mensah, "Chemical Pretreatment Methods for the Production of Cellulosic Ethanol: Technologies and Innovations," *International Journal of Chemical Engineering,* vol. 2013, pp. 1-21, 2013.

[103] M. A. Hubbe, O. R. Rojas, L. A. Lucia and M. Sain, "Cellulosic Nanocomposite: A Review," *Bio Resources,* vol. 3, no. 3, pp. 929-980, 2008.

[104] A. Coletti, A. Valerio and E. Vismara, "Posidonia oceanica as a Renewable Lignocellulosic Biomass for the Synthesis of Cellulose Acetate and Glycidyl Methacrylate Grafted Cellulose," *Materials,* vol. 6, pp. 2043-2058, May 2013.

[105] S. K. B. Zain, "Catalytic Depolymerization of Cellulose to Nanocellulose using Heteropoly Acid," Kuala Lumpur, 2015.

[106] C. J. Chirayil, L. Mathew and S. Thomas, "Review of recent research in nano cellulose preparation from different lignocellulosic fibers," *Advanced Materials,* vol. 37, pp. 20-28, November 2014.

[107] P. Satyamurthy and .. Vigneshwaran, "A novel process for synthesis of spherical nanocellulose by controlled hydrolysis of microcrystalline cellulose using anaerobic microbial consortium," *Enzyme and Microbial Technology,* vol. 52, no. 1, pp. 20-25, 2013.

[108] A. d. Campos, A. C. Correa, D. Cannella, E. d. M. Teixeira, J. M. Marconcini, A. Dufresne, L. H. C. Mattoso, P. Cassland and A. R. Sanadi, "Obtaining nanofibers from curaua and sugarcane bagasse fibers using enzymatic hydrolysis followed by sonication," *Cellulose,* vol. 20, p. 1491–1500, 2013.

[109] J. P. S. Morais, M. D. F. Rosa, M. D. S. M. D. S. Filho, L. D. Nascimento, D. M. D. Nascimento and A. R. Cassales, "Extraction and characterization of nanocellulose structures from raw cotton linter," *Carbohydrate Polymers,* vol.

91, no. 1, pp. 229-235, 2013.

[110] R. Xiong, X. Zhang, D. Tian, Z. Zhou and C. Lu, "Comparing microcrystalline with spherical nanocrystalline cellulose from waste cotton fabrics," *Cellulose,* vol. 19, no. 4, p. 1189–1198, 2012.

[111] H. Yu, Z. Qin, B. Liang, N. Liu, Z. Zhou and L. Chen, "Facile extraction of thermally stable cellulose nanocrystals with a high yield of 93% through hydrochloric acid hydrolysis under hydrothermal conditions," *Materials Chemistry A,* vol. 1, pp. 3938-3944, 2013.

[112] F. Jiang and Y. Hsieh, "Chemically and mechanically isolated nanocellulose and their self-assembled structures," *Carbohydrate Polymers,* vol. 95, pp. 32-40, 2013.

[113] L. Wagberg, G. Decher, M. Norgren, T. Lindstrom, M. Ankerfors and K. Axnas, "The build-up of polyelectrolyte multilayers of microfibrillated cellulose and cationic polyelectrolytes," *Langmuir,* vol. 24, no. 3, pp. 784-95., 2008.

[114] J. A. Sirviö, M. Visanko, O. Laitinen, A. Ämmälä and H. Liimatainen, "Amino-modified cellulose nanocrystals with adjustable hydrophobicity from combined regioselective oxidation and reductive amination," *Carbohydrate Polymers,* vol. 136, p. 581–587, 2016.

[115] V. S. Chauhan and S. K. Chakrabarti, "Use of nanotechnology for high performance cellulosic and papermaking products," *Cellulose Chemistry and Technology,* vol. 46, no. 5-6, p. 389–400., 2012.

[116] A. N. Frone, D. M. Panaitescu and D. Donescu, "Some aspects concerning the iso-lation of cellulose micro- and nano-fibers.," *U.P.B. Science Bulletin, Series B,C,* vol. 73, no. 2, p. 133–152, January 2011.

[117] J. Li, X. Wei, Q. Wang, J. Chen, G. Chang, L. Kong, J. Su and Y. Liu, "Homogeneous isolation of nanocellulose from sugarcane bagasse by high pressure homogenization," *Carbohydrate Polymers,* vol. 90, no. 4, p. 1609–1613, 2012.

[118] J. Leitner, B. Hinterstoisser, M. Wastyn, J. Keckes and W. Gindl, "Sugar beet cellulose nanofibril-reinforced composite," *Cellulose,* vol. 14, p. 419–425, 2007.

[119] Y. Habibi, M. Mahrouz and M. R. Vignon, "Microfibrillated cellulose from the peel of prickly pear fruits," *Food Chemistry,* vol. 115, p. 423–429, 2009.

[120] T. Zimmermann, N. Bordeanu and E. Strub, "Properties of nanofibrillated cellulose from different raw materials and its reinforcement potential," *Carbohydrate Polymers,* vol. 79, p. 1086–1093, 2010.

[121] N. Lavoine, I. Desloges, A. Dufresne and J. Bras, "Microfibrillated cellulose – Its barrier properties and applications in cellulosic materials: A review," *Carbohydrate Polymers,* vol. 90, p. 735– 764, 2012.

[122] S. Iwamoto, A. N. Nakagaito and H. Yano, "Nano-fibrillation of pulp fibers for the processing of transparent nanocomposites," *Applied Physics A,* vol. 89, no. 2, p. 461–466, 2007.

[123] Q. Q. Wang, J. Y. Zhu, R. Gleisner, T. Kuster, U. Baxa and S. E. McNeil, "Morphological development of cellulose fibrils of a bleached eucalyptus pulp bymechanical fibrillation," *Cellulose,* vol. 19, p. 1631–1643, 2012.

[124] S. P. Mishra, A. S. Manent, B. Chabot and C. Daneault, "Production of nanocel-lulose from native cellulose-various options utilizing ultrasound.," *BioResources,* vol. 7, no. 1, p. 422–436, 2012.

[125] Y. Peng, D. J. Gardner, Y. Han, A. Kiziltas, Z. Cai and M. A. Tshabalala, "Influence of drying method on the material properties of nanocellulose I: thermostability and crystallinity," *Cellulose,* vol. 20, no. 5, pp. 2379-2392, 2013.

[126] S. Beck, J. Bouchard and R. Berry, "Dispersibility in water of dried nanocrystalline cellulose," *Biomacromolecules,* vol. 13, p. 1486–1494., 2012.

[127] P. Nechita and D. M. Panaitescu, "Improving the Dispersibility of Cellulose Microfibrillated Structures in Polymer Matrix by Controlling Drying Conditions and Chemical Surface Modifications," *Cellulose Chemistry and Technology,* vol. 47, no. 10, pp. 711-719, 2013.

[128] G. V. Laivins and A. M. Scallan, "The Mechanism of Hornification of Wood Pulps. Products of Papermaking," in *Tenth Fundamental Research Symposium*, Oxford, 1993.

[129] Y. Peng, D. J. Gardner and Y. Han, "Drying cellulose nanofibrils: in search of a suitable method," *Cellulose,* vol. 19, no. 1, p. 91–102, 2012.

[130] M. Kılınçel, E. Toklu and F. Polat, "Classification of Supercritical Drying Methods and a Reactor Design," *Journal of Engineering Research and Applied Science,* vol. 3, no. 1, pp. 217-225, 2014.

[131] H. Kangas, P. Lahtinen, A. Sneck, A. Saariaho, O. Laitinen and E. Hellén, "Characterization of fibrillated celluloses. A short review and evaluation of characteristics with a combination of methods," *Nordic Pulp & Paper Research Journal,* vol. 29, no. 1, pp. 129-143, 2014.

[132] G. Tonoli, E. M. Teixeira, A. C. Corrêa, J. M. Marconcini, L. A. Caixeta , M. A. Pereira-da-Silva and L. H. C. Mattoso , "Cellulose micro/nanofibres from Eucalyptus kraft pulp: Preparation and properties," *Carbohydrate Polymers,* vol. 89, p. 80–88, 2012.

[133] J. I. Moran, V. A. Alvarez, V. P. Cyras and A. Vazquez, "Extraction of cellulose and preparation of nanocellulose from sisal fibers," *Cellulose,* vol. 15, p. 149–159, 2008.

[134] H. S. Yang and D. J. Gardner, "Morphological characteristics of cellulose nanofibril-filled polypropylene composites," *Wood and Fiber Science,* vol. 43, no. 2, pp. 215-224, 2011.

[135] S. Kampangkaewa, C. Thongpina and O. Santawteeb, "The synthesis of Cellulose nanofibers from Sesbania Javanica for filler in Thermoplastic starch," *Energy Procedia* , vol. 56, p. 318 – 325, 2014.

[136] D. Ciolacu, F. Ciolacu and V. I. Popa, "Amorphous Cellulose - Structure and Characterization," *Cellulose Chemistry and Technology,* vol. 45, pp. 13-21, 2011.

[137] N. F. M. Zain, S. M. Yusop and I. Ahmad, "Preparation and Characterization of Cellulose and Nanocellulose From Pomelo (Citrus grandis) Albedo," *Journal of Nutrition & Food Sciences* , vol. 5, no. 1, p. 334, 2014.

[138] M. R. K. Sofla, R. J. Brown, T. Tsuzuki and T. J. Rainey, "A comparison of cellulose nanocrystals and cellulose nanofibres extracted from bagasse using acid and ball milling methods," *Advances in Natural Sciences: Nanoscience and Nanotechnology,* vol. 7, pp. 1-10, 2016.

[139] C. Karunakaran, C. R. Christensen, C. Gaillard, R. Lahlali, L. M. Blair, V. Perumal, S. S. Miller and A. P. Hitchcock, "introduction of soft x-ray spectromicroscopy as an advanced technique for plant biopolymers research," *PLOS ONE,* pp. 1-18, 2015.

[140] I. Cumpstey, "Review Article - Chemical Modification of Polysaccharides," *Organic Chemistry,* vol. 2013, pp. 1-27, 2013.

[141] L. Heux, G. Chauve and C. Bonini, "Nonflocculating and chiral-nematic selfordering of cellulose microcrystals suspensions in nonpolar solvents," *Langmuir,* vol. 16, no. 21, p. 8210–8212., 2000.

[142] N. Lin, "Cellulose nanocrystals : surface modification and advanced materials," Grenoble, 2014.

[143] M. Salajková, "Wood Nanocellulose Materials and Effects from Surface Modification of Nanoparticles," Stockholm, 2013.

[144] "Surface modification in WPC with pre-treatment methods," in *Recent Advances in the Processing of Wood-Plastic Composites,* New York, Springer, 2010, pp. 23-57.

[145] J. Z. Lu, Q. Wu and H. S. McNabb, "Chemical Coupling Wood Fiber and Polymer Composites: A Review of Coupling Agents and Treatments.," *Wood*

Fiber and Science, vol. 32, no. 1, pp. 88-104, 2000.

[146] R. T. Coutts and G. B. Baker, "Gas Chromatography," in *Handbook of Neurochemistry*, 2 ed., A. Lajtha, Ed., New York, Plenum publishing corparation, 1982, pp. 429-445.

[147] A. Aravamudhan, D. M. Ramos, A. A. Nada and S. G. Kumb, "Natural Polymers: Polysaccharides and Their Derivatives for Biomedical Applications," in *Natural and Synthetic Biomedical Polymers*, Burlington, Elsevier, 2014, p. 67–89.

[148] Y. Xie, C. A. S. Hill, Z. Xiao, H. Militz and C. Mai, "Silane coupling agents used for natural fiber/polymer composites: A review," *Composites: Part A*, vol. 41, p. 806–819, 2010.

[149] C. O. Ufodike, "Modified Natural Fibrils for Structural Hybrid Composites: Towards an Investigation of Textile Reduction," Gainesville, 2016.

[150] L. A. Pothan and S. Thomas, "Polarity parameters and dynamic mechanical behaviour of chemically modified banana fiber reinforced polyester composites," *Composites Science and Technology*, vol. 63, pp. 1231-1240, 2003.

[151] M. Andresen, L. Johansson, B. S. Tanem and P. Stenius, "Properties and characterization of hydrophobized microfibrillated cellulose," *CelluloseMartin Andresen1,*, Leena-Sisko Johansson2*, vol. 13, p. 665 –677, 2006.

[152] D. Loof, M. Hiller, H. Oschkinat and K. Koschek, "Quantitative and Qualitative Analysis of Surface Modified Cellulose Utilizing TGA-MS," *Materials*, vol. 9, pp. 415-429, 2016.

[153] A. Rachini, M. L. Troedec, C. Peyratout and A. Smith, "Chemical Modification of Hemp Fibers by Silane Coupling Agents," *Journal of Applied Polymer Science*, vol. 123, p. 601–610, 2012.

[154] Y. B. Tee, R. A. Talib, K. Abdan, N. L. Chin, R. K. Basha and K. F. M. Yunos, "Thermally Grafting Aminosilane onto Kenaf-Derived Cellulose and Its Influence on the Thermal Properties of Poly(Lactic Acid) Composites," *BioResources* , vol. 8, no. 3, pp. 4468-4483, 2013.

[155] S. Ifuku, M. Nogi, K. Abe, K. Handa, F. Nakatsubo and H. Yano, "Surface modification of bacterial cellulose nanofibers for property enhancement of opticallytransparent composites: Dependence on acetyl-group DS," *Biomacromolecules*, vol. 8, no. 6, p. 1973–1978, 2007.

[156] M. Bulota, K. Kreitsmann, M. Hughes and J. Paltakari, "Acetylated microfibrillated cellulose as a toughening agent in poly(lactic acid)," *Journal of Applied Polymer Science*, vol. 126, no. 1, p. 448–457, 2012.

[157] N. Olaru, L. Olaru, C. Vasile and P. Ander, "Surface modified cellulose obtained by acetylation without solvents of bleached and unbleached kraft pulps," *Polymery,* pp. 834-840, 2011.

[158] X. Xu, M. Zhang, Q. Qiang, J. Song and W. He, "Study on the performance of the acetylated bamboo fiber/PBS composites by molecular dynamics simulation," *Composite Materials ,* pp. 1-9, 2015.

[159] G. Gurdag and S. Sarmad, "Cellulose Graft Copolymers: Synthesis, Properties and Applications," in *Polysaccharide Based Graft Copolymers*, Heidelberg, Springer, 2013, pp. 15-57.

[160] D. Roy, M. Semsarilar, J. T. Guthrie and S. Perrier, "Cellulose modification by polymer grafting: A review," *Chemical Society Reviews,* vol. 38, no. 7, pp. 2046-2064, 2009.

[161] E. Bianchi, A. Bonazza, E. Marsano and S. Russo, "Free radical grafting onto cellulose in homogeneous conditions. 2. Modified cellulose–methyl methacrylate system.," *Carbohydrate Polymers,* vol. 41, p. 47–53, 2000.

[162] L. Andreozzi, V. Castelvetro , G. Ciardelli, L. Corsi, M. Faetti, E. Fatarella and F. Zulli, "Free radical generation upon plasma treatment of cotton fibers and their initiation efficiency in surface-graft polymerization," *Journal of Colloid and Interface Science,* vol. 289, p. 455–465, 2005.

[163] K. Matyjaszewski, "Radical nature of cu-catalyzed controlled radical polymerizations (atom transfer radical polymerization)," *Macromolecules ,* vol. 31, p. 4710–4717, 1998.

[164] J. H. Xia and K. Matyjaszewski, "Controlled/“living” radical polymerization. Atom transfer radical polymerization catalyzed by copper(I) and picolylamine complexes," *Macromolecules,* vol. 32, p. 2434–2437, 1999.

[165] N. Tsubokawa, T. Iida and T. Takayama, "Modification of cellulose powder surface by grafting of polymers with controlled molecular weight and narrow molecular weight distribution," *Journal of Applied Polymer Science,* vol. 75, no. 4, pp. 515-522, 2000.

[166] S. T. Sundar, "Chemical Modification of Wood Fiber to Enhance the Interface Between Wood and Polymer in Wood Plastic Composites," Moscow , 2005.

[167] M. I. Mendelson, Learning Bio-Micro-Nanotechnology, 1 ed., Boca Raton: CRC Press, 2013.

[168] T. Tadros, Encyclopedia of Colloid and Interface Science, New York: Springer, 2013.

[169] B. L. Tardy, S. Yokota, M. Ago, W. Xiang, T. Kondo, R. Bordes and O. J. Rojas, "Nanocellulose-surfactant interactions," *Current Opinion in Colloid &*

Interface Science, vol. 29, pp. 57-67, March 2017.

[170] J. Kim, G. Montero, Y. Habibi, J. P. Hinest, J. Genzer, D. S. Argyropoulos and O. J. Rojas, "Dispersion of Cellulose Crystallites by Nonionic Surfactants in a Hydrophobic Polymer Matrix," *Polymer Engineering and Science,* vol. 49, no. 10, pp. 2054-2061, October 2009.

[171] S. Iwamoto, S. Yamamoto, S. Lee and T. Endo, "Mechanical properties of polypropylene composites reinforced by surface-coated microfibrillated cellulose," *Composites Part A Applied Science and Manufacturing,* vol. 59, pp. 26-29, April 2014.

[172] C. Bruce, "Surface Modification of Cellulose by Covalent Grafting and Physical Adsorption for Biocomposite Applications," Stockholm, 2014.

[173] L. Wågberg, "Polyelectrolyte adsorption on cellulose fibres - A review," Sundsvall, 2001.

[174] H. Li, S. Fu, L. Peng and H. Zhan, "Surface modification of cellulose fibers with layer-by-layer self-assembly of lignosulfonate and polyelectrolyte: effects on fibers wetting properties and paper strength," *Cellulose,* vol. 19, p. 533–546, 2012.

[175] M. Jonoobi, J. Harun, A. P. Mathew and K. Oksman, "Mechanical properties of cellulose nanofiber (CNF) reinforced polylactic acid (PLA) prepared by twin screw extrusion," *Composites Science and Technology,* vol. 70, no. 12, pp. 1742-1747, 2010.

[176] T. Wang and L. T. Drzal, "Cellulose-Nanofiber-Reinforced Poly(lactic acid) Composites Prepared by a Water-Based Approach," *ACS Applied Materials & Interfaces,* vol. 4, no. 10, p. 5079–5085, 2012.

[177] A. Iwatake, M. Nogi and H. Yano, "Cellulose nanofiber reinforced polylactic acid," *Composites Science and Technology,* vol. 68, no. 9, pp. 2103-2106, 2008.

[178] M. Hietala, A. P. Mathew and K. Oksman, "Bionanocomposites of thermoplastic starch and cellulose nanofibers manufactured using twin-screw extrusion," *European Polymer Journal,* vol. 49, no. 4, pp. 950-956, 2013.

[179] A. Kaushik, M. Singh and G. Verma, "Green nanocomposites based on thermoplastic starch and steam exploded cellulose nanofibrils from wheat straw," *Carbohydrate Polymers,* vol. 82, no. 2, pp. 337-345, 2010.

[180] B. N. Nasrabadia, M. Mehrasab, M. Rafienia, S. Bonakdar, T. Behzad and S. Gavanji, "Porous starch/cellulose nanofibers composite prepared by salt leaching technique for tissue engineering," *Carbohydrate Polymers,* vol. 108, no. 8, pp. 232-238, 2014.

[181] U. Bhardwaj, P. Dhar, A. Kumar and V. Katiyar, "Polyhydroxyalkanoates (PHA)-Cellulose Based Nanobiocomposites for Food Packaging Applications," in *Food Additives and Packaging*, V. Komolprasert and P. Turowski, Eds., Washington, American Chemical Society, 2014, p. 275–314.

[182] M. P. Arrieta, E. Fortunati, F. Dominici, J. Lopez and J. M. Kenny, "Bionanocomposite Films Based on plasticized PLA–PHB/cellulose Nanocrystals Blends," *Carbohydrate Polymers,* vol. 121, pp. 265-275, 2015.

[183] E. Ten, D. F. Bahr, B. Li, L. Jiang and M. P. Wolcott, "Effects of Cellulose Nanowhiskers on Mechanical, Dielectric, and Rheological Properties of Poly(3-hydroxybutyrate-co-3-hydroxyvalerate)/Cellulose Nanowhisker Composites," *Industrial & Engineering Chemistry Research,* vol. 51, no. 7, p. 2941–2951, 2012.

[184] Y. Peng, S. A. Gallegos, D. J. Gardner, Y. Han and Z. Cai, "Maleic Anhydride Polypropylene Modified Cellulose Nanofibril Polypropylene Nanocomposites With Enhanced Impact Strength," *Polymer Composites,* vol. 37, no. 3, p. 782–793, 2016.

[185] E. Yakkan, T.Uysalman, M. Atagür, H. Kara, K. Sever, A. Yıldırım, B. Girginer and M. O. Seydibeyoğlu, 2016. [Online]. Available: https://biltek.sanayi.gov.tr/Bilimsel%20almalarmz/Nanocellulose_1.pdf.

[186] S. H. Lee, Y. Teramoto and T. Endo, "Cellulose nanofiber-reinforced polycaprolactone/polypropylene hybrid nanocomposite," *Composites Part A: Applied Science and Manufacturing,* vol. 42, no. 2, pp. 151-156, 2011.

[187] A. Kiziltas, B. Nazari, E. E. Kiziltas, D. J. S. Gardner, Y. Han and T. S. Rushing, "Cellulose NANOFIBER-polyethylene nanocomposites modified by polyvinyl alcohol," *Applied Polymer Science,* vol. 133, no. 6, pp. 1-8, 2016.

[188] M. A. Shamsabadi, T. Behzad, R. Bagheri and B. N. Nasrabadi, "Preparation and Characterization of Low-Density Polyethylene/Thermoplastic Starch Composites," *Polymer Composites,* vol. 36, no. 12, p. 2309–2316, 2015.

[189] M. L. Auad, T. Richardson, W. J. Orts, E. S. Medeiros, L. H. C. Mattoso, M. A. Mosiewicki, N. E. Marcovich and M. I. Aranguren, "Polyaniline-modified cellulose nanofibrils as reinforcement of a smart polyurethane," *Polymer International,* vol. 60, no. 5, p. 743–750, 2011.

[190] P. Nechita and D. M. Panaitescu, "Improving the Dispersibility of Cellulose Microfibrillated Structures in Polymer Matrix by Controlling Drying Conditions and Chemical Surface Modifications," *Cellulose Chemistry and Technology,* vol. 47, no. 9, pp. 711-719, 2013.

[191] M. Bhattacharya, "Polymer Nanocomposites—A Comparison between Carbon Nanotubes, Graphene, and Clay as Nanofillers," *Materials,* vol. 9, no. 4, pp.

262-297, 2016.

[192] O. J. Rojas, G. A. Montero and Y. Habibi, "Electrospun Nanocomposites from Polystyrene Loaded with Cellulose Nanowhiskers," *Applied Polymer Science,* vol. 113, p. 927–935, 2009.

[193] X. Cao, Y. Habibi and L. A. Lucia, "One-pot polymerization, surface grafting, and processing of waterborne polyurethane-cellulose nanocrystal nanocomposites," *Materials Chemistry*, vol. 19, p. 7137–7145, 2009.

[194] A. Dufresne, "Processing of Polymer Nanocomposites Reinforced with Polysaccharide Nanocrystals," *Molecules,* vol. 15, pp. 4111-4128, 2010.

[195] A. M. Gumel and S. M. Annuar, "Nanocomposites of Polyhydroxyalkanoates (PHAs)," in *Polyhydroxyalkanoate (PHA) based Blends, Composites and Nanocomposites*, I. Roy and P. M. Visakh, Eds., Cambridge, The Royal Society of Chemistry, 2015, pp. 98-118.

[196] J. Kim, G. Montero, Y. Habibi, J. P. Hinestroza, J. Genzer, D. S. Argyropoulos and O. J. Rojas, "Dispersion of Cellulose Crystallites by Nonionic Surfactants in a Hydrophobic Polymer Matrix," *Polymer Engineering and Science*, vol. 49, no. 10, p. 2054–2061, 2009.

[197] N. Ljungberg, J. Cavaille and L. Heux, "Nanocomposites of isotactic polypropylene reinforced with rod-like cellulose whiskers," *Polymer,* vol. 47, no. 18, pp. 6285-6292, 2006.

[198] W. S. Khan, N. N. Hamadneh and W. A. Khan, "Polymer nanocomposites - synthesis techniques, classification and properties," in *Science and applications of Tailored Nanostructures*, P. D. Sia, Ed., Padova, One Central Press, 2017, pp. 50-67.

[199] H. M. Hassanabadi, A. Alemder and D. Rodrigue, "Polyporpylene reinforced with nanocrystalline cellulose: Coupling agent optimization," *Applied Polymer Science,* vol. 132, no. 34, pp. 1-10, 2015.

[200] A. Dufresne, Nanocellulose: From Nature to High Performance Tailored Materials, Berlin: hubert & co. gottingen, 2012.

[201] K. Rodrıguez, P. Gatenholm and S. Renneckar, "Electrospinning cellulosic nanofibers for biomedical applications: structure and in vitro biocompatibility," *Cellulose* , vol. 19, p. 1583–1598, 2012.

[202] R. L. Razalli, M. M. Abdi, P. M. Tahir, A. Moradbak, Y. Sulaiman and L. Y. Heng, "Polyaniline-modified nanocellulose prepared from Semantan bamboo by chemical polymerization: preparation and characterization," *RSC Advances,* vol. 7, pp. 25191-25198, 2017.

[203] M. Abdelmouleh, S. Boufi, M. Belgacem and A. Dufresne, "Short natural-fibre

reinforced polyethylene and natural rubber composites: Effect of silane coupling agents and fibres loading," *Composites Science and Technology,* vol. 67, p. 1627–1639, 2007.

[204] T. T. Loan, "Investigation on jute fibres and their composites based on polypropylene and epoxy matrices," Dresden, 2006.

[205] M. J. Chen, J. J. Meister, D. W. Gunnells and D. J. Gardner, "A process for coupling wood to thermoplastic using graft copolymers," *Advanced Polymer Technology,* vol. 14, no. 2, pp. 97-109, 1995.

[206] G. E. Myers, I. S. Chahyadi, C. Gonzalez, C. A. Coberly and D. S. Ermer, "Wood flour and polypropylene or high-density polyethylene composites: Influence of maleated polypropylene concentration and extrusion temperature on properties," *Polymeric Materials and Polymeric Biomaterials,* vol. 15, no. 3, pp. 49-56, 1991.

[207] S. Takase and N. Shiraishi, "Studies on composites from wood and polypropylenes. II," *Applied Polymer Science,* vol. 37, no. 3, pp. 645-659, 1989.

[208] G. Suaria, C. G. Avio, A. Mineo, G. L. Lattin, M. G. Magaldi, G. Belmonte, C. J. Moore, F. Regoli and S. Aliani, "The Mediterranean Plastic Soup: synthetic polymers in Mediterranean surface waters," *Scientific Reports,* vol. 6, pp. 1-10, 2016.

[209] G. M. Glenn, W. Orts, S. Imam, B. Chiou and D. F. Wood, "Starch Plastic Packaging and Agriculture Applications," *Starch Polymers,* pp. 421-452, 2014.

[210] M. F. Maitz, "Applications of synthetic polymers in clinical medicine," *Biosurface and Biotribology,* vol. 1, no. 3, pp. 161-176, 2015.

[211] Y. Lu, H. L. Tekinalp, C. C. Eberle, W. Peter, A. K. Naskar and S. Ozcan, "Nanocellulose in Polymer Composites and Biomedical Applications," *Tappi Journal,* vol. 13, no. 6, pp. 47-54, 2014.

[212] L. D. Rajapaksha and H. A. D. Saumyadi, "Investigation of Mechanical Properties of Microcrystalline Cellulose Based Composites," University of Moratuwa, Moratuwa, 2017.

[213] A. B. Fall, "Colloidal interactions and orientation of nanocellulose," Stockholm, 2013.

[214] M. Fan, D. Dai and B. Huang, "Fourier Transform Infrared Spectroscopy for Natural Fibres," in *Fourier Transform - Materials Analysis*, Shanghai, InTech, 2012, pp. 45-68.

[215] R. Morent, N. De Geyter, C. Leys, L. Gengembre and E. Payen, "Comparison between XPS- and FTIR-analysis of plasma-treated polypropylene film

surfaces," *Surface and Interface Analysis,* vol. 40, p. 597–600, 2008.

[216] S. Devasahayam, V. Sahajwalla and M. Sng, "Investigation into Failure in Mining Wire Ropes—Effect of Crystallinity," *Open Journal of Organic Polymer Materials, 2013, 3, 34-40,* vol. 3, pp. 34-40, 2013.

[217] U. W. Gedde, Polymer Physics, stockholm: Springer, 1999.

[218] E. Andreassen, "Infrared and Raman Spectroscopy of Polypropylene," in *Polypropylene: An A-Z reference,* Springer, 1999, pp. 320-328.

[219] S. Park, J. O. Baker, M. E. Himmel and P. A. Parill, "Cellulose crystallinity index: measurement techniques and their impact on interpreting cellulase performance," *Biotechnol Biofuels. 2010; 3: 10. ,* vol. 3, no. 10, pp. 1-10, 2010.

[220] A. Kumar, Y. S. Nege, N. K. Bhardwaj and V. Choudhary, "Synthesis and characterization of cellulose nanocrystals/PVA based bionanocomposite," *Advanced materials letters,* vol. 4, no. 8, pp. 626-631, 2013.

[221] N. H. Mohd, N. F. H. Ismail, J. I. Zahari, W. F. Fathilah, H. Kargarzadeh, S. Ramli, I. Ahmad, M. A. Yarmo and R. Othaman, "Effect of Aminosilane Modification on Nanocrystalline Cellulose Properties," *Journal of Nanomaterials,* vol. 2016, pp. 1-8, 2016.

[222] M. Poletto, A. J. Zattera and V. Pistor, "Structural Characteristics and Thermal Properties of Native Cellulose," in *Cellulose - Fundamental Aspects*, T. V. de Ven and L. Godbout, Eds., Intech, 2013, pp. 45-68.

[223] K. Y. Lee, Y. Aitomäki, L. A. Berglund, K. Oksman and A. Bismarck, "On the use of nanocellulose as reinforcement in polymer matrix composites," *Composites Science and Technology,* vol. 105, pp. 15-27, 2014.

[224] E. M. Troisi, H. J. M. Caelers and G. W. M. Peters, "Full Characterization of Multiphase, Multimorphological Kinetics in Flow-Induced Crystallization of IPP at Elevated Pressure," *Macromolecules,* vol. 50, pp. 3868-3882, 2017.

[225] L. Guo, X. Ma, B. Zhang, Z. Wang and P. Huang, "Synthesis of polyether imidazole ionic liquid and its modification on polypropylene crystal structure and mechanical properties," *e-Polymers,* vol. 15, no. 1, p. 33–37, 2015.

[226] E. Lêzak and Z. Bartczak, "Experimental Study of the Formation of β- and γ-phase Isotactic Polypropylene and Estimation of the Phase Composition by Wide-Angle X-Ray Scattering," *Fibres & Textiles in Eastern Europe,* vol. 13, no. 5, pp. 51-56, 2005.

[227] A. Sluiter, B. Hames, R. Ruiz, C. Scarlata, J. Sluiter and D. Templeton, "Determination of Ash in Biomass - Laboratory Analytical Procedure (LAP)," National Renewable Energy Laboratory, Colorado, 2008.

[228] A. Valadez-Gonzalez, J. M. Cervantes, R. Olayo and P. J. Herrera-Franco, "Chemical modification of heneque´n fibers with an organosilane coupling agent," *Composites: Part B* , vol. 30, p. 321–331, 1999.

[229] L. Britcher, D. Kehoe, J. Matisons and G. Swincer, "Siloxane coupling agents," *Macromolecules,* vol. 28, p. 3110–3118, 1995.

[230] H. Khanjanzadeh, R. Behrooz, N. Bahramifar, W. Gindl-Altmutter, M. Bache, M. Edler and T. Griesser, "Surface chemical functionalization of cellulose nanocrystals by 3-aminopropyltriethoxysilane," *International Journal of Biological Macromolecules,* vol. 106, pp. 1288-1296, 2018.

[231] H. G. Brittain and R. D. Bruce, "Thermal analysis," in *Comprehensive Analytical Chemistry,* A. Cappiello and P. Palma, Eds., 2006, pp. 63-109.

[232] R. M. Sheltami, H. Kargarzadeh and I. Abdullah, "Effects of Silane Surface Treatment of Cellulose Nanocrystals on the Tensile Properties of Cellulose-Polyvinyl Chloride Nanocomposite," *Sains Malaysiana,* vol. 44, no. 6, p. 801–810, 2015.

[233] E. Pavlidou, D. Bikiaris, A. Vassiliou, M. Chiotelli and G. Karayammidis, "Mechanical properties and morphological examination of isotactic polypropylene/SiO2 nanocomposites containing PP-g-MA as compatibilizer," *Journal of Physics: Conference Series,* vol. 10, pp. 190-193, 2005.

[234] H. Salmah, M. Marliza and P. L. Teh, "Treated Coconut Shell Reinforced Unsaturated Polyester," *International Journal of Engineering and Technology,* vol. 13, no. 2, pp. 94-103, 2013.

[235] A. F. Yee and H. J. Sue, "Impact Resistance," in *Encyclopedia of Polymer Science and Technology,* John Wiley & Sons, 2002, pp. 528-563.

[236] "Composites," in *Materials Science and Engineering: an Introduction*, New York, John Wiley & Sons, 2007, pp. 577-617.

[237] N. F. Aris, R. A. Majid, W. H. W. Hassan, M. F. A. Rahman and N. Y. Mun, "Effects of Stone Powder on Water Absorption and Biodegradability of Low Density Polyethylene/Palm Pressed Fibre Composite Film," *Applied Mechanics and Materials,* vol. 554, pp. 123-127, 2014.

[238] Z. X. Zhang, J. Zhang, B. Lu, Z. X. Xin, C. K. Kang and J. K. Kim, "Effect of flame retardants on mechanical properties, flammability and foamability of PP/wood–fiber composites," *Composites: Part B,* vol. 43, p. 150–158, 2012.

[239] W. Minoshima, J. L. White and J. E. Spruiell, "Experimental Investigation of the Influence of Molecular Weight Distribution on the Rheological Properties of Polypropylene Melts," *Polymer Engineering and Science,* vol. 20, no. 17, pp. 1166-1176, 1980.

Appendix A

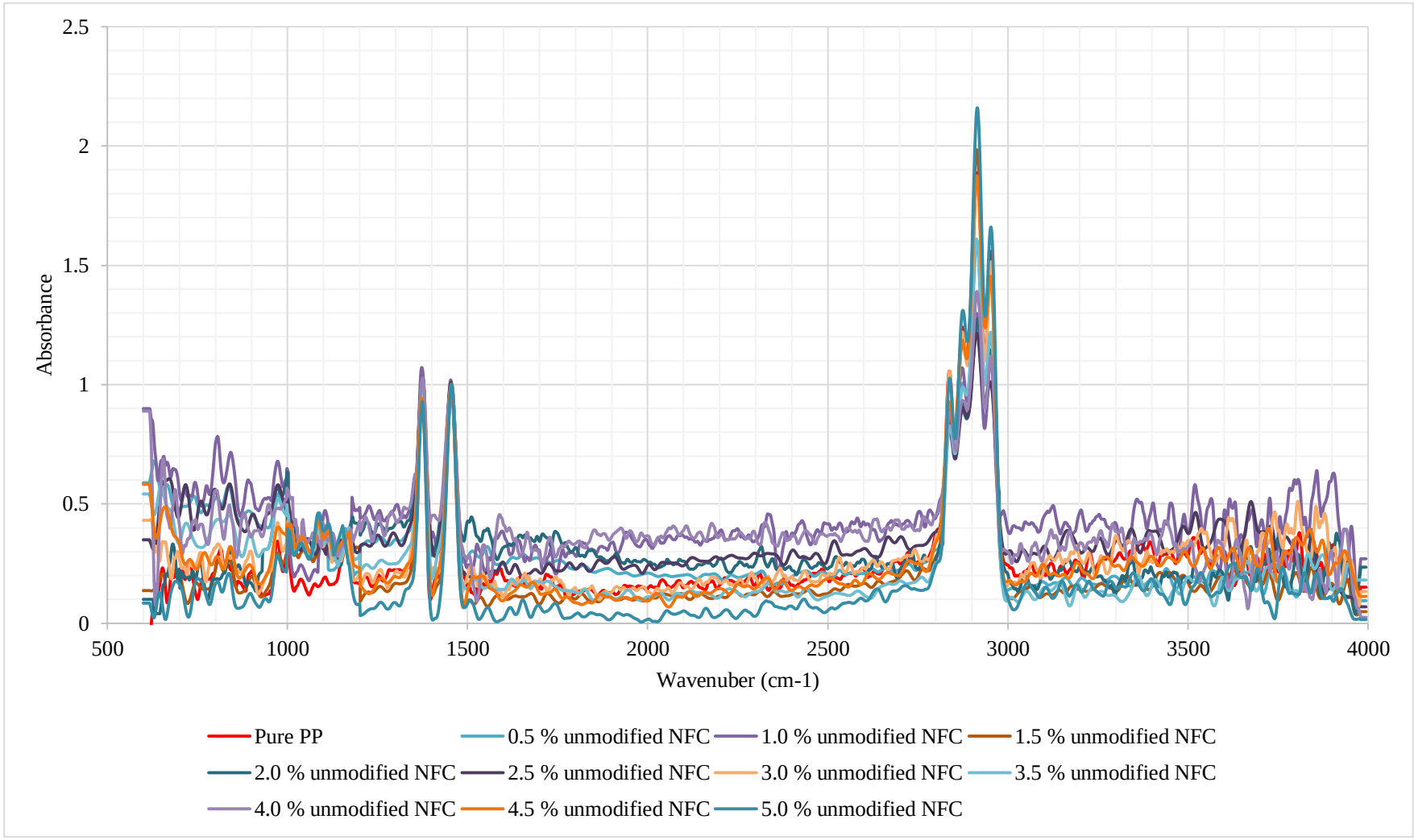
2.5
2
1.5
1
0.5
0
Absorbance
500
1000
1500
2000
2500
3000
3500
4000
Wavenuber (cm-1)
Pure PP
0.5 % unmodified NFC
1.0 % unmodified NFC
1.5 % unmodified NFC
2.0 % unmodified NFC
2.5 % unmodified NFC
3.0 % unmodified NFC
3.5 % unmodified NFC
4.0 % unmodified NFC
4.5 % unmodified NFC
5.0 % unmodified NFC

Appendix B

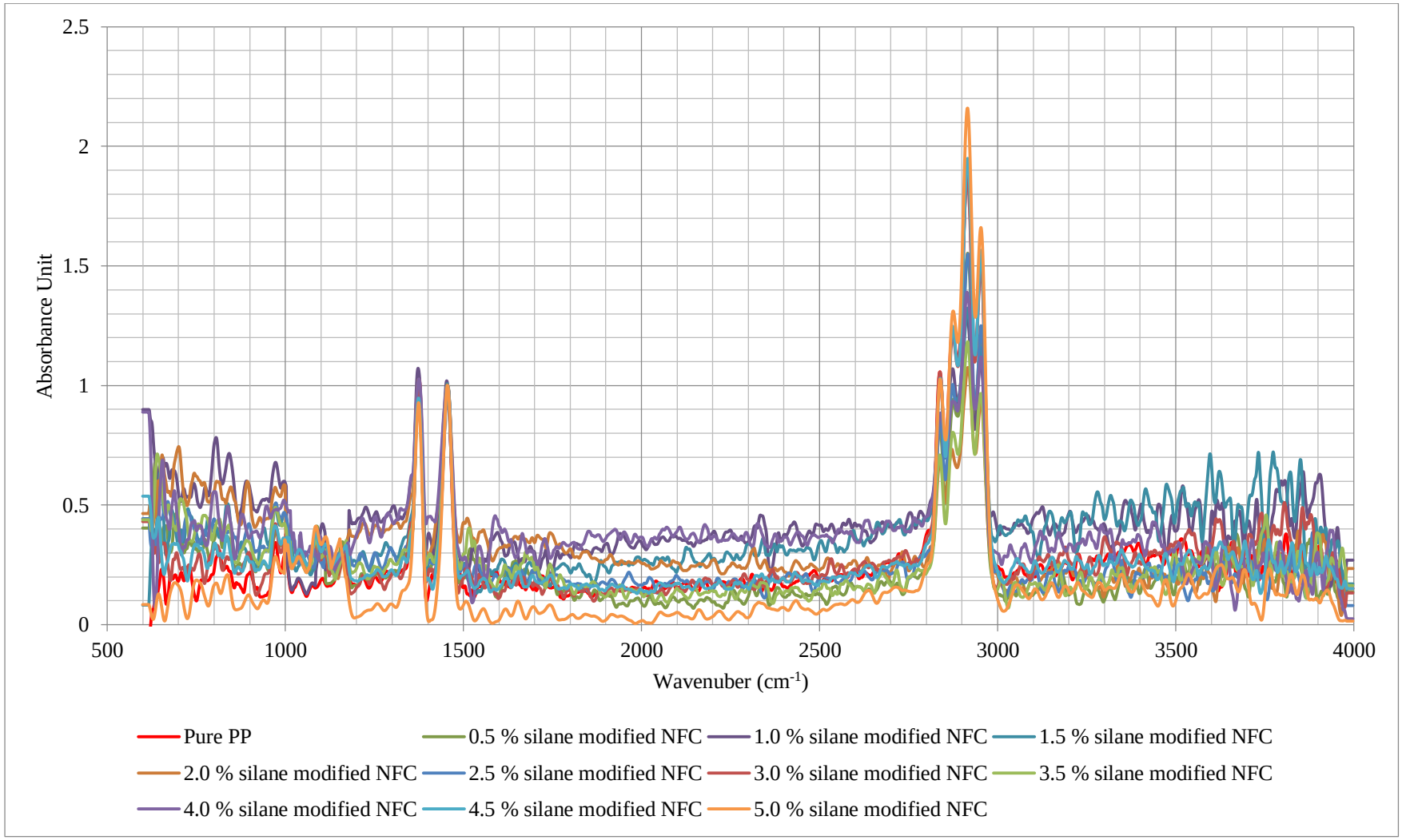
2.5
2
1.5
1
0.5
0
Absorbance Unit
500
1000
1500
2000
2500
3000
3500
4000
Wavenuber (cm-1)
Pure PP
0.5 % silane modified NFC
1.0 % silane modified NFC
1.5 % silane modified NFC
2.0 % silane modified NFC
2.5 % silane modified NFC
3.0 % silane modified NFC
3.5 % silane modified NFC
4.0 % silane modified NFC
4.5 % silane modified NFC
5.0 % silane modified NFC

Appendix C

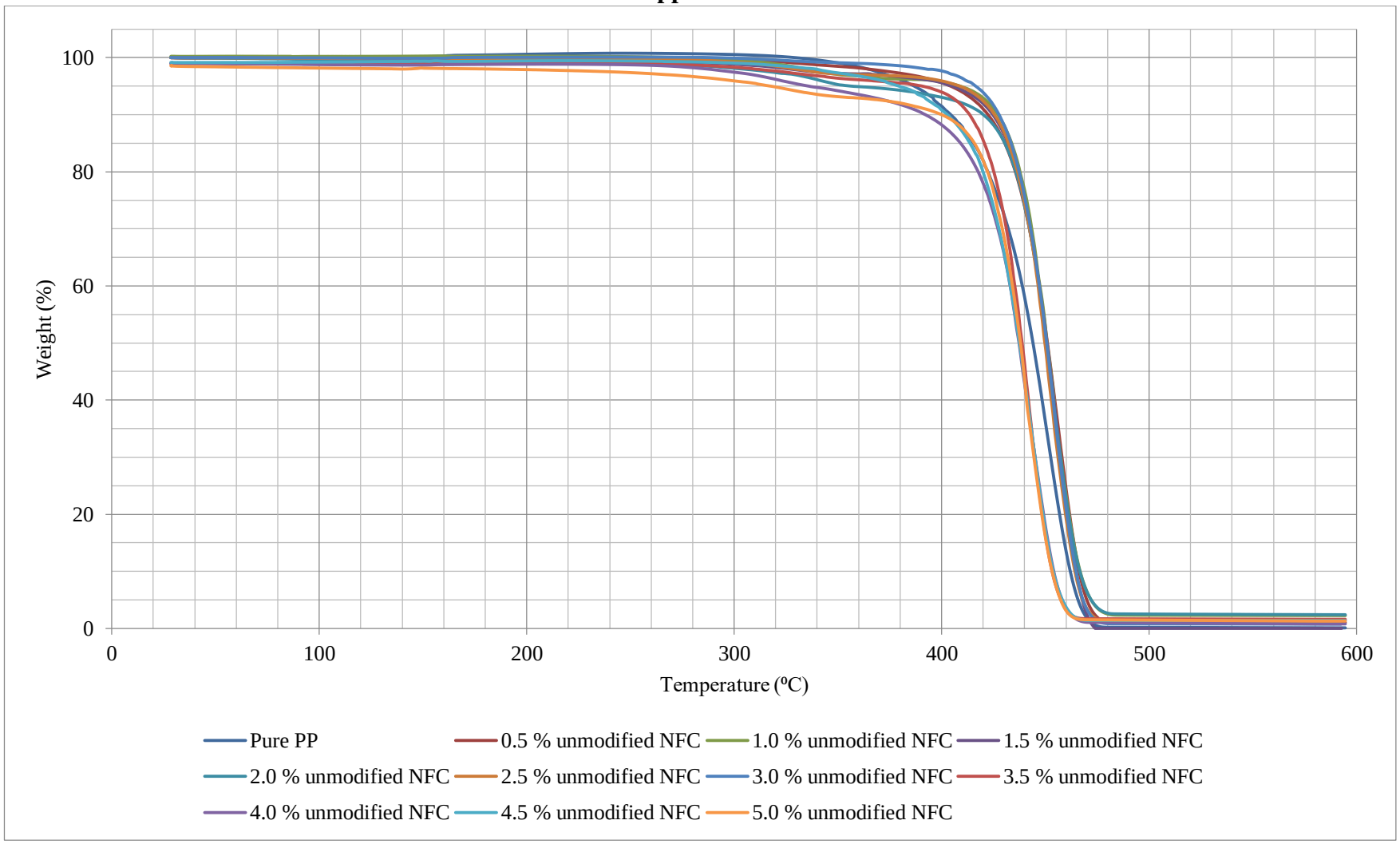
100
80
60
40
20
0
Weight (%)
0
100
200
300
400
500
600
Temperature (ºC)
Pure PP
0.5 % unmodified NFC
1.0 % unmodified NFC
1.5 % unmodified NFC
2.0 % unmodified NFC
2.5 % unmodified NFC
3.0 % unmodified NFC
3.5 % unmodified NFC
4.0 % unmodified NFC
4.5 % unmodified NFC
5.0 % unmodified NFC

Appendix D

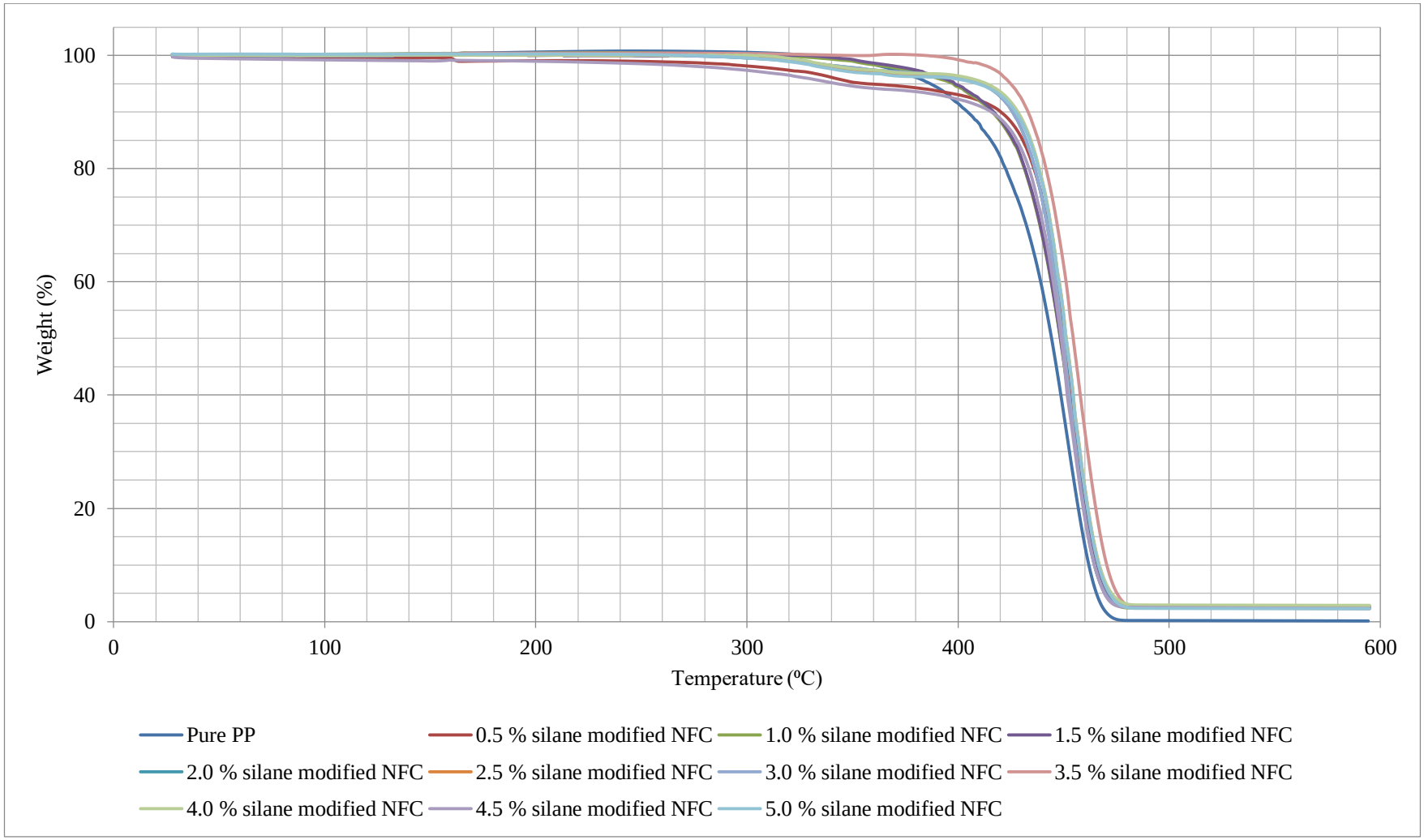
100
80
60
40
20
0
Weight (%)
0
100
200
300
400
500
600
Temperature (ºC)
Pure PP
0.5 % silane modified NFC
1.0 % silane modified NFC
1.5 % silane modified NFC
2.0 % silane modified NFC
2.5 % silane modified NFC
3.0 % silane modified NFC
3.5 % silane modified NFC
4.0 % silane modified NFC
4.5 % silane modified NFC
5.0 % silane modified NFC

Appendix E

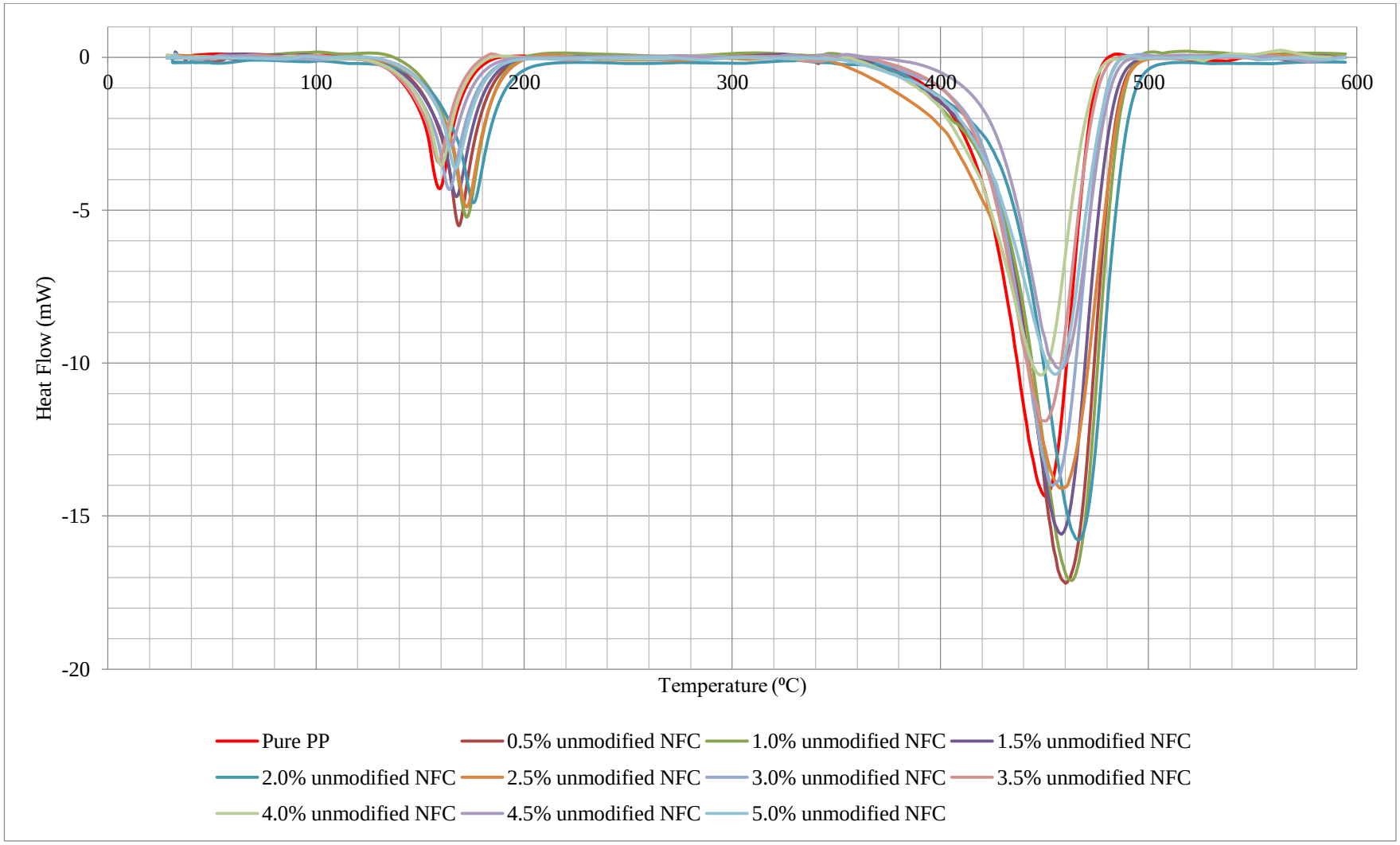
0
-5
-10
-15
-20
0
100
200
300
400
500
600
Heat Flow (mW)
Temperature (ºC)
Pure PP
0.5% unmodified NFC
1.0% unmodified NFC
1.5% unmodified NFC
2.0% unmodified NFC
2.5% unmodified NFC
3.0% unmodified NFC
3.5% unmodified NFC
4.0% unmodified NFC
4.5% unmodified NFC
5.0% unmodified NFC

Appendix F

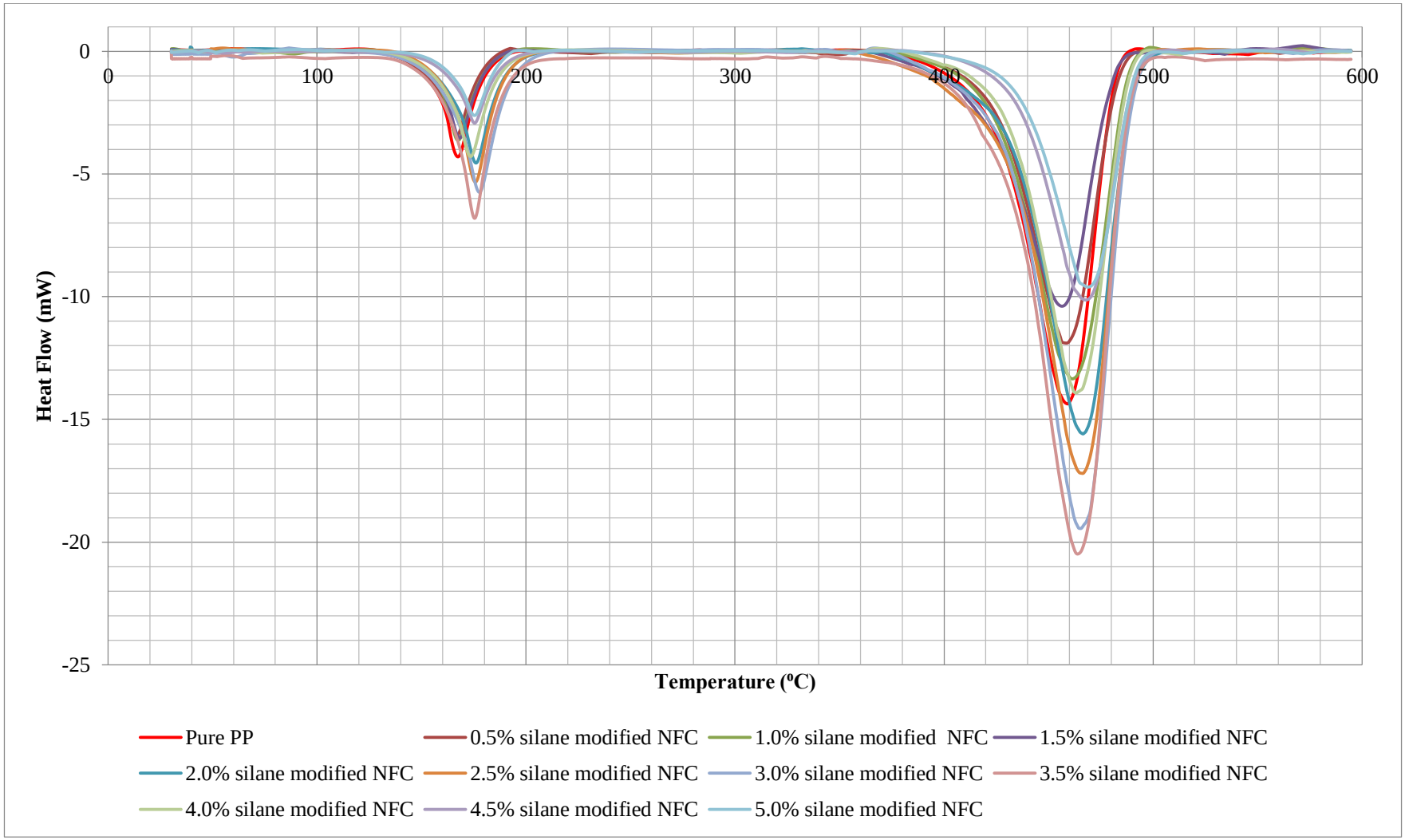
0
-5
-10
-15
-20
-25
0
100
200
300
400
500
600
Heat Flow (mW)
Temperature (ºC)
Pure PP
0.5% silane modified NFC
1.0% silane modified NFC
1.5% silane modified NFC
2.0% silane modified NFC
2.5% silane modified NFC
3.0% silane modified NFC
3.5% silane modified NFC
4.0% silane modified NFC
4.5% silane modified NFC
5.0% silane modified NFC